

Spring 1-1-2017

Fully-Coupled Dynamical Jitter Modeling of Momentum Exchange Devices

John Alcorn

University of Colorado at Boulder, john.b.alcorn@gmail.com

Follow this and additional works at: https://scholar.colorado.edu/asen_gradetds

 Part of the [Aerospace Engineering Commons](#), [Applied Mathematics Commons](#), and the [Mechanical Engineering Commons](#)

Recommended Citation

Alcorn, John, "Fully-Coupled Dynamical Jitter Modeling of Momentum Exchange Devices" (2017). *Aerospace Engineering Sciences Graduate Theses & Dissertations*. 232.
https://scholar.colorado.edu/asen_gradetds/232

This Thesis is brought to you for free and open access by Aerospace Engineering Sciences at CU Scholar. It has been accepted for inclusion in Aerospace Engineering Sciences Graduate Theses & Dissertations by an authorized administrator of CU Scholar. For more information, please contact cuscholaradmin@colorado.edu.

**Fully-Coupled Dynamical Jitter Modeling of Momentum
Exchange Devices**

by

John Alcorn

B.S., University of Alabama in Huntsville, 2014

A thesis submitted to the
Faculty of the Graduate School of the
University of Colorado in partial fulfillment
of the requirements for the degree of
Master of Science
Department of Aerospace Engineering Sciences
2017

This thesis entitled:
Fully-Coupled Dynamical Jitter Modeling of Momentum Exchange Devices
written by John Alcorn
has been approved for the Department of Aerospace Engineering Sciences

Prof. Hanspeter Schaub

Dr. Daniel G. Kubitschek

Dr. Robert R. Leben

Date _____

The final copy of this thesis has been examined by the signatories, and we find that both the content and the form meet acceptable presentation standards of scholarly work in the above mentioned discipline.

Alcorn, John (M.S., Aerospace Engineering Sciences)

Fully-Coupled Dynamical Jitter Modeling of Momentum Exchange Devices

Thesis directed by Prof. Hanspeter Schaub

A primary source of spacecraft jitter is due to mass imbalances within momentum exchange devices (MEDs) used for fine pointing, such as reaction wheels (RWs) and variable-speed control moment gyroscopes (VSCMGs). Although these effects are often characterized through experimentation in order to validate pointing stability requirements, it is of interest to include jitter in a computer simulation of the spacecraft in the early stages of spacecraft development. An estimate of jitter amplitude may be found by modeling MED imbalance torques as external disturbance forces and torques on the spacecraft. In this case, MED mass imbalances are lumped into static and dynamic imbalance parameters, allowing jitter force and torque to be simply proportional to wheel speed squared. A physically realistic dynamic model may be obtained by defining mass imbalances in terms of a wheel center of mass location and inertia tensor. The fully-coupled dynamic model allows for momentum and energy validation of the system. This is often critical when modeling additional complex dynamical behavior such as flexible dynamics and fuel slosh. Furthermore, it is necessary to use the fully-coupled model in instances where the relative mass properties of the spacecraft with respect to the RWs cause the simplified jitter model to be inaccurate. This thesis presents a generalized approach to MED imbalance modeling of a rigid spacecraft hub with N RWs or VSCMGs. A discussion is included to convert from manufacturer specifications of RW imbalances to the parameters introduced within each model. Implementations of the fully-coupled RW and VSCMG models derived within this thesis are released open-source as part of the Basilisk astrodynamics software.

Dedication

Dedicated to all of the great friends I made in Boulder
and to the mountains of Colorado – a source of infinite inspiration and endless possibilities.

Acknowledgements

I would like to acknowledge my advisor, Dr. Hanspeter Schaub, for his support of this thesis.

Extra special thanks to bug-hunter Cody Allard for finding all the problems with the software I wrote in support of this research. I definitely owe you a few more IPAs!

Contents

Chapter	
1	Introduction 1
1.1	Background 1
1.2	Motivation 5
1.3	Literature Review 9
1.4	Research Scope 10
2	Imbalanced Reaction Wheel 13
2.1	Problem Statement 13
2.1.1	Reference Frame Definitions 13
2.1.2	Variable Definitions 14
2.2	Equations of Motion 14
2.2.1	Translational Motion 15
2.2.2	Rotational Motion 16
2.2.3	Motor Torque Equation 21
3	Imbalanced Variable Speed Control Moment Gyroscope 25
3.1	Problem Statement 25
3.1.1	Reference Frame Definitions 25
3.1.2	Variable Definitions 26
3.2	Equations of Motion 27

3.2.1	Translational Motion	27
3.2.2	Rotational Motion	29
3.2.3	Gimbal Torque Equation	40
3.2.4	Wheel Torque Equation	43
4	Imbalance Parameter Adaptation	46
4.1	Simplified Imbalance Model	46
4.2	Imbalance Parameter Adaptation	47
5	Software Implementation	50
5.1	Back-Substitution Method	50
5.1.1	Equations of Motion	52
5.1.2	Derivation of Back-Substitution	55
5.1.3	Back-Substitution Contribution Matrices	57
5.2	Energy and Angular Momentum Validation Method	58
5.2.1	Angular Momentum	58
5.2.2	Energy	59
5.2.3	Energy Rate	59
6	Numerical Simulation Results	61
6.1	Spacecraft with N Imbalanced Reaction Wheels	61
6.2	Reaction Wheel Jitter Comparison Using a Fixed-Axis Rotation Scenario	64
6.3	Spacecraft with N Imbalanced VSCMGs	66
7	Conclusions	73

Bibliography	75
---------------------	-----------

Appendix

A	Basilisk Software Architecture	78
A.1	Basilisk Overview	78
A.2	Basilisk Dynamics Architecture	82
A.3	Visualization	83
B	Additional Back-Substitution Derivations	85
B.1	Back-Substitution Derivations	85
B.1.1	Balanced Reaction Wheel Back-Substitution	85
B.1.2	Imbalanced Reaction Wheel Back-Substitution	87
B.1.3	Balanced VSCMG Back-Substitution	90

Tables

Table

6.1	: Simulation parameters for the fully-coupled model. Note that wheel parameters apply to all wheels unless otherwise specified.	62
6.2	: Simulation parameters for the fully-coupled model. Note that wheel parameters apply to all wheels unless otherwise specified.	67

Figures

Figure

1.1	Various types of reaction wheels.	3
1.2	A control moment gyro used on the BETTII mission at NASA Goddard Space Flight Center.	4
1.3	An astronaut handles one of the International Space Station's 275 kg control moment gyros.	5
1.4	Diagram from Häussermann's patent of a spherical reaction wheel. One of the earliest conceptions of a momentum exchange device.	6
1.5	An example of the jitter smearing effect on imagery taken from space.	7
1.6	Reaction wheel static and dynamic imbalance.	8
2.1	Reference frame setup and variable definitions for the spacecraft + RW problem. . .	14
3.1	Reference frame setup and variable definitions for the spacecraft + VSCMG problem.	26
6.1	Attitude, principle angle, and body rates of spacecraft	64
6.2	Position and velocity of the spacecraft	65
6.3	Wheel angle, wheel speed, and motor torque of RWs	65
6.4	Change in energy and momentum of the spacecraft	65
6.5	Comparison of results for the fully-coupled and simplified models with $N = 1$	66
6.6	Attitude and body rates of the spacecraft	69
6.7	Principle angle and jitter of the spacecraft	69

6.8	Position and velocity of the spacecraft	69
6.9	Wheel speed and gimbal rate of the VSCMGs	70
6.10	Wheel torque and gimbal torque of the VSCMGs	70
6.11	Change in energy and angular momentum of the system	70
6.12	Energy rate and energy rate error of the system	71
A.1	The Basilisk logo.	79
A.2	Basilisk simulation and FSW architecture	80
A.3	Basilisk message passing interface	81
A.4	Basilisk visualization example of a Mars orbiting spacecraft.	84

Chapter 1

Introduction

1.1 Background

Momentum exchange devices (MEDs) are a fundamental component of most spacecraft. Used primarily for attitude reconfiguration and pointing, MEDs trade angular momentum with the body of a spacecraft using spinning flywheels. MEDs are an attractive device for attitude control since they do not consume fuel as thrusters do, and are typically capable of achieving significantly greater pointing precision than other actuators.[1] Examples of important uses for MEDs include pointing a spacecraft's solar panels towards the sun, pointing an instrument toward a target, and reorienting a spacecraft to perform a thrust maneuver.

Reaction wheels (RWs), a very popular device due to their mechanical simplicity and associated lower cost, consist of a flywheel attached to a motor and bearing. Figure 1.1 shows examples of various types reaction wheels. Spacecraft of all purposes and sizes, from CubeSats to Hubble, use RWs for attitude control. RWs trade angular momentum with a spacecraft solely by changing the speed of rotation of the flywheel. Other than spinning about a single body-fixed spin axis, the flywheel is fixed with respect to the spacecraft and does not change orientation. When a torque is applied using an electric motor, the flywheel experiences angular acceleration. Due to conservation of angular momentum, the rotational analog of Newton's third law of motion, the total angular momentum of the spacecraft and reaction wheel must remain constant. Thus, the spacecraft counter-rotates and its attitude is changed. Euler's equation is the fundamental equation governing the motion of a spacecraft and the MED system, and relates torque to the time derivative of

angular momentum. This equation is,

$$\mathbf{L} = \frac{N_d}{dt} \mathbf{H} \quad (1.1)$$

where \mathbf{L} is torque and \mathbf{H} is angular momentum. This equation is the main building block of the derivations presented within this thesis. Spacecraft typically have three or more reaction wheels dedicated to attitude control. This enables a full solution to the attitude control problem, since a single reaction wheel can only rotate the spacecraft about one axis. When three reaction wheels are used, it is advantageous to position them so that the three flywheel spin axes are mutually orthogonal. In this case, torquing a reaction wheel does not directly effect the spacecraft's motion about the other two axes. Many spacecraft have more than three reaction wheels in order to create a redundant attitude control solution or achieve larger control torques. This may be achieved by placing the reaction wheels in a "pyramid" or tetrahedral orientation, in which the reaction wheels work together to produce a net torque on the spacecraft. Utilizing more than three RWs also has the added benefit of maintaining a 3D attitude solution in the case that one reaction wheel fails, which is actually not uncommon.[2] RWs typically require "desaturation" due to momentum buildup from external sources, such as drag, magnetic torquing, and gravity gradient torquing. An external torque may increase the speed of the reaction wheel until it reaches its limit, at which point loss of control and system brownout are of concern. Thus, particular attention must be paid to controlling wheel speeds. Desaturation may be achieved using thrusters or, in the case of an earth orbiting spacecraft, magnetic torque rods. In certain cases, spacecraft may also dissipate angular momentum stored within the reaction wheels by assuming an orientation which allows an external torque to lower the wheels speeds. In addition to saturation, high wheel speeds are undesirable because they can cause the spacecraft to become dynamically "stiff" and require relatively large torques to perform a maneuver due to the presence of gyroscopic torques caused by the spinning reaction wheels. Numerous missions have employed reaction wheels for attitude control since the dawn of spaceflight.

Control moment gyroscopes (CMGs) are a popular method to control larger spacecraft. A



(a) A reaction wheel manufactured by Honeywell.



(b) A reaction wheel manufactured by Clyde Space showing the sealed casing, rotor, and motor/supporting electronics.



(c) A micro reaction wheel specifically for CubeSats manufactured by Blue Canyon Technologies.

Figure 1.1: Various types of reaction wheels.



Figure 1.2: A control moment gyro used on the BETTII mission at NASA Goddard Space Flight Center.

CMG, like a RW, trades angular momentum with the spacecraft body using a flywheel. However, instead of changing the rate of rotation of the flywheel like a RW, a CMG changes the direction of the spin axis of the flywheel and keeps wheel speed near constant. The axis about which the CMG rotates the flywheel is called the gimbal axis. Thus, a CMG must have dedicated electric motors for the flywheel and gimbal. CMGs have multiple benefits over reaction wheels. CMGs are typically more power efficient because they only require a torque on the gimbal axis to actuate. The wheel motor must simply maintain a constant wheel speed after the initial spin up of the wheel. Thus, CMGs are particularly good at delivering large torques very quickly. However, a minimum of three CMGs are required for a full 3D control solution, and a cluster of CMGs can encounter singularities which prevent torque about certain axes and can lead to loss of control. Furthermore, some CMGs are limited in the range that they can gimbal. This is usually due to hard stops on the motor or to prevent cables from becoming twisted (see Figure 1.2). CMGs are much more complex than reaction wheels and typically more expensive. Dual-gimbal control moment gyros (DGCMGs), CMGs containing two gimbal axes, have been leveraged as an actuator that can provide any torque vector. However, the additional complexity and cost of such a device often outweighs the benefits. Prominent examples of CMGs being used in flight include Skylab and the International Space Station (see Figure 1.3).

Several futuristic MEDs have been proposed. Of these, variable-speed control moment gyro-

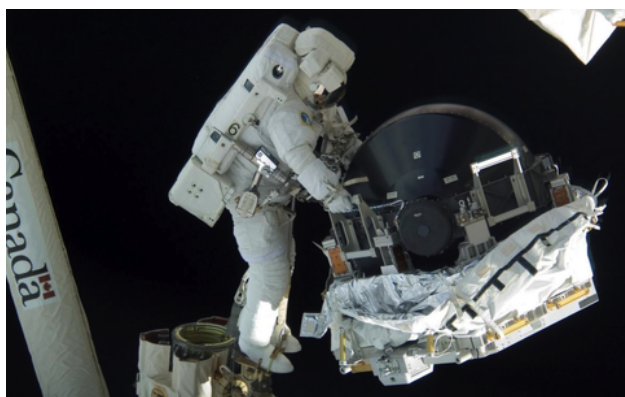


Figure 1.3: An astronaut handles one of the International Space Station's 275 kg control moment gyros.

scopes (VSCMGs) have gathered significant academic interest due to having properties of both RWs and CMGs. By nature, a CMG and VSCMG are fundamentally the same device. Unlike CMGs, VSCMGs leverage the additional degree of freedom in the rate of rotation of the flywheel. Cleverly devised control strategies allow the VSCMG to maneuver to avoid singularities by combining wheel speed changes and gimbal rates. "Null-motion" reconfiguration allows a cluster of VSCMGs to reconfigure without applying a net torque to the spacecraft hub.[3] Dual-gimbal variable-speed control moment gyroscopes (DGVSCMGs) are an attractive attitude actuator due to their ability to generate any 3D torque. DGVSCMGs have also been proposed as dual-function devices for both attitude control and energy storage in place of chemical batteries.[4] This concept is called integrated power/attitude control system (IPACS). Other futuristic MEDs include spherical reaction wheels[5], which were originally proposed at the dawn of the space era by German engineer Walter Häussermann in support of the Apollo program[6] (see Figure 1.4). Such devices pose high risk to space missions due to their additional complexity and are mainly academic.

1.2 Motivation

A problem with using MEDs for attitude control is that they usually cause vibration or "jitter" due to mass imbalances in the flywheels.[7, 8, 1] Characterization and mitigation of MED induced jitter on a spacecraft is of interest to many missions due to increasingly rigorous attitude

Jan. 23, 1962 W. HAEUSSERMANN 3,017,777
 SPACE VEHICLE ATTITUDE CONTROL MECHANISM
 Filed Oct. 14, 1960 4 Sheets-Sheet 1

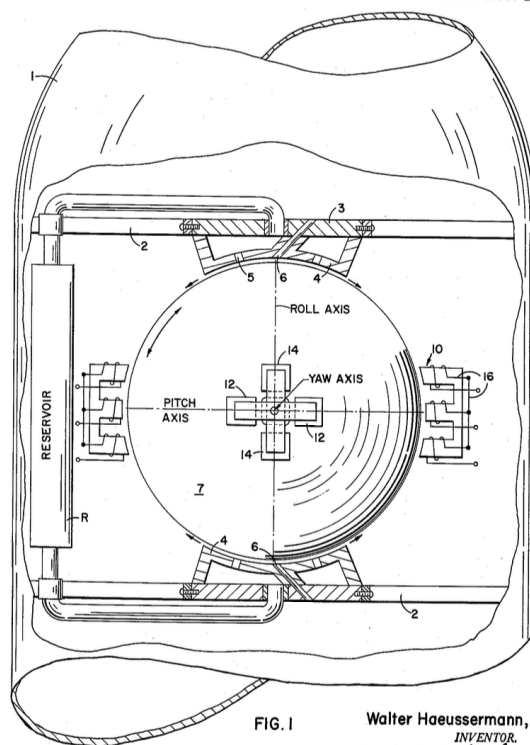


FIG. 1

Walter Haeussermann,
 INVENTOR,
 S. J. Rotondi,
 BY A. T. Dupont,
 and
 Alvin E. Moore,
 ATTORNEYS

Figure 1.4: Diagram from Häussermann's patent of a spherical reaction wheel. One of the earliest conceptions of a momentum exchange device.

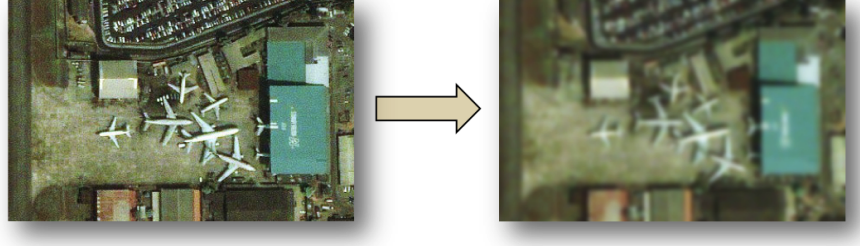


Figure 1.5: An example of the jitter smearing effect on imagery taken from space.

stability requirements and the necessity of avoiding excitation of the spacecraft's structural modes. Many instruments require the spacecraft to be held extremely still in order to effectively operate or collect data. Figure 1.5 illustrates the necessity of this. Optical instruments in particular often require attitude stability of less than one arcsecond per second in order to avoid optical smear or similar effects.[9, 10] Additionally, excessive vibration of a spacecraft may be detrimental to its instruments and operation.

Mass imbalances are inherent within the manufacturing process of flywheels. There are two primary types of mass imbalance: static imbalance and dynamic imbalance. Figure 1.6 demonstrates the difference between these within the context of a wheel. In this figure, \hat{g}_s represents the spin axis of the wheel and I_p represents a principle axis of inertia of the wheel. Static imbalance is caused by an offset in the center of mass of the wheel from the spin axis of the wheel. As the wheel rotates, the static imbalance effectively causes a force orthogonal to the spin axis of the wheel. Fundamentally, this motion is governed by the equation

$$\mathbf{F}_s = md\Omega^2\hat{u} \quad (1.2)$$

where \mathbf{F}_s is the force resulting from the imbalanced spinning wheel, Ω is the spin rate of the wheel, d is the offset of the wheel spin axis from the center of mass, m is the mass of the wheel, and \hat{u} is a unit vector pointing from the spin axis to the center of mass. This equation is essentially the force resulting from a centripetal acceleration, but it must be noted that when attached to a spacecraft, this must be treated as an *internal* force, rather than an external disturbance. Because static imbalance acts as a force, if the wheel is not located near the center of mass of the spacecraft

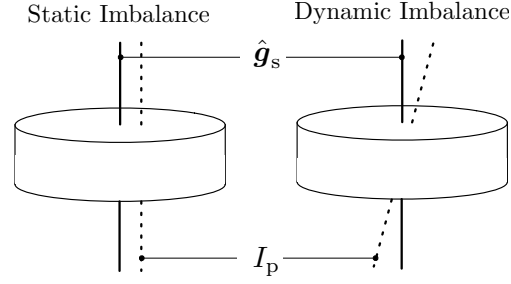


Figure 1.6: Reaction wheel static and dynamic imbalance.

it will cause an additional disturbance torque. Dynamic imbalance is caused by the spin axis of the wheel not being a principle axis of inertia, as shown in Figure 1.6. Spinning a dynamically imbalanced wheel causes a wobbling effect. The equation governing the motion of a dynamically imbalanced wheel is

$$\mathbf{L}_d = J\Omega^2\hat{\mathbf{v}} \quad (1.3)$$

where \mathbf{L}_d is the torque resulting from the imbalance, J is the magnitude of the off-diagonal inertia, and $\hat{\mathbf{v}}$ is a unit vector pointing in the direction of the mass imbalance. Again, when attached to a spacecraft, dynamic imbalance acts as an internal torque, and the total angular momentum of the system must remain constant without an external disturbance present. Note that in Eq. (1.2) and Eq. (1.3) the magnitude of the force/torque is proportional to wheel speed squared, which may be problematic for MEDs that operate at large wheel speeds. Since it is of interest to spacecraft manufacturers to reduce mass imbalance as much as possible, MED flywheels are often put through a “fine balancing” process to minimize the center of mass offset and off-diagonal inertia component. This process involves identify the location of the imbalances by spinning the wheel and measuring the phase and amplitude of jitter using load cells.[11] This process can be time consuming and expensive, and does not completely remove the imbalance. Various methods of vibration isolation have been proposed, including magnetic suspension of RWs as a means of circumventing the jitter problem.[12, 13, 14]

1.3 Literature Review

MED induced vibration on a spacecraft is usually characterized through experimentation prior to flight in order to validate requirements. Empirical models of MEDs allow imbalance parameters to be extracted.[15, 16] In addition to experimental demonstration of MED performance on an integrated spacecraft, it is of interest to use an analytic model of a MED for simulation in the early stages of spacecraft development. A simplified model of MED jitter involves including the forces (Eq. (1.2)) and torques (Eq. (1.3)) resulting from MED imbalance as external disturbances.[8, 17, 18, 19] This model is well established and is attractive due to its non-computationally expensive formulation – force and torque of jitter are simply proportional to wheel speed squared. Furthermore, the simplified formulation allows a model to be constructed directly from the typical MED manufacturer imbalance specifications: static imbalance and dynamic imbalance. This allows MED mass imbalances to be implemented as lumped parameters instead of using specific terms such as MED center of mass location and inertia tensor.[8] Previous literature puts emphasis on empirical modeling of MED jitter and the effects of MED jitter within context of spacecraft flexible dynamics.[20, 21, 22] Zhang and Zhang discuss a fully-coupled model of control moment gyro (CMG) imbalance[23], but present the results without a full derivation and fail to provide the complete system equations of motion. Furthermore, to the authors' knowledge there has been no direct method of implementing manufacturers' imbalance specifications directly in a fully-coupled model of a reaction wheel.

The simplified “lumped parameter” method of modeling MED jitter is not physically realistic due to the nonconservative nature of adding a system-internal forcing effect as an external disturbance.[24] Since angular momentum is not conserved in this model, a time varying bias in angular velocity is observed. The magnitude of the bias is dependent on the relative magnitude of the spacecraft inertia versus the reaction wheel imbalance and the wheel speed. For analysis purposes this does not necessarily present a problem. The overall effect of the angular velocity bias is quite small for spacecraft that have small wheel imbalance to spacecraft inertia ratios. The

amplitude of MED induced jitter may be computed by subtracting a polynomial fit of appropriate order from the resulting angular velocity. For spacecraft with poorly balanced reaction wheels or small wheel mass/imbalance to spacecraft inertia ratios this approach may become problematic. Additionally, the simplified model does not allow for energy and momentum checks. For a simulation that only includes MED jitter, validation of the model would not be too cumbersome because of the simplicity of the model. However, if the model of spacecraft has other complex behavior such as solar panel flexing or fuel slosh, the importance of energy and momentum validation increases dramatically. The coupled nature of these complex spacecraft systems results in extreme difficulty with debugging and validation. The energy and momentum checks become essential in this process. Furthermore, more complicated momentum exchange devices such as variable-speed control moment gyros (VSCMGs) violate conservation of momentum more so than a MED without using a fully-coupled model due simply to the additional complexity of a gimble axis.

1.4 Research Scope

This primary goal of this thesis is to present a general method of deriving the equations of motion (EOMs) for a spacecraft containing N MEDs with imbalanced flywheels. The derivations are shown for both RWs and VSCMGs. Naturally, the equations of motion governing a VSCMG apply to a CMG as well. The derivations take a classical mechanics approach, rather than generalized coordinates. Both derivations treat the jitter disturbances as true mass imbalances rather than external disturbances forces and torques, and thus represents the true physics governing this fully coupled phenomenon. Static imbalance takes the form of a center of mass offset from the spin axis of the wheel, and dynamic imbalance takes the form of off-diagonal elements within the wheel's inertia tensor. As a result, energy and momentum validation tools are available using these models due to the fact that the models obey conservation of angular momentum. A Newtonian/Eulerian formulation approach is employed within both derivations. Since the spacecraft hub is considered to be rigid, flexible dynamics are not considered. However, the formulation is developed in such a way that adding other modes such as flexing and fuel slosh is relatively simple.[25, 26] Another key

aspect of this thesis is the ability to take manufacturers specifications characterizing RW imbalances and convert them to the parameters introduced in this new derivation. A discussion is included on this important conversion.

In summary, the goals of the research presented are:

- (1) Derive from basic principles the translational, rotational, and motor torque equations for reaction wheels and variable-speed control moment gyroscopes.
- (2) Present a method of implementing standard manufacturer imbalance specifications within the models developed.
- (3) Demonstrate a software-friendly method of solving the equations of motion for each model.
- (4) Use energy and angular momentum validation checks to demonstrate the validity of the derived equations of motion
- (5) Demonstrate the validity of the software implementation method by comparing the results of VSCMG EOMs from two independent software implementations.
- (6) Present numerical simulation results of each model and make recommendations for appropriate use of each fully-coupled model versus the simplified wheel jitter model.

The logic behind presenting the RW EOMs and VSCMG EOMs separately is to introduce the reader to the methodology of the derivation before involving the added complexity of a gimbal axis. Naturally, the EOMs of an imbalanced RW could easily be obtained from the imbalanced VSCMG equations by simply zeroing out gimbal related terms. However, it is the author's opinion that there is value in presenting them separately if only because the majority of readers will likely be most interested in the RW derivation.

A goal of the research presented within this thesis was to validate the EOMs and software implementation using with energy and angular momentum results from two completely independent software suites. This level of validation shows that the EOMs and software implementation

method are correct beyond doubt. Implementations of the fully-coupled RW and VSCMG models derived within this thesis will be released open-source in 2017 as part of the Basilisk astrodynamics software.¹

¹ <http://hanspeterschaub.info/bskMain.html>

Chapter 2

Imbalanced Reaction Wheel

2.1 Problem Statement

When deriving the equations of motion (EOMs) for a spacecraft with N MEDs, an important assumption is made in that the MEDs are symmetric and results in the EOMs to be simplified to a convenient and compact form.[24] However, if the MEDs are imbalanced the EOMs have to be rederived to account for the fully-coupled dynamics between the MEDs and the spacecraft. This derivation follows a development path using Newtonian and Eulerian mechanics using a formulation that uses a minimal coordinate description.[24]

2.1.1 Reference Frame Definitions

Figure 2.1 shows the frame and variable definitions used for the imbalanced RW problem. The formulation involves a rigid hub with its center of mass location labeled as point B_c , and N RWs with their center of mass locations labeled as W_{c_i} . The frames being used for this formulation are the body frame, $\mathcal{B} : \{\hat{\mathbf{b}}_1, \hat{\mathbf{b}}_2, \hat{\mathbf{b}}_3\}$, the motor frame of the i^{th} RW, $\mathcal{M}_i : \{\hat{\mathbf{m}}_{s_i}, \hat{\mathbf{m}}_{2_i}, \hat{\mathbf{m}}_{3_i}\}$, and the wheel frame of the i^{th} RW, $\mathcal{W}_i : \{\hat{\mathbf{g}}_{s_i}, \hat{\mathbf{w}}_{2_i}, \hat{\mathbf{w}}_{3_i}\}$. The dynamics are modeled with respect to the \mathcal{B} frame which can be oriented in any direction. The \mathcal{W}_i frame is oriented such that the $\hat{\mathbf{g}}_{s_i}$ axis is aligned with the spin axis of the RW, the $\hat{\mathbf{w}}_{2_i}$ axis is perpendicular to $\hat{\mathbf{g}}_{s_i}$ and points in the direction towards W_{c_i} . The $\hat{\mathbf{w}}_{3_i}$ completes the right hand rule. The \mathcal{M}_i frame is defined as being equal to the \mathcal{W}_i frame at the beginning of the simulation and therefore the \mathcal{W}_i and \mathcal{M}_i frames are offset by an angle, θ_i , about the $\hat{\mathbf{m}}_{s_i} = \hat{\mathbf{g}}_{s_i}$ axes. These are the necessary frame and variable

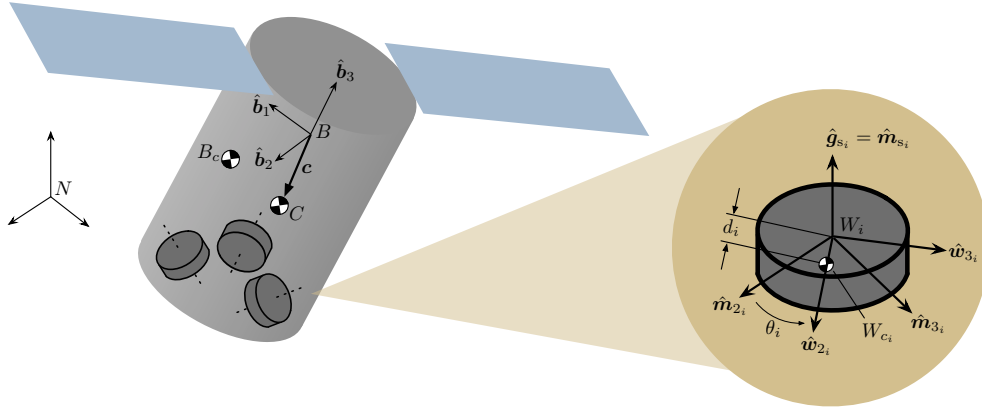


Figure 2.1: Reference frame setup and variable definitions for the spacecraft + RW problem.

definitions needed for this formulation.

2.1.2 Variable Definitions

A few more key variables in Figure 2.1 need to be defined. Point B is the origin of the \mathcal{B} frame and is a general body-fixed point that does not have to be identical to the spacecraft center of mass. Point W_i is the origin of the \mathcal{W}_i frame and can also have any location relative to point B . Point C is the center of mass of the spacecraft including the RWs and vector \mathbf{c} points from point B to point C . Variable d_i is the center of mass offset of the RW, or the distance from the spin axis, $\hat{\mathbf{g}}_{s_i}$ to W_{c_i} . These variable and frame definitions are leveraged throughout the paper to derive the EOMs.

2.2 Equations of Motion

The system under consideration is an $N+6$ degrees-of-freedom (DOF) system with the following second order terms: inertial acceleration $\ddot{\mathbf{r}}_{B/N}$, angular acceleration $\dot{\boldsymbol{\omega}}_{B/N}$, and the acceleration of each RW $\dot{\Omega}_1, \dots, \dot{\Omega}_N$. Thus, a total of $N+6$ equations must be developed in order to solve for all second order terms. Section 2.2.1 describes the derivation of the translational EOM and represents 3 DOF, section 2.2.2 describes the rotational motion and represents 3 DOF, and section 2.2.3

describes the motor torque equation and represents N DOF.

2.2.1 Translational Motion

For the dynamical system considered, the center of mass of the spacecraft is not constant with respect to the body frame. This results in the necessity to track the center of mass of the spacecraft and its corresponding acceleration. Following a similar derivation as seen in Reference [25], the derivation begins with Newton's second law of motion for the center of mass of the spacecraft seen in Eq. (2.1).

$$\ddot{\mathbf{r}}_{C/N} = \frac{\mathbf{F}}{m_{sc}} \quad (2.1)$$

\mathbf{F} is the sum of the external forces on the spacecraft which has a mass labeled as m_{sc} . The notation being used for this work can be seen in Reference [24]. For example, the vector $\mathbf{v}_{B/A}$ is a vector that points from point A to B . The inertial time derivative of $\mathbf{v}_{B/A}$ is denoted by $\dot{\mathbf{v}}_{B/A}$ and the time derivative taken with respect to the body frame is $\mathbf{v}'_{B/A}$.

Ultimately the acceleration of the body frame or point B is desired, which is expressed through

$$\ddot{\mathbf{r}}_{B/N} = \ddot{\mathbf{r}}_{C/N} - \ddot{\mathbf{c}} \quad (2.2)$$

where the center of mass equation is rewritten to yield

$$\mathbf{c} = \frac{1}{m_{sc}} (m_B \mathbf{r}_{B_c/B} + \sum_{i=1}^N m_{W_i} \mathbf{r}_{W_{c_i}/B}) \quad (2.3)$$

Taking the first and second body frame time derivatives of point \mathbf{c} results in

$$\mathbf{c}' = \frac{1}{m_{sc}} \sum_{i=1}^N m_{W_i} \mathbf{r}'_{W_{c_i}/B} \quad (2.4)$$

$$\mathbf{c}'' = \frac{1}{m_{sc}} \sum_{i=1}^N m_{W_i} \mathbf{r}''_{W_{c_i}/B} \quad (2.5)$$

Taking the first and second body frame time derivatives of $\mathbf{r}_{W_{c_i}/B}$ results in

$$\mathbf{r}_{W_{c_i}/B} = \mathbf{r}_{W_i/B} + \mathbf{r}_{W_{c_i}/W_i} = \mathbf{r}_{W_i/B} + d_i \hat{\mathbf{w}}_{2_i} \quad (2.6)$$

$$\mathbf{r}'_{W_{c_i}/B} = d \hat{\mathbf{w}}'_{2_i} = \boldsymbol{\omega}_{W_i/B} \times d_i \mathbf{w}_{2_i} = \Omega_i \hat{\mathbf{g}}_{s_i} \times d_i \mathbf{w}_{2_i} = d_i \Omega_i \hat{\mathbf{w}}_{3_i} \quad (2.7)$$

$$\mathbf{r}''_{W_{c_i}/B} = \Omega_i \hat{\mathbf{g}}_{s_i} \times d_i \Omega_i \hat{\mathbf{w}}_{3_i} = d_i \dot{\Omega}_i \hat{\mathbf{w}}_{3_i} - d_i \Omega_i^2 \hat{\mathbf{w}}_{2_i} \quad (2.8)$$

Using the transport theorem [24] the inertial and body-relative time derivatives of \mathbf{c} are related through

$$\ddot{\mathbf{c}} = \mathbf{c}'' + 2\boldsymbol{\omega}_{B/N} \times \mathbf{c}' + \dot{\boldsymbol{\omega}}_{B/N} \times \mathbf{c} + \boldsymbol{\omega}_{B/N} \times (\boldsymbol{\omega}_{B/N} \times \mathbf{c}) \quad (2.9)$$

Substituting Eq. (2.8) and (2.9) into Eq. (3.6) and grouping second order terms on the left-hand side yields the translational equation of motion.

$$\ddot{\mathbf{r}}_{B/N} - [\tilde{\mathbf{c}}] \dot{\boldsymbol{\omega}}_{B/N} + \frac{1}{m_{sc}} \sum_{i=1}^N m_{W_i} d_i \hat{\mathbf{w}}_{3_i} \dot{\Omega}_i = \ddot{\mathbf{r}}_{C/N} - 2[\tilde{\boldsymbol{\omega}}_{B/N}] \mathbf{c}' - [\tilde{\boldsymbol{\omega}}_{B/N}] [\tilde{\boldsymbol{\omega}}_{B/N}] \mathbf{c} + \frac{1}{m_{sc}} \sum_{i=1}^N m_{W_i} d_i \Omega_i^2 \hat{\mathbf{w}}_{2_i} \quad (2.10)$$

Equation (2.10) shows that the translational acceleration, $\ddot{\mathbf{r}}_{B/N}$, is coupled with the rotational acceleration, $\dot{\boldsymbol{\omega}}_{B/N}$, and the wheel accelerations, $\dot{\Omega}_i$. This is a result of the fact that the reaction wheels are imbalanced and therefore change the center of mass location of the spacecraft.[24]

2.2.2 Rotational Motion

The rotational motion equation of the spacecraft also needs to be modified. This derivation starts with the angular momentum of the spacecraft about point B :

$$\mathbf{H}_{sc,B} = \mathbf{H}_{B,B} + \sum_{i=1}^N \mathbf{H}_{W_i,B} \quad (2.11)$$

The EOM for the rotational motion is found using the definition of the inertial time derivative of angular momentum when the body fixed coordinate frame origin is not coincident with the center of mass of the body.[24]

$$\dot{\mathbf{H}}_{sc,B} = \mathbf{L}_B + m_{sc} \ddot{\mathbf{r}}_{B/N} \times \mathbf{c} \quad (2.12)$$

The inertial derivative of the spacecraft angular momentum is expressed as

$$\dot{\mathbf{H}}_{sc,B} = \dot{\mathbf{H}}_{B,B} + \sum_{i=1}^N \dot{\mathbf{H}}_{W_i,B} \quad (2.13)$$

Thus, in order to use Eq. (3.28), each derivative on the right-hand side of Eq. (3.29) needs to be evaluated. The equation for finding the angular momentum about a point not coincident with the center of mass of that object [24] is utilized and the following definitions are found

$$\mathbf{H}_{B,B} = \mathbf{H}_{B,B_c} + m_B \mathbf{r}_{B_c/B} \times \dot{\mathbf{r}}_{B_c/B} \quad (2.14)$$

$$\mathbf{H}_{W_i,B} = \mathbf{H}_{W_i,W_{c_i}} + m_{W_i} \mathbf{r}_{W_{c_i}/B} \times \dot{\mathbf{r}}_{W_{c_i}/B} \quad (2.15)$$

where the angular momentum of the hub and reaction wheel about their respective center of masses are

$$\mathbf{H}_{B,B_c} = [I_{B,B_c}] \boldsymbol{\omega}_{B/N} \quad (2.16)$$

$$\mathbf{H}_{W_i,W_{c_i}} = [I_{W_i,W_{c_i}}] \boldsymbol{\omega}_{W_i/N} = [I_{W_i,W_{c_i}}] (\boldsymbol{\omega}_{B/N} + \Omega_i \hat{\mathbf{g}}_{s_i}) \quad (2.17)$$

Taking the inertial time derivative of hub's angular momentum yields

$$\dot{\mathbf{H}}_{B,B} = [I_{B,B_c}] \dot{\boldsymbol{\omega}}_{B/N} + \boldsymbol{\omega}_{B/N} \times [I_{B,B_c}] \boldsymbol{\omega}_{B/N} + m_B \mathbf{r}_{B_c/B} \times \ddot{\mathbf{r}}_{B_c/B} \quad (2.18)$$

and knowing that $\mathbf{r}_{B_c/B}$ is fixed with respect to the body the following are defined

$$\dot{\mathbf{r}}_{B_c/B} = \mathbf{r}'_{B_c/B} + \boldsymbol{\omega}_{B/N} \times \mathbf{r}_{B_c/B} = \boldsymbol{\omega}_{B/N} \times \mathbf{r}_{B_c/B} \quad (2.19)$$

$$\ddot{\mathbf{r}}_{B_c/B} = \dot{\boldsymbol{\omega}}_{B/N} \times \mathbf{r}_{B_c/B} + \boldsymbol{\omega}_{B/N} \times (\boldsymbol{\omega}_{B/N} \times \mathbf{r}_{B_c/B}) \quad (2.20)$$

Substitute Eq. (3.34) into Eq. (3.32) yields

$$\begin{aligned} \dot{\mathbf{H}}_{B,B} &= [I_{B,B_c}] \dot{\boldsymbol{\omega}}_{B/N} + \boldsymbol{\omega}_{B/N} \times [I_{B,B_c}] \boldsymbol{\omega}_{B/N} \\ &\quad + m_B \mathbf{r}_{B_c/B} \times (\dot{\boldsymbol{\omega}}_{B/N} \times \mathbf{r}_{B_c/B}) + m_B \mathbf{r}_{B_c/B} \times (\boldsymbol{\omega}_{B/N} \times (\boldsymbol{\omega}_{B/N} \times \mathbf{r}_{B_c/B})) \end{aligned} \quad (2.21)$$

Employing the Jacobi triple-product identity, $\mathbf{a} \times (\mathbf{b} \times \mathbf{c}) = (\mathbf{a} \times \mathbf{b}) \times \mathbf{c} + \mathbf{b} \times (\mathbf{a} \times \mathbf{c})$, on the right-hand side of Eq. (3.35) and using the parallel axis theorem $[I_{B,B}] = [I_{B,B_c}] + m_B [\tilde{\mathbf{r}}_{B_c/B}] [\tilde{\mathbf{r}}_{B_c/B}]^T$, the hub angular momentum derivative is finally written after extensive algebra as

$$\begin{aligned} \dot{\mathbf{H}}_{B,B} &= [I_{B,B_c}] \dot{\boldsymbol{\omega}}_{B/N} + [\tilde{\boldsymbol{\omega}}_{B/N}] [I_{B,B_c}] \boldsymbol{\omega}_{B/N} \\ &\quad + m_B [\tilde{\mathbf{r}}_{B_c/B}] [\tilde{\mathbf{r}}_{B_c/B}]^T \dot{\boldsymbol{\omega}}_{B/N} + m_B [\tilde{\boldsymbol{\omega}}_{B/N}] [\tilde{\mathbf{r}}_{B_c/B}] [\tilde{\mathbf{r}}_{B_c/B}]^T \boldsymbol{\omega}_{B/N} \\ &= [I_{B,B}] \dot{\boldsymbol{\omega}}_{B/N} + [\tilde{\boldsymbol{\omega}}_{B/N}] [I_{B,B}] \boldsymbol{\omega}_{B/N} \end{aligned} \quad (2.22)$$

Following an equivalent derivation procedure, the inertial time derivative of reaction wheel angular momentum about point B is

$$\begin{aligned} \dot{\mathbf{H}}_{W_i,B} = & [I_{W_i,W_{c_i}}]'(\boldsymbol{\omega}_{B/N} + \Omega_i \hat{\mathbf{g}}_{s_i}) + [I_{W_i,W_{c_i}}](\dot{\boldsymbol{\omega}}_{B/N} + \dot{\Omega}_i \hat{\mathbf{g}}_{s_i}) + \boldsymbol{\omega}_{B/N} \times [I_{W_i,W_{c_i}}](\boldsymbol{\omega}_{B/N} + \Omega_i \hat{\mathbf{g}}_{s_i}) \\ & + m_{W_i} \mathbf{r}_{W_{c_i}/B} \times \ddot{\mathbf{r}}_{W_{c_i}/B} \end{aligned} \quad (2.23)$$

The body relative inertia tensor time derivative $[I_{W_i,W_{c_i}}]'$ needs to be defined. For this general RW model, the inertia matrix of the RW in the \mathcal{W}_i frame is defined as

$$[I_{W_i/W_{c_i}}] = {}^{\mathcal{W}_i} \begin{bmatrix} J_{11_i} & J_{12_i} & J_{13_i} \\ J_{12_i} & J_{22_i} & J_{23_i} \\ J_{13_i} & J_{23_i} & J_{33_i} \end{bmatrix} \quad (2.24)$$

The definition of $[I_{W_i/W_{c_i}}]$ allows for any RW inertia matrix to be considered. Section 4 describes the characterization of the dynamic imbalance of the RW by defining parameters in $[I_{W_i/W_{c_i}}]$.

In order to take the body frame derivative of $[I_{W_i/W_{c_i}}]$, Eq. (3.62) is rewritten in a general form using outer product expansions.

$$\begin{aligned} [I_{W_i/W_{c_i}}] = & J_{11_i} \hat{\mathbf{g}}_{s_i} \hat{\mathbf{g}}_{s_i}^T + J_{12_i} \hat{\mathbf{g}}_{s_i} \hat{\mathbf{w}}_{2_i}^T + J_{13_i} \hat{\mathbf{g}}_{s_i} \hat{\mathbf{w}}_{3_i}^T \\ & + J_{12_i} \hat{\mathbf{w}}_{2_i} \hat{\mathbf{g}}_{s_i}^T + J_{22_i} \hat{\mathbf{w}}_{2_i} \hat{\mathbf{w}}_{2_i}^T + J_{23_i} \hat{\mathbf{w}}_{2_i} \hat{\mathbf{w}}_{3_i}^T \\ & + J_{13_i} \hat{\mathbf{w}}_{3_i} \hat{\mathbf{g}}_{s_i}^T + J_{23_i} \hat{\mathbf{w}}_{3_i} \hat{\mathbf{w}}_{2_i}^T + J_{33_i} \hat{\mathbf{w}}_{3_i} \hat{\mathbf{w}}_{3_i}^T \end{aligned} \quad (2.25)$$

The body frame derivatives of wheel frame basis vectors are

$$\hat{\mathbf{g}}'_{s_i} = \boldsymbol{\omega}_{\mathcal{W}_i/B} \times \hat{\mathbf{g}}_{s_i} = \Omega_i \hat{\mathbf{g}}_{s_i} \times \hat{\mathbf{g}}_{s_i} = \mathbf{0} \quad (2.26)$$

$$\hat{\mathbf{w}}'_{2_i} = \boldsymbol{\omega}_{\mathcal{W}_i/B} \times \hat{\mathbf{w}}_{2_i} = \Omega_i \hat{\mathbf{g}}_{s_i} \times \hat{\mathbf{w}}_{2_i} = \Omega_i \hat{\mathbf{w}}_{3_i} \quad (2.27)$$

$$\hat{\mathbf{w}}'_{3_i} = \boldsymbol{\omega}_{\mathcal{W}_i/B} \times \hat{\mathbf{w}}_{3_i} = \Omega_i \hat{\mathbf{g}}_{s_i} \times \hat{\mathbf{w}}_{3_i} = -\Omega_i \hat{\mathbf{w}}_{2_i} \quad (2.28)$$

Taking the body frame time derivative and using Eq. (2.26)-(2.28) to simplify yields

$$\begin{aligned}
[I_{W_i/W_{c_i}}]' &= J_{12_i} \Omega_i \hat{\mathbf{g}}_{s_i} \hat{\mathbf{w}}_{3_i}^T - J_{13_i} \Omega_i \hat{\mathbf{g}}_{s_i} \hat{\mathbf{w}}_{2_i}^T \\
&+ J_{12_i} \Omega_i \hat{\mathbf{w}}_{3_i} \hat{\mathbf{g}}_{s_i}^T + J_{22_i} \Omega_i \hat{\mathbf{w}}_{3_i} \hat{\mathbf{w}}_{2_i}^T + J_{22_i} \Omega_i \hat{\mathbf{w}}_{2_i} \hat{\mathbf{w}}_{3_i}^T + J_{23_i} \Omega_i \hat{\mathbf{w}}_{3_i} \hat{\mathbf{w}}_{3_i}^T - J_{23_i} \Omega_i \hat{\mathbf{w}}_{2_i} \hat{\mathbf{w}}_{2_i}^T \\
&- J_{13_i} \Omega_i \hat{\mathbf{w}}_{2_i} \hat{\mathbf{g}}_{s_i}^T - J_{23_i} \Omega_i \hat{\mathbf{w}}_{2_i} \hat{\mathbf{w}}_{2_i}^T + J_{23_i} \Omega_i \hat{\mathbf{w}}_{3_i} \hat{\mathbf{w}}_{3_i}^T - J_{33_i} \Omega_i \hat{\mathbf{w}}_{2_i} \hat{\mathbf{w}}_{3_i}^T - J_{33_i} \Omega_i \hat{\mathbf{w}}_{3_i} \hat{\mathbf{w}}_{2_i}^T
\end{aligned} \tag{2.29}$$

Eq. (2.29) is expressed in the wheel frame as

$$[I_{W_i/W_{c_i}}]' = \begin{matrix} \mathcal{W}_i \\ \left[\begin{array}{ccc} 0 & -J_{13_i} & J_{12_i} \\ -J_{13_i} & -2J_{23_i} & J_{22_i} - J_{33_i} \\ J_{12_i} & J_{22_i} - J_{33_i} & 2J_{23_i} \end{array} \right] \Omega_i \end{matrix} \tag{2.30}$$

The remaining term in Eq. (2.23) that needs to be defined is $\ddot{\mathbf{r}}_{W_{c_i}/B}$. Following its definition, the time derivatives are:

$$\mathbf{r}_{W_{c_i}/B} = \mathbf{r}_{W_i/B} + d_i \hat{\mathbf{w}}_{2_i} \tag{2.31}$$

$$\dot{\mathbf{r}}_{W_{c_i}/B} = \mathbf{r}'_{W_i/B} + d_i \hat{\mathbf{w}}'_{2_i} + \boldsymbol{\omega}_{B/N} \times (\mathbf{r}_{W_i/B} + d_i \hat{\mathbf{w}}_{2_i}) = d_i \Omega_i \hat{\mathbf{w}}_{3_i} + \boldsymbol{\omega}_{B/N} \times (\mathbf{r}_{W_i/B} + d_i \hat{\mathbf{w}}_{2_i}) \tag{2.32}$$

$$\ddot{\mathbf{r}}_{W_{c_i}/B} = d_i \dot{\Omega}_i \hat{\mathbf{w}}_{3_i} - d_i \Omega_i^2 \hat{\mathbf{w}}_{2_i} + \dot{\boldsymbol{\omega}}_{B/N} \times \mathbf{r}_{W_{c_i}/B} + 2\boldsymbol{\omega}_{B/N} \times d_i \Omega_i \hat{\mathbf{w}}_{3_i} + \boldsymbol{\omega}_{B/N} \times (\boldsymbol{\omega}_{B/N} \times \mathbf{r}_{W_{c_i}/B}) \tag{2.33}$$

Substituting Eq. (2.33) into Eq. (2.23) and applying the triple product identity and parallel axis theorem $[I_{W_i,B}] = [I_{W_i,W_{c_i}}] + m_{W_i} [\tilde{\mathbf{r}}_{W_{c_i}/B}] [\tilde{\mathbf{r}}_{W_{c_i}/B}]^T$ results in

$$\begin{aligned}
\dot{\mathbf{H}}_{W_i,B} &= [I_{W_i,B}]' \boldsymbol{\omega}_{B/N} + [I_{W_i,B}] \dot{\boldsymbol{\omega}}_{B/N} + [\tilde{\boldsymbol{\omega}}_{B/N}] [I_{W_i,B}] \boldsymbol{\omega}_{B/N} \\
&+ [I_{W_i,W_{c_i}}]' \Omega_i \hat{\mathbf{g}}_{s_i} + [I_{W_i,W_{c_i}}] \dot{\Omega}_i \hat{\mathbf{g}}_{s_i} + [\tilde{\boldsymbol{\omega}}_{B/N}] [I_{W_i,W_{c_i}}] \Omega_i \hat{\mathbf{g}}_{s_i} \\
&+ m_{W_i} \mathbf{r}_{W_{c_i}/B} \times (d_i \dot{\Omega}_i \hat{\mathbf{w}}_{3_i} - d_i \Omega_i^2 \hat{\mathbf{w}}_{2_i}) + m_{W_i} \boldsymbol{\omega}_{B/N} \times (\mathbf{r}_{W_{c_i}/B} \times \mathbf{r}'_{W_{c_i}/B})
\end{aligned} \tag{2.34}$$

Note that taking the body time derivative of the parallel axis theorem equation yields

$$[I_{W_i,B}]' = [I_{W_i,W_{c_i}}]' + m_{W_i} [\tilde{\mathbf{r}}'_{W_{c_i}/B}] [\tilde{\mathbf{r}}_{W_{c_i}/B}]^T + m_{W_i} [\tilde{\mathbf{r}}_{W_{c_i}/B}] [\tilde{\mathbf{r}}'_{W_{c_i}/B}]^T \tag{2.35}$$

Now the definition of the inertial time derivatives of the hub's angular momentum and reaction wheels' angular momentum, Eq. (2.22) and (2.34) respectively, are substituted into Eq. (3.29)

$$\begin{aligned}
\dot{\mathbf{H}}_{sc,B} = & [I_{B,B}] \dot{\boldsymbol{\omega}}_{B/N} + [\tilde{\boldsymbol{\omega}}_{B/N}] [I_{B,B}] \boldsymbol{\omega}_{B/N} + \sum_{i=1}^N \left[[I_{W_i,B}]' \boldsymbol{\omega}_{B/N} + [I_{W_i,B}] \dot{\boldsymbol{\omega}}_{B/N} + [\tilde{\boldsymbol{\omega}}_{B/N}] [I_{W_i,B}] \boldsymbol{\omega}_{B/N} \right. \\
& + [I_{W_i,W_{c_i}}]' \Omega_i \hat{\mathbf{g}}_{s_i} + [I_{W_i,W_{c_i}}] \dot{\Omega}_i \hat{\mathbf{g}}_{s_i} + [\tilde{\boldsymbol{\omega}}_{B/N}] [I_{W_i,W_{c_i}}] \Omega_i \hat{\mathbf{g}}_{s_i} \\
& \left. + m_{W_i} \mathbf{r}_{W_{c_i}/B} \times (d_i \dot{\Omega}_i \hat{\mathbf{w}}_{3_i} - d_i \Omega_i^2 \hat{\mathbf{w}}_{2_i}) + m_{W_i} \boldsymbol{\omega}_{B/N} \times (\mathbf{r}_{W_{c_i}/B} \times \mathbf{r}'_{W_{c_i}/B}) \right]
\end{aligned} \tag{2.36}$$

Noting that $[I_{sc,B}] = [I_{B,B}] + \sum_{i=1}^N [I_{W_i,B}]$, Eq. (2.36) is simplified to

$$\begin{aligned}
\dot{\mathbf{H}}_{sc,B} = & [I_{sc,B}] \dot{\boldsymbol{\omega}}_{B/N} + [\tilde{\boldsymbol{\omega}}_{B/N}] [I_{sc,B}] \boldsymbol{\omega}_{B/N} + [I_{sc,B}]' \boldsymbol{\omega}_{B/N} \\
& + \sum_{i=1}^N \left[[I_{W_i,W_{c_i}}]' \Omega_i \hat{\mathbf{g}}_{s_i} + [I_{W_i,W_{c_i}}] \dot{\Omega}_i \hat{\mathbf{g}}_{s_i} + [\tilde{\boldsymbol{\omega}}_{B/N}] \left([I_{W_i,W_{c_i}}] \Omega_i \hat{\mathbf{g}}_{s_i} + m_{W_i} [\tilde{\mathbf{r}}_{W_{c_i}/B}] \mathbf{r}'_{W_{c_i}/B} \right) \right. \\
& \left. + m_{W_i} [\tilde{\mathbf{r}}_{W_{c_i}/B}] (d_i \dot{\Omega}_i \hat{\mathbf{w}}_{3_i} - d_i \Omega_i^2 \hat{\mathbf{w}}_{2_i}) \right]
\end{aligned} \tag{2.37}$$

Eq. (2.37) is substituted into Eq. (3.28) to yield

$$\begin{aligned}
\mathbf{L}_B + m_{sc} \ddot{\mathbf{r}}_{B/N} \times \mathbf{c} = & [I_{sc,B}] \dot{\boldsymbol{\omega}}_{B/N} + [\tilde{\boldsymbol{\omega}}_{B/N}] [I_{sc,B}] \boldsymbol{\omega}_{B/N} + [I_{sc,B}]' \boldsymbol{\omega}_{B/N} \\
& + \sum_{i=1}^N \left[[I_{W_i,W_{c_i}}]' \Omega_i \hat{\mathbf{g}}_{s_i} + [I_{W_i,W_{c_i}}] \dot{\Omega}_i \hat{\mathbf{g}}_{s_i} + [\tilde{\boldsymbol{\omega}}_{B/N}] \left([I_{W_i,W_{c_i}}] \Omega_i \hat{\mathbf{g}}_{s_i} + m_{W_i} [\tilde{\mathbf{r}}_{W_{c_i}/B}] \mathbf{r}'_{W_{c_i}/B} \right) \right. \\
& \left. + m_{W_i} [\tilde{\mathbf{r}}_{W_{c_i}/B}] (d_i \dot{\Omega}_i \hat{\mathbf{w}}_{3_i} - d_i \Omega_i^2 \hat{\mathbf{w}}_{2_i}) \right]
\end{aligned} \tag{2.38}$$

Grouping second order terms on the left-hand side yields the rotational EOM.

$$\begin{aligned}
m_{sc} [\tilde{\mathbf{c}}] \ddot{\mathbf{r}}_{B/N} + [I_{sc,B}] \dot{\boldsymbol{\omega}}_{B/N} + \sum_{i=1}^N \left([I_{W_i,W_{c_i}}] \hat{\mathbf{g}}_{s_i} + m_{W_i} d_i [\tilde{\mathbf{r}}_{W_{c_i}/B}] \hat{\mathbf{w}}_{3_i} \right) \dot{\Omega}_i \\
= \sum_{i=1}^N \left[m_{W_i} [\tilde{\mathbf{r}}_{W_{c_i}/B}] d_i \Omega_i^2 \hat{\mathbf{w}}_{2_i} - [I_{W_i,W_{c_i}}]' \Omega_i \hat{\mathbf{g}}_{s_i} - [\tilde{\boldsymbol{\omega}}_{B/N}] \left([I_{W_i,W_{c_i}}] \Omega_i \hat{\mathbf{g}}_{s_i} + m_{W_i} [\tilde{\mathbf{r}}_{W_{c_i}/B}] \mathbf{r}'_{W_{c_i}/B} \right) \right] \\
- [\tilde{\boldsymbol{\omega}}_{B/N}] [I_{sc,B}] \boldsymbol{\omega}_{B/N} - [I_{sc,B}]' \boldsymbol{\omega}_{B/N} + \mathbf{L}_B
\end{aligned} \tag{2.39}$$

Eq. (2.39) shows that the rotational EOM is coupled with the other second order variables. Similar to the translational EOM, this coupling is due to the fact that the center of mass of the spacecraft is not coincident with point B . The motor torque equation is the remaining necessary EOM to describe the motion of the spacecraft and is defined in the following section.

2.2.3 Motor Torque Equation

The motor torque equation is used to relate body rate derivative $\dot{\boldsymbol{\omega}}_{\mathcal{B}/\mathcal{N}}$ and wheel speed derivative $\dot{\Omega}_i$. The motor torque u_{s_i} is the spin axis component of wheel torque about point W_i . The transverse torques acting on the wheel $\tau_{w_{2_i}}$ and $\tau_{w_{3_i}}$ are structural torques on the wheel and do not contribute to the motor torque equation.

$$\mathbf{L}_{W_i} = \begin{matrix} \mathcal{W}_i \\ \left[\begin{array}{c} u_{s_i} \\ \tau_{w_{2_i}} \\ \tau_{w_{3_i}} \end{array} \right] \end{matrix} \quad (2.40)$$

Torque about point W_i relates to torque about W_{c_i} by [24]

$$\mathbf{L}_{W_i} = \mathbf{L}_{W_{c_i}} + \mathbf{r}_{W_{c_i}/W_i} \times m_{W_i} \ddot{\mathbf{r}}_{W_{c_i}/N} \quad (2.41)$$

Euler's equation [24] applies as follows.

$$\mathbf{L}_{W_{c_i}} = \dot{\mathbf{H}}_{W_i, W_{c_i}} \quad (2.42)$$

The RW angular momentum about W_{c_i} is expressed as

$$\mathbf{H}_{W_i, W_{c_i}} = [I_{W_i, W_{c_i}}] \boldsymbol{\omega}_{W_i/N} = [I_{W_i, W_{c_i}}] (\boldsymbol{\omega}_{\mathcal{B}/\mathcal{N}} + \Omega_i \hat{\mathbf{g}}_{s_i}) \quad (2.43)$$

To aid in the simplification of the motor torque equation, $[I_{W_i, W_{c_i}}]$ is expressed as an outer product sum and distributed into Eq. (2.43).

$$\begin{aligned} \mathbf{H}_{W_i, W_{c_i}} = & J_{11_i} \hat{\mathbf{g}}_{s_i} (\omega_{s_i} + \Omega_i) + J_{12_i} \hat{\mathbf{g}}_{s_i} \omega_{w_{2_i}} + J_{13_i} \hat{\mathbf{g}}_{s_i} \omega_{w_{3_i}} \\ & + J_{12_i} \hat{\mathbf{w}}_{2_i} (\omega_{s_i} + \Omega_i) + J_{22_i} \hat{\mathbf{w}}_{2_i} \omega_{w_{2_i}} + J_{23_i} \hat{\mathbf{w}}_{2_i} \omega_{w_{3_i}} \\ & + J_{13_i} \hat{\mathbf{w}}_{3_i} (\omega_{s_i} + \Omega_i) + J_{23_i} \hat{\mathbf{w}}_{3_i} \omega_{w_{2_i}} + J_{33_i} \hat{\mathbf{w}}_{3_i} \omega_{w_{3_i}} \end{aligned} \quad (2.44)$$

Note that the \mathcal{W}_i frame components of $\boldsymbol{\omega}_{\mathcal{B}/\mathcal{N}}$ and their corresponding derivatives are defined as

$$\omega_{s_i} = \hat{\mathbf{g}}_{s_i}^T \boldsymbol{\omega}_{\mathcal{B}/\mathcal{N}} \quad (2.45)$$

$$\omega_{w_{2_i}} = \hat{\mathbf{w}}_{2_i}^T \boldsymbol{\omega}_{\mathcal{B}/\mathcal{N}} \quad (2.46)$$

$$\omega_{w_{3_i}} = \hat{\mathbf{w}}_{3_i}^T \boldsymbol{\omega}_{\mathcal{B}/\mathcal{N}} \quad (2.47)$$

$$\dot{\omega}_{s_i} = \hat{\mathbf{g}}_{s_i}^T \dot{\boldsymbol{\omega}}_{\mathcal{B}/\mathcal{N}} \quad (2.48)$$

$$\dot{\omega}_{w_{2_i}} = \hat{\mathbf{w}}_{2_i}^T \dot{\boldsymbol{\omega}}_{\mathcal{B}/\mathcal{N}} + \Omega_i \omega_{w_{3_i}} \quad (2.49)$$

$$\dot{\omega}_{w_{3_i}} = \hat{\mathbf{w}}_{3_i}^T \dot{\boldsymbol{\omega}}_{\mathcal{B}/\mathcal{N}} - \Omega_i \omega_{w_{2_i}} \quad (2.50)$$

Grouping like terms in Eq. (2.44) yields

$$\mathbf{H}_{W_i, W_{c_i}} = (J_{11_i} \omega_{s_i} + J_{11_i} \Omega_i + J_{12_i} \omega_{w_{2_i}} + J_{13_i} \omega_{w_{3_i}}) \hat{\mathbf{g}}_{s_i} + p_i \hat{\mathbf{w}}_{2_i} + q_i \hat{\mathbf{w}}_{3_i} \quad (2.51)$$

where p_i and q_i are scalar components defined as

$$p_i = J_{12_i} \omega_{s_i} + J_{12_i} \Omega_i + J_{22_i} \omega_{w_{2_i}} + J_{23_i} \omega_{w_{3_i}} \quad (2.52)$$

$$q_i = J_{13_i} \omega_{s_i} + J_{13_i} \Omega_i + J_{23_i} \omega_{w_{2_i}} + J_{33_i} \omega_{w_{3_i}} \quad (2.53)$$

Taking the inertial derivative of wheel angular momentum about W_c gives

$$\begin{aligned} \dot{\mathbf{H}}_{W_i, W_{c_i}} &= (J_{11_i} \dot{\omega}_{s_i} + J_{11_i} \dot{\Omega}_i + J_{12_i} \dot{\omega}_{w_{2_i}} + J_{13_i} \dot{\omega}_{w_{3_i}}) \hat{\mathbf{g}}_{s_i} + \dot{p}_i \hat{\mathbf{w}}_{2_i} + \dot{q}_i \hat{\mathbf{w}}_{3_i} \\ &+ (J_{11_i} \omega_{s_i} + J_{11_i} \Omega_i + J_{12_i} \omega_{w_{2_i}} + J_{13_i} \omega_{w_{3_i}}) \dot{\hat{\mathbf{g}}}_{s_i} + p_i \dot{\hat{\mathbf{w}}}_{2_i} + q_i \dot{\hat{\mathbf{w}}}_{3_i} \end{aligned} \quad (2.54)$$

where the inertial derivatives of the \mathcal{W}_i frame basis vectors are determined by evaluating the cross product in wheel frame components such as

$$\dot{\hat{\mathbf{g}}}_{s_i} = \boldsymbol{\omega}_{\mathcal{B}/\mathcal{N}} \times \hat{\mathbf{g}}_{s_i} = \omega_{w_{3_i}} \hat{\mathbf{w}}_{2_i} - \omega_{w_{2_i}} \hat{\mathbf{w}}_{3_i} \quad (2.55)$$

Similarly, $\dot{\hat{\mathbf{w}}}_{2_i}$ and $\dot{\hat{\mathbf{w}}}_{3_i}$ are found to be

$$\dot{\hat{\mathbf{w}}}_{2_i} = -\omega_{w_{3_i}} \hat{\mathbf{g}}_{s_i} + (\omega_{s_i} + \Omega_i) \hat{\mathbf{w}}_{3_i} \quad (2.56)$$

$$\dot{\hat{\mathbf{w}}}_{3_i} = \omega_{w_{2_i}} \hat{\mathbf{g}}_{s_i} - (\omega_{s_i} + \Omega_i) \hat{\mathbf{w}}_{2_i} \quad (2.57)$$

Substituting Eq. (2.55)-(2.57) into Eq. (2.54) and grouping like terms yields

$$\begin{aligned} \dot{\mathbf{H}}_{W_i, W_{c_i}} = & [(J_{11_i} \hat{\mathbf{g}}_{s_i}^T + J_{12_i} \hat{\mathbf{w}}_{2_i}^T + J_{13_i} \hat{\mathbf{w}}_{3_i}^T) \dot{\boldsymbol{\omega}}_{B/N} + J_{11_i} \dot{\Omega}_i + \omega_{s_i} (J_{13_i} \omega_{w_{2_i}} - J_{12_i} \omega_{w_{3_i}}) \\ & + \omega_{w_{3_i}} \omega_{w_{2_i}} (J_{33_i} - J_{22_i}) + J_{23_i} (\omega_{w_{2_i}}^2 - \omega_{w_{3_i}}^2)] \hat{\mathbf{g}}_{s_i} + P_i \hat{\mathbf{w}}_{2_i} + Q_i \hat{\mathbf{w}}_{3_i} \end{aligned} \quad (2.58)$$

Scalar quantities, P_i and Q_i are the coefficients for $\hat{\mathbf{w}}_{2_i}$ and $\hat{\mathbf{w}}_{3_i}$ respectively. Since only the coefficient of $\hat{\mathbf{g}}_{s_i}$ relates directly to the motor torque equation as in Eq. (2.40)-(2.41), specifying P_i and Q_i is unnecessary as they do not contribute to u_{s_i} .

The next step is to define the remaining terms in Eq. (2.41). This begins by determining the second inertial derivative of $\ddot{\mathbf{r}}_{W_{c_i}/N}$.

$$\mathbf{r}_{W_{c_i}/N} = \mathbf{r}_{B/N} + \mathbf{r}_{W_i/B} + \mathbf{r}_{W_{c_i}/W_i} = \mathbf{r}_{B/N} + \mathbf{r}_{W_i/B} + d_i \hat{\mathbf{w}}_{2_i} \quad (2.59)$$

$$\dot{\mathbf{r}}_{W_{c_i}/N} = \dot{\mathbf{r}}_{B/N} + \boldsymbol{\omega}_{B/N} \times \mathbf{r}_{W_i/B} + (\boldsymbol{\omega}_{B/N} + \Omega_i \hat{\mathbf{g}}_{s_i}) \times d_i \hat{\mathbf{w}}_{2_i} \quad (2.60)$$

$$\begin{aligned} \ddot{\mathbf{r}}_{W_{c_i}/N} = & \ddot{\mathbf{r}}_{B/N} + \dot{\boldsymbol{\omega}}_{B/N} \times \mathbf{r}_{W_i/B} + \boldsymbol{\omega}_{B/N} \times (\boldsymbol{\omega}_{B/N} \times \mathbf{r}_{W_i/B}) + (\dot{\boldsymbol{\omega}}_{B/N} + \dot{\Omega}_i \hat{\mathbf{g}}_{s_i}) \times d_i \hat{\mathbf{w}}_{2_i} \\ & + (\boldsymbol{\omega}_{B/N} + \Omega_i \hat{\mathbf{g}}_{s_i}) \times d_i \Omega_i \hat{\mathbf{w}}_{3_i} + \boldsymbol{\omega}_{B/N} \times [(\boldsymbol{\omega}_{B/N} + \Omega_i \hat{\mathbf{g}}_{s_i}) \times d_i \hat{\mathbf{w}}_{2_i}] \end{aligned} \quad (2.61)$$

Each cross product in Eq. (2.61) is evaluated using wheel frame components. For example,

$$(\boldsymbol{\omega}_{B/N} + \Omega_i \hat{\mathbf{g}}_{s_i}) \times d_i \hat{\mathbf{w}}_{2_i} = -d_i \omega_{w_{3_i}} \hat{\mathbf{g}}_{s_i} + d_i (\omega_{s_i} + \Omega_i) \hat{\mathbf{w}}_{3_i} \quad (2.62)$$

Repeating this procedure several times yields the following expression for the right hand term of Eq. (2.41) (R_i is the coefficient in front of $\hat{\mathbf{w}}_{3_i}$ and does need to be defined because only the $\hat{\mathbf{g}}_{s_i}$ component is desired):

$$\begin{aligned} \mathbf{r}_{W_{c_i}/W_i} \times m_{W_i} \ddot{\mathbf{r}}_{W_{c_i}/N} = & m_{W_i} d_i \left[\hat{\mathbf{w}}_{3_i}^T \ddot{\mathbf{r}}_{B/N} - \hat{\mathbf{w}}_{3_i}^T [\tilde{\mathbf{r}}_{W_i/B}] \dot{\boldsymbol{\omega}}_{B/N} + \hat{\mathbf{w}}_{3_i}^T [\tilde{\boldsymbol{\omega}}_{B/N}] [\tilde{\boldsymbol{\omega}}_{B/N}] \mathbf{r}_{W_i/B} \right. \\ & \left. + d_i (\hat{\mathbf{g}}_{s_i}^T \dot{\boldsymbol{\omega}}_{B/N} + \dot{\Omega}_i) + d_i \omega_{w_{2_i}} \omega_{w_{3_i}} \right] \hat{\mathbf{g}}_{s_i} - R_i \hat{\mathbf{w}}_{3_i} \end{aligned} \quad (2.63)$$

The motor torque equation is obtained by summing the $\hat{\mathbf{g}}_{s_i}$ components of Eq. (2.58) and Eq. (2.63)

$$\begin{aligned} u_{s_i} = & (J_{11_i} \hat{\mathbf{g}}_{s_i}^T + J_{12_i} \hat{\mathbf{w}}_{2_i}^T + J_{13_i} \hat{\mathbf{w}}_{3_i}^T) \dot{\boldsymbol{\omega}}_{B/N} + J_{11_i} \dot{\Omega}_i + \omega_{s_i} (J_{13_i} \omega_{w_{2_i}} - J_{12_i} \omega_{w_{3_i}}) + \omega_{w_{3_i}} \omega_{w_{2_i}} (J_{33_i} - J_{22_i}) \\ & + J_{23_i} (\omega_{w_{2_i}}^2 - \omega_{w_{3_i}}^2) + m_{W_i} d_i \hat{\mathbf{w}}_{3_i}^T \ddot{\mathbf{r}}_{B/N} - m_{W_i} d_i \hat{\mathbf{w}}_{3_i}^T [\tilde{\mathbf{r}}_{W_i/B}] \dot{\boldsymbol{\omega}}_{B/N} \\ & + m_{W_i} d_i \hat{\mathbf{w}}_{3_i}^T [\tilde{\boldsymbol{\omega}}_{B/N}] [\tilde{\boldsymbol{\omega}}_{B/N}] \mathbf{r}_{W_i/B} + m_{W_i} d_i^2 (\hat{\mathbf{g}}_{s_i}^T \dot{\boldsymbol{\omega}}_{B/N} + \dot{\Omega}_i) + m_{W_i} d_i^2 \omega_{w_{2_i}} \omega_{w_{3_i}} \end{aligned} \quad (2.64)$$

Grouping second order terms on the left-hand side yields the simplified motor torque equation.

$$\begin{aligned}
& [m_{W_i} d_i \hat{\mathbf{w}}_{3_i}^T] \ddot{\mathbf{r}}_{B/N} + [(J_{11_i} + m_{W_i} d_i^2) \hat{\mathbf{g}}_{s_i}^T + J_{12_i} \hat{\mathbf{w}}_{2_i}^T + J_{13_i} \hat{\mathbf{w}}_{3_i}^T \\
& \quad - m_{W_i} d_i \hat{\mathbf{w}}_{3_i}^T [\tilde{\mathbf{r}}_{W_i/B}]] \dot{\boldsymbol{\omega}}_{B/N} + [J_{11_i} + m_{W_i} d_i^2] \dot{\Omega}_i \\
& = J_{23_i} (\omega_{w_{3_i}}^2 - \omega_{w_{2_i}}^2) + \omega_{s_i} (J_{12_i} \omega_{w_{3_i}} - J_{13_i} \omega_{w_{2_i}}) + \omega_{w_{2_i}} \omega_{w_{3_i}} (J_{22_i} - J_{33_i} - m_{W_i} d_i^2) \\
& \quad - m_{W_i} d_i \hat{\mathbf{w}}_{3_i}^T [\tilde{\boldsymbol{\omega}}_{B/N}] [\tilde{\boldsymbol{\omega}}_{B/N}] \mathbf{r}_{W_i/B} + u_{s_i} \quad (2.65)
\end{aligned}$$

As a form of validation, the balanced motor torque equation may be obtained by zeroing out all imbalance terms (d_i , J_{12_i} , J_{13_i} , J_{23_i}) and making the assumption $J_{22_i} = J_{33_i}$. Under these conditions, Eq. (2.65) may be simplified to

$$u_{s_i} = J_{11_i} (\hat{\mathbf{g}}_{s_i}^T \boldsymbol{\omega}_{B/N} + \dot{\Omega}_i) \quad (2.66)$$

Eq. (2.66) is equivalent to the balanced motor torque equation found in Reference [24].

This concludes the necessary derivations for the EOMs that are needed to describe the fully-coupled jitter model for imbalanced RWs. Since the simplified RW jitter model [17] assumes an external force and torque on the spacecraft, the EOMs for the fully-coupled model and the simplified RW jitter model are significantly different. However, due to the coupled nature of the EOMs, the similar terms in the simplified model compared to the fully-coupled model are not readily apparent in EOMs presented thus far. In the following section, the paper addresses this discrepancy and discusses the conversion from imbalance parameters from RW manufactures to the new parameters in the formulation.

Chapter 3

Imbalanced Variable Speed Control Moment Gyroscope

3.1 Problem Statement

The problem consists of modeling static and dynamic imbalance of any number of wheel + gimbal assemblies attached to a rigid spacecraft. In order to develop the equations of motion in a general way, we consider arbitrary locations, inertia tensors, and center of mass locations for the spacecraft hub, gimbal, and wheels. Additionally, the wheel center of mass is not assumed to lie on the gimbal axis of the VSCMG, and the wheel frame origin and gimbal frame origin are not assumed to coincide.

3.1.1 Reference Frame Definitions

The development considers the body frame and N gimbal and wheel frames as well as the inertial frame. The body frame is denoted \mathcal{B} . The basis vectors of the body frame are

$$\mathcal{B} : \{B, \hat{\mathbf{b}}_1, \hat{\mathbf{b}}_2, \hat{\mathbf{b}}_3\} \quad (3.1)$$

The i^{th} gimbal and wheel frames are denoted \mathcal{G}_i and \mathcal{W}_i , respectively. The basis vectors of \mathcal{G}_i and \mathcal{W}_i are defined as

$$\mathcal{G}_i : \{G_i, \hat{\mathbf{g}}_{s_i}, \hat{\mathbf{g}}_{t_i}, \hat{\mathbf{g}}_{g_i}\} \quad (3.2)$$

$$\mathcal{W}_i : \{W_i, \hat{\mathbf{g}}_{s_i}, \hat{\mathbf{w}}_{2_i}, \hat{\mathbf{w}}_{3_i}\} \quad (3.3)$$

It is assumed that the $\hat{\mathbf{g}}_{s_i}$ vectors of the \mathcal{G}_i and \mathcal{W}_i frames are always parallel.

3.2 Equations of Motion

The system under consideration is an $2N + 6$ degrees-of-freedom (DOF) system with the following second order terms: inertial acceleration $\ddot{\mathbf{r}}_{B/N}$, angular acceleration $\dot{\boldsymbol{\omega}}_{B/N}$, the acceleration of each wheel $\dot{\Omega}_1, \dots, \dot{\Omega}_N$, and the acceleration of the gimbal $\ddot{\gamma}_1, \dots, \ddot{\gamma}_N$. Thus, a total of $2N + 6$ equations must be developed in order to solve for all second order terms. Section 3.2.1 describes the derivation of the translational EOM and represents 3 DOF, section 3.2.2 describes the rotational motion and represents 3 DOF, section 3.2.3 describes the gimbal torque equation and represents N DOF, and section 3.2.4 describes the wheel torque equation and represents N DOF.

3.2.1 Translational Motion

The derivation of the translational EOMs begins with Newton's second law for the center of mass of the spacecraft.

$$\ddot{\mathbf{r}}_{C/N} = \frac{\mathbf{F}}{m_{sc}} \quad (3.4)$$

where

$$m_{sc} = m_B + \sum_{i=1}^N (m_{G_i} + m_{W_i}) \quad (3.5)$$

\mathbf{F} is the sum of the external forces on the spacecraft which has mass m_{sc} . Ultimately the acceleration of the body frame or point B is desired, which is expressed through

$$\ddot{\mathbf{r}}_{B/N} = \ddot{\mathbf{r}}_{C/N} - \ddot{\mathbf{c}} \quad (3.6)$$

The center of mass \mathbf{c} is time variant and is expressed as

$$\mathbf{c} = \frac{1}{m_{sc}} (m_B \mathbf{r}_{B_c/B} + \sum_{i=1}^N (m_{G_i} \mathbf{r}_{G_{c_i}/B} + m_{W_i} \mathbf{r}_{W_{c_i}/B})) \quad (3.7)$$

Find the second inertial derivative of \mathbf{c} .

$$\dot{\mathbf{c}} = \mathbf{c}' + \boldsymbol{\omega} \times \mathbf{c} \quad (3.8)$$

$$\ddot{\mathbf{c}} = \mathbf{c}'' + \dot{\boldsymbol{\omega}} \times \mathbf{c} + 2\boldsymbol{\omega} \times \mathbf{c}' + \boldsymbol{\omega} \times (\boldsymbol{\omega} \times \mathbf{c}) \quad (3.9)$$

Find the body frame derivatives of \mathbf{c} .

$$\mathbf{c}' = \frac{1}{m_{sc}} \sum_{i=1}^N (m_{G_i} \mathbf{r}'_{G_{c_i}/B} + m_{W_i} \mathbf{r}'_{W_{c_i}/B}) \quad (3.10)$$

$$\mathbf{c}'' = \frac{1}{m_{sc}} \sum_{i=1}^N (m_{G_i} \mathbf{r}''_{G_{c_i}/B} + m_{W_i} \mathbf{r}''_{W_{c_i}/B}) \quad (3.11)$$

The body frame derivatives of $\mathbf{r}_{G_{c_i}/B}$ are given by

$$\mathbf{r}_{G_{c_i}/B} = \mathbf{r}_{G_i/B} + \mathbf{r}_{G_{c_i}/G_i} \quad (3.12)$$

$$\mathbf{r}'_{G_{c_i}/B} = \mathbf{r}'_{G_{c_i}/G} = \boldsymbol{\omega}_{G_i/B} \times \mathbf{r}_{G_{c_i}/G_i} = \dot{\gamma}_i \hat{\mathbf{g}}_{g_i} \times \mathbf{r}_{G_{c_i}/G_i} \quad (3.13)$$

$$\begin{aligned} \mathbf{r}''_{G_{c_i}/B} &= \ddot{\gamma}_i \hat{\mathbf{g}}_{g_i} \times \mathbf{r}_{G_{c_i}/G_i} + \dot{\gamma}_i \dot{\hat{\mathbf{g}}}_{g_i} \times \mathbf{r}'_{G_{c_i}/B} \\ &= \ddot{\gamma}_i [\tilde{\hat{\mathbf{g}}}_{g_i}] \mathbf{r}_{G_{c_i}/G_i} + \dot{\gamma}_i [\tilde{\dot{\hat{\mathbf{g}}}}_{g_i}] \mathbf{r}'_{G_{c_i}/B} \end{aligned} \quad (3.14)$$

The body frame derivatives of $\mathbf{r}_{W_{c_i}/B}$ are given by

$$\mathbf{r}_{W_{c_i}/B} = \mathbf{r}_{W_{c_i}/G_i} + \mathbf{r}_{G_i/B} = d_i \hat{\mathbf{w}}_{2_i} + \ell_i \hat{\mathbf{g}}_{s_i} + L_i \hat{\mathbf{g}}_{g_i} + \mathbf{r}_{G_i/B} \quad (3.15)$$

$$\mathbf{r}'_{W_{c_i}/B} = \mathbf{r}'_{W_{c_i}/G} = d_i \hat{\mathbf{w}}'_{2_i} + \ell_i \hat{\mathbf{g}}'_{s_i} = d_i \Omega_i \hat{\mathbf{w}}_{3_i} - d_i \dot{\gamma}_i c \theta_i \hat{\mathbf{g}}_{s_i} + \ell_i \dot{\gamma}_i \hat{\mathbf{g}}_{t_i} \quad (3.16)$$

$$\begin{aligned} \mathbf{r}''_{W_{c_i}/B} &= \mathbf{r}''_{W_{c_i}/G} = d_i \dot{\Omega}_i \hat{\mathbf{w}}_{3_i} + d_i \Omega_i \hat{\mathbf{w}}'_{3_i} - d_i \ddot{\gamma}_i c \theta_i \hat{\mathbf{g}}_{s_i} + d_i \dot{\gamma}_i \Omega_i s \theta_i \hat{\mathbf{g}}_{s_i} - d_i \dot{\gamma}_i c \theta_i \hat{\mathbf{g}}'_{s_i} + \ell_i \ddot{\gamma}_i \hat{\mathbf{g}}_{t_i} + \ell_i \dot{\gamma}_i \hat{\mathbf{g}}'_{t_i} \\ &= (2d_i \dot{\gamma}_i \Omega_i s \theta_i - d_i \ddot{\gamma}_i c \theta_i - \ell_i \dot{\gamma}_i^2) \hat{\mathbf{g}}_{s_i} + (\ell_i \ddot{\gamma}_i - d_i \dot{\gamma}_i^2 c \theta_i) \hat{\mathbf{g}}_{t_i} - d_i \Omega_i^2 \hat{\mathbf{w}}_{2_i} + d_i \dot{\Omega}_i \hat{\mathbf{w}}_{3_i} \end{aligned} \quad (3.17)$$

Note that the body frame derivatives of the gimbal and wheel frame basis vectors are given by,

$$\hat{\mathbf{g}}'_{s_i} = \dot{\gamma}_i \hat{\mathbf{g}}_{g_i} \times \hat{\mathbf{g}}_{s_i} = \dot{\gamma}_i \hat{\mathbf{g}}_{t_i} \quad (3.18)$$

$$\hat{\mathbf{g}}'_{t_i} = \dot{\gamma}_i \hat{\mathbf{g}}_{g_i} \times \hat{\mathbf{g}}_{t_i} = -\dot{\gamma}_i \hat{\mathbf{g}}_{s_i} \quad (3.19)$$

$$\hat{\mathbf{g}}'_{g_i} = \mathbf{0} \quad (3.20)$$

$$\hat{\mathbf{w}}'_{2_i} = (\dot{\gamma}_i \hat{\mathbf{g}}_{g_i} + \Omega_i \hat{\mathbf{g}}_{s_i}) \times \hat{\mathbf{w}}_{2_i} = \Omega_i \hat{\mathbf{w}}_{3_i} - \dot{\gamma}_i c \theta_i \hat{\mathbf{g}}_{s_i} \quad (3.21)$$

$$\hat{\mathbf{w}}'_{3_i} = (\dot{\gamma}_i \hat{\mathbf{g}}_{g_i} + \Omega_i \hat{\mathbf{g}}_{s_i}) \times \hat{\mathbf{w}}_{3_i} = \dot{\gamma}_i s \theta_i \hat{\mathbf{g}}_{s_i} - \Omega_i \hat{\mathbf{w}}_{2_i} \quad (3.22)$$

Expanding Eq. (3.11) gives,

$$\begin{aligned} \mathbf{c}'' = & \frac{1}{m_{sc}} \sum_{i=1}^N \left[m_{G_i} \left(\dot{\gamma}_i [\tilde{\mathbf{g}}_{g_i}] \mathbf{r}_{G_{c_i}/G_i} + \dot{\gamma}_i [\tilde{\mathbf{g}}_{g_i}] \mathbf{r}'_{G_{c_i}/B} \right) \right. \\ & \left. + m_{W_i} \left((2d_i \dot{\gamma}_i \Omega_i s \theta_i - d_i \dot{\gamma}_i c \theta_i - \ell_i \dot{\gamma}_i^2) \hat{\mathbf{g}}_{s_i} + (\ell_i \dot{\gamma}_i - d_i \dot{\gamma}_i^2 c \theta_i) \hat{\mathbf{g}}_{t_i} - d_i \Omega_i^2 \hat{\mathbf{w}}_{2_i} + d_i \dot{\Omega}_i \hat{\mathbf{w}}_{3_i} \right) \right] \end{aligned} \quad (3.23)$$

Substitute $\ddot{\mathbf{c}}$ into Eq. (3.6).

$$\ddot{\mathbf{r}}_{B/N} = \ddot{\mathbf{r}}_{C/N} - \mathbf{c}'' + [\ddot{\mathbf{c}}] \dot{\boldsymbol{\omega}} - 2[\dot{\boldsymbol{\omega}}] \mathbf{c}' - [\dot{\boldsymbol{\omega}}][\dot{\boldsymbol{\omega}}] \mathbf{c} \quad (3.24)$$

Substitute Eq. (3.23) into Eq. (3.24) and group second-order terms to obtain the translational equations of motion.

$$\begin{aligned} \ddot{\mathbf{r}}_{B/N} - [\ddot{\mathbf{c}}] \dot{\boldsymbol{\omega}} + \frac{1}{m_{sc}} \sum_{i=1}^N \left[m_{G_i} [\tilde{\mathbf{g}}_{g_i}] \mathbf{r}_{G_{c_i}/G_i} - m_{W_i} d_i c \theta_i \hat{\mathbf{g}}_{s_i} + m_{W_i} \ell_i \hat{\mathbf{g}}_{t_i} \right] \dot{\gamma}_i + \frac{1}{m_{sc}} \sum_{i=1}^N \left[m_{W_i} d_i \hat{\mathbf{w}}_{3_i} \right] \dot{\Omega}_i \\ = \ddot{\mathbf{r}}_{C/N} - 2[\dot{\boldsymbol{\omega}}] \mathbf{c}' - [\dot{\boldsymbol{\omega}}][\dot{\boldsymbol{\omega}}] \mathbf{c} - \frac{1}{m_{sc}} \sum_{i=1}^N \left[m_{G_i} \dot{\gamma}_i [\tilde{\mathbf{g}}_{g_i}] \mathbf{r}'_{G_{c_i}/B} \right. \\ \left. + m_{W_i} \left[(2d_i \dot{\gamma}_i \Omega_i s \theta_i - \ell_i \dot{\gamma}_i^2) \hat{\mathbf{g}}_{s_i} - d_i \dot{\gamma}_i^2 c \theta_i \hat{\mathbf{g}}_{t_i} - d_i \Omega_i^2 \hat{\mathbf{w}}_{2_i} \right] \right] \end{aligned} \quad (3.25)$$

This equation represents 3 DOF and contains all second order states ($\ddot{\mathbf{r}}_{B/N}$, $\dot{\boldsymbol{\omega}}$, $\dot{\gamma}_i$, $\dot{\Omega}_i$). Removing wheel imbalance terms and assuming a symmetrical VSCMG (i.e. $\mathbf{r}_{G_{c_i}/G_i} = \mathbf{0}$, $\ell_i = 0$, $d_i = 0$) gives the following equation.

$$m_{sc} \ddot{\mathbf{r}}_{B/N} - m_{sc} [\ddot{\mathbf{c}}] \dot{\boldsymbol{\omega}} = \mathbf{F} - 2m_{sc} [\dot{\boldsymbol{\omega}}] \mathbf{c}' - m_{sc} [\dot{\boldsymbol{\omega}}]^2 \mathbf{c} \quad (3.26)$$

Thus, the balanced VSCMG translational equation of motion does not contain any second-order terms relating to the wheel or gimbal, and agrees with Reference [24]. The following section shows the derivation of the rotational equations of motion.

3.2.2 Rotational Motion

The derivation of rotational EOMs starts with the angular momentum of the spacecraft about point B .

$$\mathbf{H}_{sc,B} = \mathbf{H}_{B,B} + \sum_{i=1}^N (\mathbf{H}_{G_i,B} + \mathbf{H}_{W_i,B}) \quad (3.27)$$

The inertial time derivative of angular momentum when the body fixed coordinate frame origin is not coincident with the center of mass of the body is

$$\dot{\mathbf{H}}_{sc,B} = \mathbf{L}_B + m_{sc}\ddot{\mathbf{r}}_{B/N} \times \mathbf{c} \quad (3.28)$$

where \mathbf{L}_B is the vector sum of external torques acting on the spacecraft. Differentiating Eq. (3.27), the inertial derivative of the spacecraft angular momentum is expressed as

$$\dot{\mathbf{H}}_{sc,B} = \dot{\mathbf{H}}_{B,B} + \sum_{i=1}^N (\dot{\mathbf{H}}_{G_i,B} + \dot{\mathbf{H}}_{W_i,B}) \quad (3.29)$$

Thus, in order to use Eq. (3.28), each derivative on the right-hand side of Eq. (3.29) needs to be evaluated. The first step is to derive the hub angular momentum derivative $\dot{\mathbf{H}}_{B,B}$. The hub angular momentum about point B_c is given by

$$\mathbf{H}_{B,B_c} = [I_{B,B_c}]\boldsymbol{\omega}_{B/N} \quad (3.30)$$

Angular momentum about point B_c is related to point B using the following equation.

$$\mathbf{H}_{B,B} = \mathbf{H}_{B,B_c} + m_B \mathbf{r}_{B_c/B} \times \dot{\mathbf{r}}_{B_c/B} \quad (3.31)$$

Taking the inertial time derivative of the hub's angular momentum yields

$$\dot{\mathbf{H}}_{B,B} = [I_{B,B_c}]\dot{\boldsymbol{\omega}} + [\tilde{\boldsymbol{\omega}}][I_{B,B_c}]\boldsymbol{\omega} + m_B \mathbf{r}_{B_c/B} \times \ddot{\mathbf{r}}_{B_c/B} \quad (3.32)$$

Note that the body rate pseudovector $\boldsymbol{\omega}_{B/N}$ will be abbreviated as $\boldsymbol{\omega}$ henceforth. Knowing that $\mathbf{r}_{B_c/B}$ is fixed with respect to the body frame, the following are defined

$$\dot{\mathbf{r}}_{B_c/B} = \mathbf{r}'_{B_c/B} + \boldsymbol{\omega} \times \mathbf{r}_{B_c/B} = \boldsymbol{\omega} \times \mathbf{r}_{B_c/B} \quad (3.33)$$

$$\ddot{\mathbf{r}}_{B_c/B} = \dot{\boldsymbol{\omega}} \times \mathbf{r}_{B_c/B} + \boldsymbol{\omega} \times (\boldsymbol{\omega} \times \mathbf{r}_{B_c/B}) \quad (3.34)$$

Substitute Eq. (3.34) into Eq. (3.32) yields

$$\dot{\mathbf{H}}_{B,B} = [I_{B,B_c}]\dot{\boldsymbol{\omega}} + [\tilde{\boldsymbol{\omega}}][I_{B,B_c}]\boldsymbol{\omega} + m_B \mathbf{r}_{B_c/B} \times (\dot{\boldsymbol{\omega}} \times \mathbf{r}_{B_c/B}) + m_B \mathbf{r}_{B_c/B} \times (\boldsymbol{\omega} \times (\boldsymbol{\omega} \times \mathbf{r}_{B_c/B})) \quad (3.35)$$

Employing the Jacobi triple-product identity, $\mathbf{a} \times (\mathbf{b} \times \mathbf{c}) = (\mathbf{a} \times \mathbf{b}) \times \mathbf{c} + \mathbf{b} \times (\mathbf{a} \times \mathbf{c})$, on the right-hand side of Eq. (3.35)

$$\dot{\mathbf{H}}_{B,B} = [I_{B,B_c}] \dot{\boldsymbol{\omega}} + [\tilde{\boldsymbol{\omega}}][I_{B,B_c}] \boldsymbol{\omega} + m_B [\tilde{\mathbf{r}}_{B_c/B}] [\tilde{\mathbf{r}}_{B_c/B}]^T \dot{\boldsymbol{\omega}} + m_B [\tilde{\boldsymbol{\omega}}] [\tilde{\mathbf{r}}_{B_c/B}] [\tilde{\mathbf{r}}_{B_c/B}]^T \boldsymbol{\omega} \quad (3.36)$$

The parallel axis theorem relates inertia about the hub center of B_c to the hub origin B .

$$[I_{B,B}] = [I_{B,B_c}] + m_B [\tilde{\mathbf{r}}_{B_c/B}] [\tilde{\mathbf{r}}_{B_c/B}]^T \quad (3.37)$$

The hub angular momentum derivative simplifies to

$$\dot{\mathbf{H}}_{B,B} = [I_{B,B}] \dot{\boldsymbol{\omega}} + [\tilde{\boldsymbol{\omega}}][I_{B,B}] \boldsymbol{\omega} \quad (3.38)$$

The next step is to derive the gimbal angular momentum derivative $\dot{\mathbf{H}}_{G_i,B}$. Recall that the i^{th} gimbal frame is defined as

$$\mathcal{G}_i : \{G_i, \hat{\mathbf{g}}_{s_i}, \hat{\mathbf{g}}_{t_i}, \hat{\mathbf{g}}_{g_i}\}$$

Angular velocity of the gimbal frame with respect to inertial is

$$\boldsymbol{\omega}_{\mathcal{G}_i/N} = \boldsymbol{\omega}_{B/N} + \boldsymbol{\omega}_{\mathcal{G}_i/B} = \boldsymbol{\omega} + \dot{\gamma}_i \hat{\mathbf{g}}_{g_i} \quad (3.39)$$

The gimbal angular momentum about point G_{c_i} is given by

$$\mathbf{H}_{G_i,G_{c_i}} = [I_{G_i,G_{c_i}}] \boldsymbol{\omega}_{\mathcal{G}_i/N} = [I_{G_i,G_{c_i}}] (\boldsymbol{\omega} + \dot{\gamma}_i \hat{\mathbf{g}}_{g_i}) \quad (3.40)$$

Angular momentum about point G_{c_i} is related to point B using the following equation.

$$\mathbf{H}_{G_i,B} = \mathbf{H}_{G_i,G_{c_i}} + m_{G_i} \mathbf{r}_{G_{c_i}/B} \times \dot{\mathbf{r}}_{G_{c_i}/B} \quad (3.41)$$

Take the inertial derivative.

$$\dot{\mathbf{H}}_{G_i,B} = [I_{G_i,G_{c_i}}] (\dot{\boldsymbol{\omega}} + \ddot{\gamma}_i \hat{\mathbf{g}}_{g_i}) + [I_{G_i,G_{c_i}}]' \boldsymbol{\omega}_{\mathcal{G}_i/N} + [\tilde{\boldsymbol{\omega}}][I_{G_i,G_{c_i}}] \boldsymbol{\omega}_{\mathcal{G}_i/N} + m_{G_i} \mathbf{r}_{G_{c_i}/B} \times \ddot{\mathbf{r}}_{G_{c_i}/B} \quad (3.42)$$

The next step is to define the gimbal inertia tensor about the gimbal center of mass $[I_{G_i,G_{c_i}}]$ and its body frame derivative $[I_{G_i,G_{c_i}}]'$. Expressed in the gimbal frame,

$$[I_{G_i,G_{c_i}}] = \begin{matrix} \mathcal{G}_i \\ \left[\begin{array}{ccc} I_{G_{s_i}} & I_{G_{12_i}} & I_{G_{13_i}} \\ I_{G_{12_i}} & I_{G_{t_i}} & I_{G_{23_i}} \\ I_{G_{13_i}} & I_{G_{23_i}} & I_{G_{g_i}} \end{array} \right] \end{matrix} \quad (3.43)$$

This tensor may be rewritten in a frame independent form as,

$$\begin{aligned}
[I_{G_i, G_{c_i}}] &= I_{G_{s_i}} \hat{\mathbf{g}}_{s_i} \hat{\mathbf{g}}_{s_i}^T + I_{G_{12_i}} \hat{\mathbf{g}}_{s_i} \hat{\mathbf{g}}_{t_i}^T + I_{G_{13_i}} \hat{\mathbf{g}}_{s_i} \hat{\mathbf{g}}_{g_i}^T \\
&+ I_{G_{12_i}} \hat{\mathbf{g}}_{t_i} \hat{\mathbf{g}}_{s_i}^T + I_{G_{t_i}} \hat{\mathbf{g}}_{t_i} \hat{\mathbf{g}}_{t_i}^T + I_{G_{23_i}} \hat{\mathbf{g}}_{t_i} \hat{\mathbf{g}}_{g_i}^T \\
&+ I_{G_{13_i}} \hat{\mathbf{g}}_{g_i} \hat{\mathbf{g}}_{s_i}^T + I_{G_{23_i}} \hat{\mathbf{g}}_{g_i} \hat{\mathbf{g}}_{t_i}^T + I_{G_{g_i}} \hat{\mathbf{g}}_{g_i} \hat{\mathbf{g}}_{g_i}^T
\end{aligned} \tag{3.44}$$

Taking the body frame derivative of this equation results in,

$$\begin{aligned}
[I_{G_i, G_{c_i}}]' &= I_{G_{s_i}} \hat{\mathbf{g}}'_{s_i} \hat{\mathbf{g}}_{s_i}^T + I_{G_{s_i}} \hat{\mathbf{g}}_{s_i} \hat{\mathbf{g}}_{s_i}^{T'} + I_{G_{12_i}} \hat{\mathbf{g}}'_{s_i} \hat{\mathbf{g}}_{t_i}^T + I_{G_{12_i}} \hat{\mathbf{g}}_{s_i} \hat{\mathbf{g}}_{t_i}^{T'} + I_{G_{13_i}} \hat{\mathbf{g}}'_{s_i} \hat{\mathbf{g}}_{g_i}^T \\
&+ I_{G_{12_i}} \hat{\mathbf{g}}'_{t_i} \hat{\mathbf{g}}_{s_i}^T + I_{G_{12_i}} \hat{\mathbf{g}}_{t_i} \hat{\mathbf{g}}_{s_i}^{T'} + I_{G_{t_i}} \hat{\mathbf{g}}'_{t_i} \hat{\mathbf{g}}_{t_i}^T + I_{G_{t_i}} \hat{\mathbf{g}}_{t_i} \hat{\mathbf{g}}_{t_i}^{T'} + I_{G_{23_i}} \hat{\mathbf{g}}'_{t_i} \hat{\mathbf{g}}_{g_i}^T \\
&+ I_{G_{13_i}} \hat{\mathbf{g}}'_{g_i} \hat{\mathbf{g}}_{s_i}^T + I_{G_{23_i}} \hat{\mathbf{g}}_{g_i} \hat{\mathbf{g}}_{t_i}^{T'}
\end{aligned} \tag{3.45}$$

Recall the following body frame derivatives.

$$\begin{aligned}
\hat{\mathbf{g}}'_{s_i} &= \dot{\gamma} \hat{\mathbf{g}}_{t_i} \\
\hat{\mathbf{g}}'_{t_i} &= -\dot{\gamma} \hat{\mathbf{g}}_{s_i} \\
\hat{\mathbf{g}}'_{g_i} &= \mathbf{0}
\end{aligned}$$

Simplifying Eq. (3.45) gives the expanded form of the body frame derivative of the gimbal inertia.

$$\begin{aligned}
[I_{G_i, G_{c_i}}]' &= I_{G_{s_i}} \dot{\gamma} \hat{\mathbf{g}}_{t_i} \hat{\mathbf{g}}_{s_i}^T + I_{G_{s_i}} \dot{\gamma} \hat{\mathbf{g}}_{s_i} \hat{\mathbf{g}}_{t_i}^T + I_{G_{12_i}} \dot{\gamma} \hat{\mathbf{g}}_{t_i} \hat{\mathbf{g}}_{t_i}^T - I_{G_{12_i}} \dot{\gamma} \hat{\mathbf{g}}_{s_i} \hat{\mathbf{g}}_{s_i}^T + I_{G_{13_i}} \dot{\gamma} \hat{\mathbf{g}}_{t_i} \hat{\mathbf{g}}_{g_i}^T \\
&- I_{G_{12_i}} \dot{\gamma} \hat{\mathbf{g}}_{s_i} \hat{\mathbf{g}}_{s_i}^T + I_{G_{12_i}} \dot{\gamma} \hat{\mathbf{g}}_{t_i} \hat{\mathbf{g}}_{t_i}^T - I_{G_{t_i}} \dot{\gamma} \hat{\mathbf{g}}_{s_i} \hat{\mathbf{g}}_{t_i}^T - I_{G_{t_i}} \dot{\gamma} \hat{\mathbf{g}}_{t_i} \hat{\mathbf{g}}_{s_i}^T - I_{G_{23_i}} \dot{\gamma} \hat{\mathbf{g}}_{s_i} \hat{\mathbf{g}}_{g_i}^T \\
&+ I_{G_{13_i}} \dot{\gamma} \hat{\mathbf{g}}_{g_i} \hat{\mathbf{g}}_{t_i}^T - I_{G_{23_i}} \dot{\gamma} \hat{\mathbf{g}}_{g_i} \hat{\mathbf{g}}_{s_i}^T
\end{aligned} \tag{3.46}$$

This tensor may be written in gimbal frame components as,

$$[I_{G_i, G_{c_i}}]' = \dot{\gamma}_i \begin{bmatrix} G_i & & \\ -2I_{G_{12_i}} & (I_{G_{s_i}} - I_{G_{t_i}}) & -I_{G_{23_i}} \\ (I_{G_{s_i}} - I_{G_{t_i}}) & 2I_{G_{12_i}} & I_{G_{13_i}} \\ -I_{G_{23_i}} & I_{G_{13_i}} & 0 \end{bmatrix} \tag{3.47}$$

The second inertial derivative of $\mathbf{r}_{G_{c_i}/B}$ is needed. Define the body frame derivative and first inertial derivative of $\mathbf{r}_{G_{c_i}/B}$, noting that point G_i is fixed with respect to point B .

$$\mathbf{r}_{G_{c_i}/B} = \mathbf{r}_{G_{c_i}/G_i} + \mathbf{r}_{G_i/B} \tag{3.48}$$

$$\mathbf{r}'_{G_{c_i}/B} = \mathbf{r}'_{G_{c_i}/G_i} = \dot{\gamma}_i \hat{\mathbf{g}}_{g_i} \times \mathbf{r}_{G_{c_i}/G_i} \tag{3.49}$$

$$\dot{\mathbf{r}}_{G_{c_i}/B} = \mathbf{r}'_{G_{c_i}/B} + \boldsymbol{\omega} \times \mathbf{r}_{G_{c_i}/B} = \dot{\gamma}_i \hat{\mathbf{g}}_{g_i} \times \mathbf{r}_{G_{c_i}/G_i} + \boldsymbol{\omega} \times \mathbf{r}_{G_{c_i}/B} \tag{3.50}$$

The second inertial derivative of $\mathbf{r}_{G_{c_i}/B}$ is

$$\begin{aligned}\ddot{\mathbf{r}}_{G_{c_i}/B} &= \ddot{\gamma}_i \hat{\mathbf{g}}_{g_i} \times \mathbf{r}_{G_{c_i}/G_i} + \dot{\gamma}_i \hat{\mathbf{g}}_{g_i} \times \mathbf{r}'_{G_{c_i}/G_i} + \dot{\boldsymbol{\omega}} \times \mathbf{r}_{G_{c_i}/B} + \boldsymbol{\omega} \times \mathbf{r}'_{G_{c_i}/B} + \boldsymbol{\omega} \times \dot{\mathbf{r}}_{G_{c_i}/B} \\ &= \ddot{\gamma}_i [\tilde{\hat{\mathbf{g}}}_{g_i}] \mathbf{r}_{G_{c_i}/G_i} + \dot{\gamma}_i [\tilde{\hat{\mathbf{g}}}_{g_i}] \mathbf{r}'_{G_{c_i}/G_i} + [\tilde{\mathbf{r}}_{G_{c_i}/B}]^T \dot{\boldsymbol{\omega}} + 2[\tilde{\mathbf{r}}'_{G_{c_i}/B}]^T \boldsymbol{\omega} + [\tilde{\boldsymbol{\omega}}][\tilde{\boldsymbol{\omega}}] \mathbf{r}_{G_{c_i}/B}\end{aligned}\quad (3.51)$$

Note that ,

$$\mathbf{r}''_{G_{c_i}/B} = \mathbf{r}''_{G_{c_i}/G} = \ddot{\gamma}_i [\tilde{\hat{\mathbf{g}}}_{g_i}] \mathbf{r}_{G_{c_i}/G_i} + \dot{\gamma}_i [\tilde{\hat{\mathbf{g}}}_{g_i}] \mathbf{r}'_{G_{c_i}/G_i} \quad (3.52)$$

Substitute into Eq. (3.42).

$$\begin{aligned}\dot{\mathbf{H}}_{G_i,B} &= [I_{G_i,G_{c_i}}](\dot{\boldsymbol{\omega}} + \dot{\gamma}_i \hat{\mathbf{g}}_{g_i}) + [I_{G_i,G_{c_i}}]' \boldsymbol{\omega}_{g_i/\mathcal{N}} + [\tilde{\boldsymbol{\omega}}][I_{G_i,G_{c_i}}] \boldsymbol{\omega}_{g_i/\mathcal{N}} \\ &\quad + m_{G_i} [\tilde{\mathbf{r}}_{G_{c_i}/B}] \left[\ddot{\gamma}_i [\tilde{\hat{\mathbf{g}}}_{g_i}] \mathbf{r}_{G_{c_i}/G_i} + \dot{\gamma}_i [\tilde{\hat{\mathbf{g}}}_{g_i}] \mathbf{r}'_{G_{c_i}/G_i} + [\tilde{\mathbf{r}}_{G_{c_i}/B}]^T \dot{\boldsymbol{\omega}} + 2[\tilde{\mathbf{r}}'_{G_{c_i}/B}]^T \boldsymbol{\omega} + [\tilde{\boldsymbol{\omega}}][\tilde{\boldsymbol{\omega}}] \mathbf{r}_{G_{c_i}/B} \right]\end{aligned}\quad (3.53)$$

The parallel axis theorem relating the gimbal inertia about point B to the gimbal inertia about point G_{c_i} is given by

$$[I_{G_i,B}] = [I_{G_i,G_{c_i}}] + m_{G_i} [\tilde{\mathbf{r}}_{G_{c_i}/B}] [\tilde{\mathbf{r}}_{G_{c_i}/B}]^T \quad (3.54)$$

Note the following simplification (using the triple product identity):

$$[\tilde{\mathbf{r}}_{G_{c_i}/B}] [\tilde{\boldsymbol{\omega}}][\tilde{\boldsymbol{\omega}}] \mathbf{r}_{G_{c_i}/B} = [\tilde{\boldsymbol{\omega}}][\tilde{\mathbf{r}}_{G_{c_i}/B}] [\tilde{\mathbf{r}}_{G_{c_i}/B}]^T \boldsymbol{\omega}$$

Using Eq. (3.54), Eq. (3.53) simplifies to

$$\begin{aligned}\dot{\mathbf{H}}_{G_i,B} &= [I_{G_i,B}] \dot{\boldsymbol{\omega}} + [I_{G_i,G_{c_i}}] \dot{\gamma}_i \hat{\mathbf{g}}_{g_i} + [I_{G_i,G_{c_i}}]' \boldsymbol{\omega}_{g_i/\mathcal{N}} + [\tilde{\boldsymbol{\omega}}][I_{G_i,B}] \boldsymbol{\omega} + [\tilde{\boldsymbol{\omega}}][I_{G_i,G_{c_i}}] \dot{\gamma}_i \hat{\mathbf{g}}_{g_i} \\ &\quad + m_{G_i} [\tilde{\mathbf{r}}_{G_{c_i}/B}] \left[\ddot{\gamma}_i [\tilde{\hat{\mathbf{g}}}_{g_i}] \mathbf{r}_{G_{c_i}/G_i} + \dot{\gamma}_i [\tilde{\hat{\mathbf{g}}}_{g_i}] \mathbf{r}'_{G_{c_i}/G_i} + 2[\tilde{\mathbf{r}}'_{G_{c_i}/B}]^T \boldsymbol{\omega} \right]\end{aligned}\quad (3.55)$$

The next step is to employ the body frame derivative of the parallel axis theorem.

$$[I_{G_i,B}]' = [I_{G_i,G_{c_i}}]' + m_{G_i} [\tilde{\mathbf{r}}'_{G_{c_i}/B}] [\tilde{\mathbf{r}}_{G_{c_i}/B}]^T + m_{G_i} [\tilde{\mathbf{r}}_{G_{c_i}/B}] [\tilde{\mathbf{r}}'_{G_{c_i}/B}]^T \quad (3.56)$$

Note the following simplification (using the triple product identity):

$$\begin{aligned}\mathbf{r}_{G_{c_i}/B} \times (\boldsymbol{\omega} \times \mathbf{r}'_{G_{c_i}/B}) &= (\mathbf{r}_{G_{c_i}/B} \times \boldsymbol{\omega}) \times \mathbf{r}'_{G_{c_i}/B} + \boldsymbol{\omega} \times (\mathbf{r}_{G_{c_i}/B} \times \mathbf{r}'_{G_{c_i}/B}) \\ &= [\tilde{\mathbf{r}}'_{G_{c_i}/B}] [\tilde{\mathbf{r}}_{G_{c_i}/B}]^T \boldsymbol{\omega} + [\tilde{\boldsymbol{\omega}}][\tilde{\mathbf{r}}_{G_{c_i}/B}] \mathbf{r}'_{G_{c_i}/B}\end{aligned}$$

Eq. (3.55) is further simplified using Eq. (3.56) to give the gimbal angular momentum derivative.

$$\begin{aligned} \dot{\mathbf{H}}_{G_i,B} = & [I_{G_i,B}] \dot{\boldsymbol{\omega}} + [I_{G_i,B}]' \boldsymbol{\omega} + [\tilde{\boldsymbol{\omega}}][I_{G_i,B}] \boldsymbol{\omega} + [I_{G_i,G_{c_i}}] \ddot{\gamma}_i \hat{\mathbf{g}}_{g_i} + [I_{G_i,G_{c_i}}]' \dot{\gamma}_i \hat{\mathbf{g}}_{g_i} + [\tilde{\boldsymbol{\omega}}][I_{G_i,G_{c_i}}] \dot{\gamma}_i \hat{\mathbf{g}}_{g_i} \\ & + m_{G_i} [\tilde{\mathbf{r}}_{G_{c_i}/B}] \left[\ddot{\gamma}_i [\tilde{\hat{\mathbf{g}}}_{g_i}] \mathbf{r}_{G_{c_i}/G_i} + \dot{\gamma}_i [\tilde{\hat{\mathbf{g}}}_{g_i}] \mathbf{r}'_{G_{c_i}/G_i} \right] + m_{G_i} [\tilde{\boldsymbol{\omega}}] [\tilde{\mathbf{r}}_{G_{c_i}/B}] \mathbf{r}'_{G_{c_i}/B} \end{aligned} \quad (3.57)$$

The next step is to derive the wheel angular momentum derivative $\dot{\mathbf{H}}_{W_i,B}$. Recall that the i^{th} wheel frame is defined as

$$\mathcal{W}_i : \{W_i, \hat{\mathbf{g}}_{s_i}, \hat{\mathbf{w}}_{2_i}, \hat{\mathbf{w}}_{3_i}\}$$

Angular velocity of the wheel with respect to inertial is

$$\boldsymbol{\omega}_{\mathcal{W}_i/\mathcal{N}} = \boldsymbol{\omega}_{\mathcal{B}/\mathcal{N}} + \boldsymbol{\omega}_{\mathcal{G}_i/B} + \boldsymbol{\omega}_{\mathcal{W}_i/\mathcal{G}_i} = \boldsymbol{\omega} + \dot{\gamma}_i \hat{\mathbf{g}}_{g_i} + \Omega_i \hat{\mathbf{g}}_{s_i} \quad (3.58)$$

The wheel angular momentum about point W_{c_i} is given by

$$\mathbf{H}_{W_i,W_{c_i}} = [I_{W_i,W_{c_i}}] \boldsymbol{\omega}_{\mathcal{W}_i/\mathcal{N}} = [I_{W_i,W_{c_i}}] (\boldsymbol{\omega} + \dot{\gamma}_i \hat{\mathbf{g}}_{g_i} + \Omega_i \hat{\mathbf{g}}_{s_i}) \quad (3.59)$$

Angular momentum about point W_{c_i} is related to point B using the following equation.

$$\mathbf{H}_{W_i,B} = \mathbf{H}_{W_i,W_{c_i}} + m_{W_i} \mathbf{r}_{W_{c_i}/B} \times \dot{\mathbf{r}}_{W_{c_i}/B} \quad (3.60)$$

Take the inertial derivative.

$$\begin{aligned} \dot{\mathbf{H}}_{W_i,B} = & [I_{W_i,W_{c_i}}] (\dot{\boldsymbol{\omega}} + \ddot{\gamma}_i \hat{\mathbf{g}}_{g_i} + \dot{\Omega}_i \hat{\mathbf{g}}_{s_i} + \Omega_i \dot{\gamma}_i \hat{\mathbf{g}}_{t_i}) + [I_{W_i,W_{c_i}}]' \boldsymbol{\omega}_{\mathcal{W}_i/\mathcal{N}} \\ & + [\tilde{\boldsymbol{\omega}}][I_{W_i,W_{c_i}}] \boldsymbol{\omega}_{\mathcal{W}_i/\mathcal{N}} + m_{W_i} \mathbf{r}_{W_{c_i}/B} \times \ddot{\mathbf{r}}_{W_{c_i}/B} \end{aligned} \quad (3.61)$$

The body relative inertia tensor time derivative $[I_{r_{w_i},W_{c_i}}]'$ needs to be defined. For this general RW model, the inertia matrix of the RW in the \mathcal{W}_i frame is defined as

$$[I_{W_i,W_{c_i}}] = \begin{matrix} \mathcal{W}_i \\ \begin{bmatrix} J_{11_i} & J_{12_i} & J_{13_i} \\ J_{12_i} & J_{22_i} & J_{23_i} \\ J_{13_i} & J_{23_i} & J_{33_i} \end{bmatrix} \end{matrix} \quad (3.62)$$

The definition of $[I_{W_i, W_{c_i}}]$ allows for any RW inertia matrix to be considered. In order to take the body frame derivative of $[I_{W_i, W_{c_i}}]$, Eq. (3.62) is rewritten in a general form using outer product expansions.

$$\begin{aligned}
[I_{W_i, W_{c_i}}] &= J_{11_i} \hat{\mathbf{g}}_{s_i} \hat{\mathbf{g}}_{s_i}^T + J_{12_i} \hat{\mathbf{g}}_{s_i} \hat{\mathbf{w}}_{2_i}^T + J_{13_i} \hat{\mathbf{g}}_{s_i} \hat{\mathbf{w}}_{3_i}^T \\
&\quad + J_{12_i} \hat{\mathbf{w}}_{2_i} \hat{\mathbf{g}}_{s_i}^T + J_{22_i} \hat{\mathbf{w}}_{2_i} \hat{\mathbf{w}}_{2_i}^T + J_{23_i} \hat{\mathbf{w}}_{2_i} \hat{\mathbf{w}}_{3_i}^T \\
&\quad + J_{13_i} \hat{\mathbf{w}}_{3_i} \hat{\mathbf{g}}_{s_i}^T + J_{23_i} \hat{\mathbf{w}}_{3_i} \hat{\mathbf{w}}_{2_i}^T + J_{33_i} \hat{\mathbf{w}}_{3_i} \hat{\mathbf{w}}_{3_i}^T
\end{aligned} \tag{3.63}$$

Take the body frame derivative.

$$\begin{aligned}
[I_{W_i, W_{c_i}}]' &= J_{11_i} \hat{\mathbf{g}}'_{s_i} \hat{\mathbf{g}}_{s_i}^T + J_{11_i} \hat{\mathbf{g}}_{s_i} \hat{\mathbf{g}}'^{T'}_{s_i} + J_{12_i} \hat{\mathbf{g}}'_{s_i} \hat{\mathbf{w}}_{2_i}^T + J_{12_i} \hat{\mathbf{g}}_{s_i} \hat{\mathbf{w}}'^{T'}_{2_i} + J_{13_i} \hat{\mathbf{g}}'_{s_i} \hat{\mathbf{w}}_{3_i}^T + J_{13_i} \hat{\mathbf{g}}_{s_i} \hat{\mathbf{w}}'^{T'}_{3_i} \\
&\quad + J_{12_i} \hat{\mathbf{w}}'_{2_i} \hat{\mathbf{g}}_{s_i}^T + J_{12_i} \hat{\mathbf{w}}_{2_i} \hat{\mathbf{g}}'^{T'}_{s_i} + J_{22_i} \hat{\mathbf{w}}'_{2_i} \hat{\mathbf{w}}_{2_i}^T + J_{22_i} \hat{\mathbf{w}}_{2_i} \hat{\mathbf{w}}'^{T'}_{2_i} + J_{23_i} \hat{\mathbf{w}}'_{2_i} \hat{\mathbf{w}}_{3_i}^T + J_{23_i} \hat{\mathbf{w}}_{2_i} \hat{\mathbf{w}}'^{T'}_{3_i} \\
&\quad + J_{13_i} \hat{\mathbf{w}}'_{3_i} \hat{\mathbf{g}}_{s_i}^T + J_{13_i} \hat{\mathbf{w}}_{3_i} \hat{\mathbf{g}}'^{T'}_{s_i} + J_{23_i} \hat{\mathbf{w}}'_{3_i} \hat{\mathbf{w}}_{2_i}^T + J_{23_i} \hat{\mathbf{w}}_{3_i} \hat{\mathbf{w}}'^{T'}_{2_i} + J_{33_i} \hat{\mathbf{w}}'_{3_i} \hat{\mathbf{w}}_{3_i}^T + J_{33_i} \hat{\mathbf{w}}_{3_i} \hat{\mathbf{w}}'^{T'}_{3_i}
\end{aligned} \tag{3.64}$$

Recall that the body frame derivatives of wheel frame basis vectors are (reprinted for convenience)

$$\begin{aligned}
\hat{\mathbf{g}}'_{s_i} &= \dot{\gamma}_i \hat{\mathbf{g}}_{t_i} \\
\hat{\mathbf{g}}'_{t_i} &= -\dot{\gamma}_i \hat{\mathbf{g}}_{s_i} \\
\hat{\mathbf{g}}'_{g_i} &= \mathbf{0} \\
\hat{\mathbf{w}}'_{2_i} &= \Omega_i \hat{\mathbf{w}}_{3_i} - \dot{\gamma}_i c \theta_i \hat{\mathbf{g}}_{s_i} \\
\hat{\mathbf{w}}'_{3_i} &= \dot{\gamma}_i s \theta_i \hat{\mathbf{g}}_{s_i} - \Omega_i \hat{\mathbf{w}}_{2_i}
\end{aligned}$$

After an exhausting amount of algebra, Eq. 3.64 simplifies to the following tensor (given in wheel frame components).

$$\begin{aligned}
&[I_{W_i, W_{c_i}}]' = \\
&w_i \begin{bmatrix} 2\dot{\gamma}_i(J_{13_i} s \theta_i - J_{12_i} c \theta_i) & \dot{\gamma}_i(J_{a_i} c \theta_i + J_{23_i} s \theta_i) - J_{13_i} \Omega_i & \dot{\gamma}_i(J_{b_i} s \theta_i - J_{23_i} c \theta_i) + J_{12_i} \Omega_i \\ \dot{\gamma}_i(J_{a_i} c \theta_i + J_{23_i} s \theta_i) - J_{13_i} \Omega_i & 2(J_{12_i} \dot{\gamma}_i c \theta_i - J_{23_i} \Omega_i) & \dot{\gamma}_i(J_{13_i} c \theta_i - J_{12_i} s \theta_i) + J_{c_i} \Omega_i \\ \dot{\gamma}_i(J_{b_i} s \theta_i - J_{23_i} c \theta_i) + J_{12_i} \Omega_i & \dot{\gamma}_i(J_{13_i} c \theta_i - J_{12_i} s \theta_i) + J_{c_i} \Omega_i & 2(J_{23_i} \Omega_i - J_{13_i} \dot{\gamma}_i s \theta_i) \end{bmatrix}
\end{aligned} \tag{3.65}$$

Where,

$$J_{a_i} = J_{11_i} - J_{22_i} \quad (3.66)$$

$$J_{b_i} = J_{33_i} - J_{11_i} \quad (3.67)$$

$$J_{c_i} = J_{22_i} - J_{33_i} \quad (3.68)$$

Note that if we assume $J_{12} = J_{23} = 0$ this tensor becomes,

$$[I_{W_i, W_{c_i}}]' = \begin{matrix} \mathcal{W}_i \\ \left[\begin{array}{ccc} 2\dot{\gamma}_i J_{13_i} s\theta_i & \dot{\gamma}_i J_{a_i} c\theta_i - J_{13_i} \Omega_i & \dot{\gamma}_i J_{b_i} s\theta_i \\ \dot{\gamma}_i J_{a_i} c\theta_i - J_{13_i} \Omega_i & 0 & \dot{\gamma}_i J_{13_i} c\theta_i + J_{c_i} \Omega_i \\ \dot{\gamma}_i J_{b_i} s\theta_i & \dot{\gamma}_i J_{13_i} c\theta_i + J_{c_i} \Omega_i & -2J_{13_i} \dot{\gamma}_i s\theta_i \end{array} \right] \end{matrix} \quad (3.69)$$

Furthermore, by assuming $J_{22_i} = J_{33_i}$, $J_{13} = 0$, and $\theta_i = 0$ (since the wheel frame does not rotate), the equation above simplifies to

$$[I_{W_i, W_{c_i}}]' = \begin{matrix} \mathcal{W}_i \\ \left[\begin{array}{ccc} 0 & \dot{\gamma}_i J_{a_i} c\theta_i & 0 \\ \dot{\gamma}_i J_{a_i} c\theta_i & 0 & 0 \\ 0 & 0 & 0 \end{array} \right] \end{matrix} \quad (3.70)$$

The second inertial derivative of $\mathbf{r}_{W_{c_i}/B}$ is needed. Note that the static imbalance is fundamentally an impact of the wheel center of mass offset d_i . We arbitrarily allow this offset to act in the $\hat{\mathbf{w}}_{2_i}$ direction. The center of mass of the wheel with respect to point W_i is thus given by

$$\mathbf{r}_{W_{c_i}/W_i} = d_i \hat{\mathbf{w}}_{2_i} \quad (3.71)$$

Additionally, point W does not lie on the body fixed gimbal axis $\hat{\mathbf{g}}_{g_i}$ for all VSCMGs. Such an offset subtly contributes to jitter. Thus, we introduce a radial offset ℓ_i of the wheel center of mass. Point W_i is related to point G_i by

$$\mathbf{r}_{W_i/G_i} = \ell_i \hat{\mathbf{g}}_{s_i} + L_i \hat{\mathbf{g}}_{g_i} \quad (3.72)$$

where L_i is the axial offset of the wheel from the gimbal origin that is common in many VSCMGs. The time varying vector that relates the wheel center of mass to the body frame origin is then given by

$$\mathbf{r}_{W_{c_i}/B} = \mathbf{r}_{W_{c_i}/W_i} + \mathbf{r}_{W_i/G_i} + \mathbf{r}_{G_i/B} = d_i \hat{\mathbf{w}}_{2_i} + \ell_i \hat{\mathbf{g}}_{s_i} + L_i \hat{\mathbf{g}}_{g_i} + \mathbf{r}_{G_i/B} \quad (3.73)$$

Recalling that $\mathbf{r}_{G_i/B}$ and $\hat{\mathbf{g}}_{g_i}$ are both body frame fixed vectors, we define the body frame derivative and first inertial derivative of $\mathbf{r}_{W_{c_i}/B}$.

$$\mathbf{r}'_{W_{c_i}/B} = \mathbf{r}'_{W_{c_i}/G} = d_i \hat{\mathbf{w}}'_{2_i} + \ell_i \hat{\mathbf{g}}'_{s_i} = d_i \Omega_i \hat{\mathbf{w}}_{3_i} - d_i \dot{\gamma}_i c \theta_i \hat{\mathbf{g}}_{s_i} + \ell_i \dot{\gamma}_i \hat{\mathbf{g}}_{t_i} \quad (3.74)$$

$$\dot{\mathbf{r}}_{W_{c_i}/B} = \mathbf{r}'_{W_{c_i}/B} + \boldsymbol{\omega} \times \mathbf{r}_{W_{c_i}/B} \quad (3.75)$$

The second inertial derivative of $\mathbf{r}_{W_{c_i}/B}$ is

$$\begin{aligned} \ddot{\mathbf{r}}_{W_{c_i}/B} &= \mathbf{r}''_{W_{c_i}/B} + \dot{\boldsymbol{\omega}} \times \mathbf{r}_{W_{c_i}/B} + \boldsymbol{\omega} \times \mathbf{r}'_{W_{c_i}/B} + \boldsymbol{\omega} \times \dot{\mathbf{r}}_{W_{c_i}/B} \\ &= \mathbf{r}''_{W_{c_i}/B} + [\tilde{\mathbf{r}}_{W_{c_i}/B}]^T \dot{\boldsymbol{\omega}} + 2[\tilde{\mathbf{r}}'_{W_{c_i}/B}]^T \boldsymbol{\omega} + [\tilde{\boldsymbol{\omega}}][\tilde{\boldsymbol{\omega}}] \mathbf{r}_{W_{c_i}/B} \end{aligned} \quad (3.76)$$

The second body frame derivative of $\mathbf{r}_{W_{c_i}/B}$ was defined in Eq. (3.17) and is reprinted here for the reader's convenience.

$$\mathbf{r}''_{W_{c_i}/B} = (2d_i \dot{\gamma}_i \Omega_i s \theta_i - d_i \ddot{\gamma}_i c \theta_i - \ell_i \dot{\gamma}_i^2) \hat{\mathbf{g}}_{s_i} + (\ell_i \ddot{\gamma}_i - d_i \dot{\gamma}_i^2 c \theta_i) \hat{\mathbf{g}}_{t_i} - d_i \Omega_i^2 \hat{\mathbf{w}}_{2_i} + d_i \dot{\Omega}_i \hat{\mathbf{w}}_{3_i}$$

Substitute Eq. (3.76) into Eq. (3.61).

$$\begin{aligned} \dot{\mathbf{H}}_{W_i,B} &= [I_{W_i,W_{c_i}}](\dot{\boldsymbol{\omega}} + \dot{\gamma}_i \hat{\mathbf{g}}_{g_i} + \dot{\Omega}_i \hat{\mathbf{g}}_{s_i} + \Omega_i \dot{\gamma}_i \hat{\mathbf{g}}_{t_i}) + [I_{W_i,W_{c_i}}]' \boldsymbol{\omega}_{W_i/N} + [\tilde{\boldsymbol{\omega}}][I_{W_i,W_{c_i}}] \boldsymbol{\omega}_{W_i/N} \\ &\quad + m_{W_i} [\tilde{\mathbf{r}}_{W_{c_i}/B}] \left[\mathbf{r}''_{W_{c_i}/B} + [\tilde{\mathbf{r}}_{W_{c_i}/B}]^T \dot{\boldsymbol{\omega}} + 2[\tilde{\mathbf{r}}'_{W_{c_i}/B}]^T \boldsymbol{\omega} + [\tilde{\boldsymbol{\omega}}][\tilde{\boldsymbol{\omega}}] \mathbf{r}_{W_{c_i}/B} \right] \end{aligned} \quad (3.77)$$

The parallel axis theorem relating the gimbal inertia about point B to the gimbal inertia about point W_{c_i} is given by

$$[I_{W_i,B}] = [I_{W_i,W_{c_i}}] + m_{W_i} [\tilde{\mathbf{r}}_{W_{c_i}/B}] [\tilde{\mathbf{r}}_{W_{c_i}/B}]^T \quad (3.78)$$

Using Eq. (3.78), Eq. (3.77) simplifies to

$$\begin{aligned} \dot{\mathbf{H}}_{W_i,B} &= [I_{W_i,B}] \dot{\boldsymbol{\omega}} + [I_{W_i,W_{c_i}}](\dot{\gamma}_i \hat{\mathbf{g}}_{g_i} + \dot{\Omega}_i \hat{\mathbf{g}}_{s_i} + \Omega_i \dot{\gamma}_i \hat{\mathbf{g}}_{t_i}) + [\tilde{\boldsymbol{\omega}}][I_{W_i,B}] \boldsymbol{\omega} + [\tilde{\boldsymbol{\omega}}][I_{W_i,W_{c_i}}] \boldsymbol{\omega}_{W_i/B} \\ &\quad + [I_{W_i,W_{c_i}}]' \boldsymbol{\omega}_{W_i/N} + m_{W_i} [\tilde{\mathbf{r}}_{W_{c_i}/B}] \left[\mathbf{r}''_{W_{c_i}/B} + 2[\tilde{\mathbf{r}}'_{W_{c_i}/B}]^T \boldsymbol{\omega} \right] \end{aligned} \quad (3.79)$$

The next step is to employ the body frame derivative of the parallel axis theorem.

$$[I_{W_i,B}]' = [I_{W_i,W_{c_i}}]' + m_{W_i} [\tilde{\mathbf{r}}'_{W_{c_i}/B}] [\tilde{\mathbf{r}}_{W_{c_i}/B}]^T + m_{W_i} [\tilde{\mathbf{r}}_{W_{c_i}/B}] [\tilde{\mathbf{r}}'_{W_{c_i}/B}]^T \quad (3.80)$$

Note the following simplification (using the triple product identity):

$$\begin{aligned} \mathbf{r}_{W_{c_i}/B} \times (\boldsymbol{\omega} \times \mathbf{r}'_{W_{c_i}/B}) &= (\mathbf{r}_{W_{c_i}/B} \times \boldsymbol{\omega}) \times \mathbf{r}'_{W_{c_i}/B} + \boldsymbol{\omega} \times (\mathbf{r}_{W_{c_i}/B} \times \mathbf{r}'_{W_{c_i}/B}) \\ &= [\tilde{\mathbf{r}}'_{W_{c_i}/B}] [\tilde{\mathbf{r}}_{W_{c_i}/B}]^T \boldsymbol{\omega} + [\tilde{\boldsymbol{\omega}}] [\tilde{\mathbf{r}}_{W_{c_i}/B}] \mathbf{r}'_{W_{c_i}/B} \end{aligned}$$

Eq. (3.79) is further simplified using Eq. (3.80) to give the wheel angular momentum derivative.

$$\begin{aligned} \dot{\mathbf{H}}_{W_i,B} = & [I_{W_i,B}] \dot{\boldsymbol{\omega}} + [I_{W_i,B}]' \boldsymbol{\omega} + [\tilde{\boldsymbol{\omega}}][I_{W_i,B}] \boldsymbol{\omega} + [I_{W_i,W_{c_i}}](\dot{\gamma}_i \hat{\mathbf{g}}_{g_i} + \dot{\Omega}_i \hat{\mathbf{g}}_{s_i} + \Omega_i \dot{\gamma}_i \hat{\mathbf{g}}_{t_i}) + [I_{W_i,W_{c_i}}]' \boldsymbol{\omega}_{W_i/B} \\ & + [\tilde{\boldsymbol{\omega}}][I_{W_i,W_{c_i}}] \boldsymbol{\omega}_{W_i/B} + m_{W_i} [\tilde{\mathbf{r}}_{W_{c_i}/B}] \mathbf{r}_{W_{c_i}/B}'' + m_{W_i} [\tilde{\boldsymbol{\omega}}][\tilde{\mathbf{r}}_{W_{c_i}/B}] \mathbf{r}_{W_{c_i}/B}' \end{aligned} \quad (3.81)$$

We may now formulate the rotational equations of motion. Euler's equation is rearranged as

$$m_{sc} [\tilde{\mathbf{c}}] \ddot{\mathbf{r}}_{B/N} + \dot{\mathbf{H}}_{B,B} + \sum_{i=1}^N (\dot{\mathbf{H}}_{G_i,B} + \dot{\mathbf{H}}_{W_i,B}) = \mathbf{L}_B \quad (3.82)$$

The rotational equations of motion are formulated by substituting Equations (3.38), (3.57), and (3.81) into Eq. (3.82)

$$\begin{aligned} m_{sc} [\tilde{\mathbf{c}}] \ddot{\mathbf{r}}_{B/N} + [I_{sc,B}] \dot{\boldsymbol{\omega}} + \sum_{i=1}^N \left[[I_{G_i,G_{c_i}}] \hat{\mathbf{g}}_{g_i} + m_{G_i} [\tilde{\mathbf{r}}_{G_{c_i}/B}] [\tilde{\hat{\mathbf{g}}}_{g_i}] \mathbf{r}_{G_{c_i}/G_i} + [I_{W_i,W_{c_i}}] \hat{\mathbf{g}}_{g_i} \right. \\ \left. + m_{W_i} [\tilde{\mathbf{r}}_{W_{c_i}/B}] (\ell_i \hat{\mathbf{g}}_{t_i} - d_i c \theta_i \hat{\mathbf{g}}_{s_i}) \right] \dot{\gamma}_i + \sum_{i=1}^N \left[[I_{W_i,W_{c_i}}] \hat{\mathbf{g}}_{s_i} + m_{W_i} d_i [\tilde{\mathbf{r}}_{W_{c_i}/B}] \hat{\mathbf{w}}_{3_i} \right] \dot{\Omega}_i \\ = \mathbf{L}_B - [I_{sc,B}]' \boldsymbol{\omega} - [\tilde{\boldsymbol{\omega}}][I_{sc,B}] \boldsymbol{\omega} - \sum_{i=1}^N \left[[I_{G_i,G_{c_i}}]' \dot{\gamma}_i \hat{\mathbf{g}}_{g_i} + [\tilde{\boldsymbol{\omega}}][I_{G_i,G_{c_i}}] \dot{\gamma}_i \hat{\mathbf{g}}_{g_i} + m_{G_i} [\tilde{\boldsymbol{\omega}}][\tilde{\mathbf{r}}_{G_{c_i}/B}] \mathbf{r}_{G_{c_i}/B}' \right. \\ \left. + m_{G_i} \dot{\gamma}_i [\tilde{\mathbf{r}}_{G_{c_i}/B}] [\tilde{\hat{\mathbf{g}}}_{g_i}] \mathbf{r}_{G_{c_i}/G_i}' + [I_{W_i,W_{c_i}}] \Omega_i \dot{\gamma}_i \hat{\mathbf{g}}_{t_i} + [I_{W_i,W_{c_i}}]' \boldsymbol{\omega}_{W_i/B} + [\tilde{\boldsymbol{\omega}}][I_{W_i,W_{c_i}}] \boldsymbol{\omega}_{W_i/B} \right. \\ \left. + m_{W_i} [\tilde{\boldsymbol{\omega}}][\tilde{\mathbf{r}}_{W_{c_i}/B}] \mathbf{r}_{W_{c_i}/B}' + m_{W_i} [\tilde{\mathbf{r}}_{W_{c_i}/B}] \left[(2d_i \dot{\gamma}_i \Omega_i s \theta_i - \ell_i \dot{\gamma}_i^2) \hat{\mathbf{g}}_{s_i} - d_i \dot{\gamma}_i^2 c \theta_i \hat{\mathbf{g}}_{t_i} - d_i \Omega_i^2 \hat{\mathbf{w}}_{2_i} \right] \right] \end{aligned} \quad (3.83)$$

The total spacecraft inertia about point B is given by,

$$[I_{sc,B}] = [I_{B,B}] + \sum_{i=1}^N [I_{vscmg_i,B}] \quad (3.84)$$

where,

$$[I_{vscmg_i,B}] = [I_{G_i,B}] + [I_{W_i,B}] \quad (3.85)$$

The rotational equation of motion for a VSCMG with balanced wheels may be found by setting imbalance terms to zero.

$$\begin{aligned}
m_{sc}[\tilde{\mathbf{c}}]\ddot{\mathbf{r}}_{B/N} + [I_{sc,B}]\dot{\boldsymbol{\omega}} + \sum_{i=1}^N I_{V_{g_i}} \hat{\mathbf{g}}_{g_i} \ddot{\gamma}_i + \sum_{i=1}^N I_{W_{s_i}} \hat{\mathbf{g}}_{s_i} \dot{\Omega}_i \\
= \mathbf{L}_B - [\tilde{\boldsymbol{\omega}}][I_{sc,B}]\boldsymbol{\omega} - \sum_{i=1}^N \left[\omega_t \dot{\gamma}_i (I_{V_{s_i}} - I_{V_{t_i}} + I_{V_{g_i}}) \hat{\mathbf{g}}_{s_i} \right. \\
\left. + [\omega_s \dot{\gamma}_i (I_{V_{s_i}} - I_{V_{t_i}} - I_{V_{g_i}}) + I_{W_{s_i}} \Omega_i (\dot{\gamma} + \omega_g)] \hat{\mathbf{g}}_{t_i} - \omega_t I_{W_{s_i}} \Omega_i \hat{\mathbf{g}}_{g_i} \right] \quad (3.86)
\end{aligned}$$

This equation agrees with that found in the reference. However, for back-substitution, we need it in the following form.

$$\begin{aligned}
m_{sc}[\tilde{\mathbf{c}}]\ddot{\mathbf{r}}_{B/N} + [I_{sc,B}]\dot{\boldsymbol{\omega}} + \sum_{i=1}^N I_{V_{g_i}} \hat{\mathbf{g}}_{g_i} \ddot{\gamma}_i + \sum_{i=1}^N I_{W_{s_i}} \hat{\mathbf{g}}_{s_i} \dot{\Omega}_i \\
= \mathbf{L}_B - [I_{sc,B}]\dot{\boldsymbol{\omega}} - [\tilde{\boldsymbol{\omega}}][I_{sc,B}]\boldsymbol{\omega} - \sum_{i=1}^N \left[I_{W_{t_i}} \Omega \dot{\gamma} \hat{\mathbf{g}}_{t_i} + \Omega_i \dot{\gamma}_i (I_{W_{s_i}} - I_{W_{t_i}}) \hat{\mathbf{g}}_{t_i} \right. \\
\left. + [\tilde{\boldsymbol{\omega}}][I_{G_i, G_{c_i}}] \dot{\gamma}_i \hat{\mathbf{g}}_{g_i} + [\tilde{\boldsymbol{\omega}}][I_{W_i, W_{c_i}}] \boldsymbol{\omega} \mathcal{W}_i / \mathcal{B} \right] \quad (3.87)
\end{aligned}$$

The equations of motion for an imbalanced RW may be obtained by setting $\ddot{\gamma}_i = \dot{\gamma}_i = 0$ in Eq. (3.83).

$$\begin{aligned}
m_{sc}[\tilde{\mathbf{c}}]\ddot{\mathbf{r}}_{B/N} + [I_{sc,B}]\dot{\boldsymbol{\omega}} + \sum_{i=1}^N \left[[I_{W_i, W_{c_i}}] \hat{\mathbf{g}}_{s_i} + m_{W_i} d_i [\tilde{\mathbf{r}}_{W_{c_i}/B}] \hat{\mathbf{w}}_{3_i} \right] \dot{\Omega}_i \\
= \mathbf{L}_B - [I_{sc,B}]\dot{\boldsymbol{\omega}} - [\tilde{\boldsymbol{\omega}}][I_{sc,B}]\boldsymbol{\omega} - \sum_{i=1}^N \left[[I_{W_i, W_{c_i}}] \boldsymbol{\omega} \mathcal{W}_i / \mathcal{B} + [\tilde{\boldsymbol{\omega}}][I_{W_i, W_{c_i}}] \boldsymbol{\omega} \mathcal{W}_i / \mathcal{B} \right. \\
\left. + m_{W_i} [\tilde{\boldsymbol{\omega}}] [\tilde{\mathbf{r}}_{W_{c_i}/B}] \mathbf{r}'_{W_{c_i}/B} - m_{W_i} d_i \Omega_i^2 [\tilde{\mathbf{r}}_{W_{c_i}/B}] \hat{\mathbf{w}}_{2_i} \right] \quad (3.88)
\end{aligned}$$

Eq. (3.88) agrees with the formulation found in Reference [27]. Eq. (3.88) is further reduced by setting all imbalance terms to zero.

$$m_{sc}[\tilde{\mathbf{c}}]\ddot{\mathbf{r}}_{B/N} + [I_{sc,B}]\dot{\boldsymbol{\omega}} + \sum_{i=1}^N [I_{W_i, W_{c_i}}] \hat{\mathbf{g}}_{s_i} \dot{\Omega}_i = \mathbf{L}_B - [\tilde{\boldsymbol{\omega}}][I_{sc,B}]\boldsymbol{\omega} - \sum_{i=1}^N [\tilde{\boldsymbol{\omega}}][I_{W_i, W_{c_i}}] \hat{\mathbf{g}}_{s_i} \Omega_i \quad (3.89)$$

If the center of mass of the spacecraft C is coincident with point B , this equation is reduced to

$$[I_{sc,B}]\dot{\boldsymbol{\omega}} + \sum_{i=1}^N [I_{W_i, W_{c_i}}] \hat{\mathbf{g}}_{s_i} \dot{\Omega}_i = \mathbf{L}_B - [\tilde{\boldsymbol{\omega}}][I_{sc,B}]\boldsymbol{\omega} - \sum_{i=1}^N [\tilde{\boldsymbol{\omega}}][I_{W_i, W_{c_i}}] \hat{\mathbf{g}}_{s_i} \Omega_i \quad (3.90)$$

This equation represents N balanced reaction wheels, and agrees with Reference [24].

3.2.3 Gimbal Torque Equation

The gimbal torque equation is used to relate body rate derivative $\dot{\boldsymbol{\omega}}_{\mathcal{B}/\mathcal{N}}$ and gimbal rate derivative $\ddot{\gamma}_i$. The VSCMG motor torque u_{g_i} is the $\hat{\boldsymbol{g}}_{g_i}$ component of gimbal torque about point G_i . The torque acting on a VSCMG at the joint between the motor and the gimbal assembly is given by

$$\mathbf{L}_{G_i} = \begin{matrix} G_i \\ \left[\begin{array}{c} \tau_{g_{s_i}} \\ \tau_{g_{t_i}} \\ u_{g_i} \end{array} \right] \end{matrix} \quad (3.91)$$

The transverse torques acting on the gimbal $\tau_{g_{s_i}}$ and $\tau_{g_{t_i}}$ are structural torques and do not contribute to the equation. Torque about point G_i is related to torque about the VSCMG center of mass V_{c_i} using the following equation.

$$\mathbf{L}_{G_i} = \mathbf{L}_{V_{c_i}} + m_{V_i} \mathbf{r}_{V_{c_i}/G_i} \times \ddot{\mathbf{r}}_{V_{c_i}/N} \quad (3.92)$$

Euler's equation applies as follows.

$$\mathbf{L}_{V_{c_i}} = \dot{\mathbf{H}}_{G_i, V_{c_i}} + \dot{\mathbf{H}}_{W_i, V_{c_i}} \quad (3.93)$$

The VSCMG motor torque is the $\hat{\boldsymbol{g}}_{g_i}$ component of the right-hand side of Eq. (3.92). This is found in a frame independent format as

$$u_{g_i} = \hat{\boldsymbol{g}}_{g_i}^T \mathbf{L}_{G_i} = \hat{\boldsymbol{g}}_{g_i}^T (\dot{\mathbf{H}}_{G_i, V_{c_i}} + \dot{\mathbf{H}}_{W_i, V_{c_i}} + \mathbf{r}_{V_{c_i}/G_i} \times m_{V_i} \ddot{\mathbf{r}}_{V_{c_i}/N}) \quad (3.94)$$

where the gimbal and wheel angular momentum derivatives about point V_{c_i} are related to point W_{c_i} using the following equation.

$$\dot{\mathbf{H}}_{G_i, V_{c_i}} = \dot{\mathbf{H}}_{G_i, G_{c_i}} + m_{G_i} \mathbf{r}_{G_{c_i}/V_{c_i}} \times \ddot{\mathbf{r}}_{G_{c_i}/V_{c_i}} \quad (3.95)$$

$$\dot{\mathbf{H}}_{W_i, V_{c_i}} = \dot{\mathbf{H}}_{W_i, W_{c_i}} + m_{W_i} \mathbf{r}_{W_{c_i}/V_{c_i}} \times \ddot{\mathbf{r}}_{W_{c_i}/V_{c_i}} \quad (3.96)$$

The inertial derivatives of the wheel and gimbal angular momentum about their respective centers of mass were found in the previous section and are reprinted here for the reader's convenience.

$$\dot{\mathbf{H}}_{G_i, G_{c_i}} = [I_{G_i, G_{c_i}}](\dot{\boldsymbol{\omega}} + \ddot{\gamma}_i \hat{\mathbf{g}}_{g_i}) + [I_{G_i, G_{c_i}}]' \boldsymbol{\omega}_{G_i/N} + [\tilde{\boldsymbol{\omega}}][I_{G_i, G_{c_i}}] \boldsymbol{\omega}_{G_i/N} \quad (3.97)$$

$$\dot{\mathbf{H}}_{W_i, W_{c_i}} = [I_{W_i, W_{c_i}}](\dot{\boldsymbol{\omega}} + \ddot{\gamma}_i \hat{\mathbf{g}}_{g_i} + \dot{\Omega}_i \hat{\mathbf{g}}_{s_i} + \Omega \dot{\gamma} \hat{\mathbf{g}}_{t_i}) + [I_{W_i, W_{c_i}}]' \boldsymbol{\omega}_{W_i/N} + [\tilde{\boldsymbol{\omega}}][I_{W_i, W_{c_i}}] \boldsymbol{\omega}_{W_i/N} \quad (3.98)$$

Define the terms on the right-hand side of Eq. (3.95).

$$\mathbf{r}_{G_{c_i}/V_{c_i}} = \mathbf{r}_{G_{c_i}/G_i} - \mathbf{r}_{V_{c_i}/G_i} \quad (3.99)$$

$$\dot{\mathbf{r}}_{G_{c_i}/V_{c_i}} = \mathbf{r}'_{G_{c_i}/V_{c_i}} + \boldsymbol{\omega} \times \mathbf{r}_{G_{c_i}/V_{c_i}} \quad (3.100)$$

$$\ddot{\mathbf{r}}_{G_{c_i}/V_{c_i}} = \mathbf{r}''_{G_{c_i}/V_{c_i}} + \dot{\boldsymbol{\omega}} \times \mathbf{r}_{G_{c_i}/V_{c_i}} + 2\boldsymbol{\omega} \times \mathbf{r}'_{G_{c_i}/V_{c_i}} + \boldsymbol{\omega} \times (\boldsymbol{\omega} \times \mathbf{r}_{G_{c_i}/V_{c_i}}) \quad (3.101)$$

Define the terms on the right-hand side of Eq. (3.96).

$$\mathbf{r}_{W_{c_i}/V_{c_i}} = \mathbf{r}_{W_{c_i}/G_i} - \mathbf{r}_{V_{c_i}/G_i} \quad (3.102)$$

$$\dot{\mathbf{r}}_{W_{c_i}/V_{c_i}} = \mathbf{r}'_{W_{c_i}/V_{c_i}} + \boldsymbol{\omega} \times \mathbf{r}_{W_{c_i}/V_{c_i}} \quad (3.103)$$

$$\ddot{\mathbf{r}}_{W_{c_i}/V_{c_i}} = \mathbf{r}''_{W_{c_i}/V_{c_i}} + \dot{\boldsymbol{\omega}} \times \mathbf{r}_{W_{c_i}/V_{c_i}} + 2\boldsymbol{\omega} \times \mathbf{r}'_{W_{c_i}/V_{c_i}} + \boldsymbol{\omega} \times (\boldsymbol{\omega} \times \mathbf{r}_{W_{c_i}/V_{c_i}}) \quad (3.104)$$

The body frame derivatives are given by

$$\mathbf{r}'_{G_{c_i}/V_{c_i}} = \mathbf{r}'_{G_{c_i}/G_i} - \mathbf{r}'_{V_{c_i}/G_i} \quad (3.105)$$

$$\mathbf{r}''_{G_{c_i}/V_{c_i}} = \mathbf{r}''_{G_{c_i}/G_i} - \mathbf{r}''_{V_{c_i}/G_i} \quad (3.106)$$

$$\mathbf{r}'_{W_{c_i}/V_{c_i}} = \mathbf{r}'_{W_{c_i}/G_i} - \mathbf{r}'_{V_{c_i}/G_i} \quad (3.107)$$

$$\mathbf{r}''_{W_{c_i}/V_{c_i}} = \mathbf{r}''_{W_{c_i}/G_i} - \mathbf{r}''_{V_{c_i}/G_i} \quad (3.108)$$

The VSCMG center of mass location with respect to point G_i and its body frame derivatives are given by

$$\mathbf{r}_{V_{c_i}/G_i} = \frac{1}{m_{V_i}} \left(m_{G_i} \mathbf{r}_{G_{c_i}/G_i} + m_{W_i} \mathbf{r}_{W_{c_i}/G_i} \right) \quad (3.109)$$

$$\mathbf{r}'_{V_{c_i}/G_i} = \rho_{G_i} \mathbf{r}'_{G_{c_i}/G_i} + \rho_{W_i} \mathbf{r}'_{W_{c_i}/G_i} \quad (3.110)$$

$$\mathbf{r}''_{V_{c_i}/G_i} = \rho_{G_i} \mathbf{r}''_{G_{c_i}/G_i} + \rho_{W_i} \mathbf{r}''_{W_{c_i}/G_i} \quad (3.111)$$

where the mass ratios are abbreviated as

$$\rho_{G_i} = \frac{m_{G_i}}{m_{G_i} + m_{W_i}} \quad (3.112)$$

$$\rho_{W_i} = \frac{m_{W_i}}{m_{G_i} + m_{W_i}} \quad (3.113)$$

Reprint Eq. (3.49), (3.52) for convenience.

$$\begin{aligned} \mathbf{r}'_{G_{c_i}/G_i} &= \dot{\gamma}_i [\tilde{\mathbf{g}}_{s_i}] \mathbf{r}_{G_{c_i}/G_i} \\ \mathbf{r}''_{G_{c_i}/G} &= \ddot{\gamma}_i [\tilde{\mathbf{g}}_{s_i}] \mathbf{r}_{G_{c_i}/G_i} + \dot{\gamma}_i [\dot{\tilde{\mathbf{g}}}_{s_i}] \mathbf{r}'_{G_{c_i}/G_i} \end{aligned}$$

Reprint Eq. (3.16), (3.17) for convenience.

$$\begin{aligned} \mathbf{r}'_{W_{c_i}/G} &= d_i \hat{\mathbf{w}}'_{2_i} + \ell_i \hat{\mathbf{g}}'_{s_i} = d_i \Omega_i \hat{\mathbf{w}}_{3_i} - d_i \dot{\gamma}_i c \theta_i \hat{\mathbf{g}}_{s_i} + \ell_i \dot{\gamma}_i \hat{\mathbf{g}}_{t_i} \\ \mathbf{r}''_{W_{c_i}/G} &= (2d_i \dot{\gamma}_i \Omega_i s \theta_i - d_i \ddot{\gamma}_i c \theta_i - \ell_i \dot{\gamma}_i^2) \hat{\mathbf{g}}_{s_i} + (\ell_i \ddot{\gamma}_i - d_i \dot{\gamma}_i^2 c \theta_i) \hat{\mathbf{g}}_{t_i} - d_i \Omega_i^2 \hat{\mathbf{w}}_{2_i} + d_i \dot{\Omega}_i \hat{\mathbf{w}}_{3_i} \\ \mathbf{r}''_{W_{c_i}/G} &= (\ell_i \hat{\mathbf{g}}_{t_i} - d_i c \theta_i \hat{\mathbf{g}}_{s_i}) \ddot{\gamma}_i + d_i \hat{\mathbf{w}}_{3_i} \dot{\Omega}_i + (2d_i \dot{\gamma}_i \Omega_i s \theta_i - \ell_i \dot{\gamma}_i^2) \hat{\mathbf{g}}_{s_i} - d_i \dot{\gamma}_i^2 c \theta_i \hat{\mathbf{g}}_{t_i} - d_i \Omega_i^2 \hat{\mathbf{w}}_{2_i} \end{aligned}$$

Evaluate $\ddot{\mathbf{r}}_{V_{c_i}/N}$.

$$\ddot{\mathbf{r}}_{V_{c_i}/N} = \ddot{\mathbf{r}}_{V_{c_i}/B} + \ddot{\mathbf{r}}_{B/N} \quad (3.114)$$

Find the second inertial derivative of $\mathbf{r}_{V_{c_i}/B}$ (note that $\mathbf{r}'_{V_{c_i}/G} = \mathbf{r}'_{V_{c_i}/B}$ and $\mathbf{r}''_{V_{c_i}/G} = \mathbf{r}''_{V_{c_i}/B}$)

$$\dot{\mathbf{r}}_{V_{c_i}/B} = \mathbf{r}'_{V_{c_i}/B} + \boldsymbol{\omega} \times \mathbf{r}_{V_{c_i}/B} \quad (3.115)$$

$$\ddot{\mathbf{r}}_{V_{c_i}/B} = \mathbf{r}''_{V_{c_i}/B} + \dot{\boldsymbol{\omega}} \times \mathbf{r}_{V_{c_i}/B} + 2\boldsymbol{\omega} \times \mathbf{r}'_{V_{c_i}/B} + \boldsymbol{\omega} \times (\boldsymbol{\omega} \times \mathbf{r}_{V_{c_i}/B}) \quad (3.116)$$

Substituting into Eq. (3.94) and performing a massive rearrange gives the VSCMG gimbal torque equation of motion.

$$\begin{aligned}
& \hat{\mathbf{g}}_{g_i}^T \left[m_{V_i} [\tilde{\mathbf{r}}_{V_{c_i}/G_i}] \ddot{\mathbf{r}}_{B/N} + \hat{\mathbf{g}}_{g_i}^T \left[[I_{V_i, V_{c_i}}] + m_{V_i} [\tilde{\mathbf{r}}_{V_{c_i}/G_i}] [\tilde{\mathbf{r}}_{V_{c_i}/B}]^T \right] \dot{\boldsymbol{\omega}} + \hat{\mathbf{g}}_{g_i}^T \left[[I_{G_i, G_{c_i}}] \hat{\mathbf{g}}_{g_i} \right. \right. \\
& \left. \left. + [I_{W_i, W_{c_i}}] \hat{\mathbf{g}}_{g_i} + [P_i] (\ell_i \hat{\mathbf{g}}_{t_i} - d_i c \theta_i \hat{\mathbf{g}}_{s_i}) + [Q_i] [\tilde{\mathbf{g}}_{g_i}] \mathbf{r}_{G_{c_i}/G_i} \right] \ddot{\gamma}_i + \hat{\mathbf{g}}_{g_i}^T \left[[I_{W_i, W_{c_i}}] \hat{\mathbf{g}}_{s_i} + [P_i] d_i \hat{\boldsymbol{\omega}}_{3_i} \right] \dot{\Omega}_i \right. \\
& = -\hat{\mathbf{g}}_{g_i}^T \left[\dot{\gamma}_i [Q_i] [\tilde{\mathbf{g}}_{g_i}] \mathbf{r}'_{G_{c_i}/G_i} + [P_i] \left[(2d_i \dot{\gamma}_i \Omega_i s \theta_i - \ell_i \dot{\gamma}_i^2) \hat{\mathbf{g}}_{s_i} - d_i \dot{\gamma}_i^2 c \theta_i \hat{\mathbf{g}}_{t_i} - d_i \Omega_i^2 \hat{\boldsymbol{\omega}}_{2_i} \right] \right. \\
& \quad \left. + [I_{G_i, G_{c_i}}]' \boldsymbol{\omega}_{G_i/N} + [\tilde{\boldsymbol{\omega}}] [I_{G_i, G_{c_i}}] \boldsymbol{\omega}_{G_i/N} + [I_{W_i, W_{c_i}}] \Omega \dot{\gamma} \hat{\mathbf{g}}_{t_i} + [I_{W_i, W_{c_i}}]' \boldsymbol{\omega}_{W_i/N} \right. \\
& \quad \left. + [\tilde{\boldsymbol{\omega}}] [I_{W_i, W_{c_i}}] \boldsymbol{\omega}_{W_i/N} + m_{G_i} [\tilde{\mathbf{r}}_{G_{c_i}/V_{c_i}}] (2[\tilde{\boldsymbol{\omega}}] \mathbf{r}'_{G_{c_i}/V_{c_i}} + [\tilde{\boldsymbol{\omega}}]^2 \mathbf{r}_{G_{c_i}/V_{c_i}}) \right. \\
& \quad \left. + m_{W_i} [\tilde{\mathbf{r}}_{W_{c_i}/V_{c_i}}] (2[\tilde{\boldsymbol{\omega}}] \mathbf{r}'_{W_{c_i}/V_{c_i}} + [\tilde{\boldsymbol{\omega}}]^2 \mathbf{r}_{W_{c_i}/V_{c_i}}) + m_{V_i} [\tilde{\mathbf{r}}_{V_{c_i}/G_i}] (2[\tilde{\boldsymbol{\omega}}] \mathbf{r}'_{V_{c_i}/B} + [\tilde{\boldsymbol{\omega}}]^2 \mathbf{r}_{V_{c_i}/B}) \right] + u_{g_i}
\end{aligned} \tag{3.117}$$

Where,

$$[I_{V_i, V_{c_i}}] = [I_{G_i, V_{c_i}}] + [I_{W_i, V_{c_i}}] \tag{3.118}$$

$$[I_{G_i, V_{c_i}}] = [I_{G_i, G_{c_i}}] + m_{G_i} [\tilde{\mathbf{r}}_{G_{c_i}/V_{c_i}}] [\tilde{\mathbf{r}}_{G_{c_i}/V_{c_i}}]^T \tag{3.119}$$

$$[I_{W_i, V_{c_i}}] = [I_{W_i, W_{c_i}}] + m_{W_i} [\tilde{\mathbf{r}}_{W_{c_i}/V_{c_i}}] [\tilde{\mathbf{r}}_{W_{c_i}/V_{c_i}}]^T \tag{3.120}$$

$$[P_i] = m_{W_i} \rho_{G_i} [\tilde{\mathbf{r}}_{W_{c_i}/V_{c_i}}] - m_{G_i} \rho_{W_i} [\tilde{\mathbf{r}}_{G_{c_i}/V_{c_i}}] + m_{W_i} [\tilde{\mathbf{r}}_{V_{c_i}/G_i}] \tag{3.121}$$

$$[Q_i] = m_{G_i} \rho_{W_i} [\tilde{\mathbf{r}}_{G_{c_i}/V_{c_i}}] - m_{W_i} \rho_{G_i} [\tilde{\mathbf{r}}_{W_{c_i}/V_{c_i}}] + m_{G_i} [\tilde{\mathbf{r}}_{V_{c_i}/G_i}] \tag{3.122}$$

$$[\tilde{\boldsymbol{\omega}}]^2 = [\tilde{\boldsymbol{\omega}}] [\tilde{\boldsymbol{\omega}}] \tag{3.123}$$

Removing all imbalance terms, Eq. (5.24) simplifies to the equation found in Reference [24].

$$I_{V_{g_i}} (\hat{\mathbf{g}}_{g_i}^T \dot{\boldsymbol{\omega}} + \ddot{\gamma}_i) = u_{g_i} + (I_{V_{s_i}} - I_{V_{t_i}}) \omega_s \omega_t + I_{W_{s_i}} \Omega_i \omega_t \tag{3.124}$$

3.2.4 Wheel Torque Equation

The wheel torque equation is used to relate body rate derivative $\dot{\boldsymbol{\omega}}_{B/N}$ and wheel speed derivative $\dot{\Omega}_i$. The wheel motor torque u_{s_i} is the $\hat{\mathbf{g}}_{s_i}$ component of wheel torque about point W_i .

The torque acting on a RW at the joint between the RW motor and the RW rotor is given by

$$\mathbf{L}_{W_i} = \begin{matrix} \mathcal{W}_i \\ \left[\begin{array}{c} u_{s_i} \\ \tau_{w_{2_i}} \\ \tau_{w_{3_i}} \end{array} \right] \end{matrix} \quad (3.125)$$

The transverse torques acting on the gimbal $\tau_{w_{2_i}}$ and $\tau_{w_{3_i}}$ are structural torques and do not contribute to the equation. Torque about point W_i is related to torque about W_{c_i} using the following equation.

$$\mathbf{L}_{W_i} = \mathbf{L}_{W_{c_i}} + \mathbf{r}_{W_{c_i}/W_i} \times m_{W_i} \ddot{\mathbf{r}}_{W_{c_i}/N} \quad (3.126)$$

Euler's equation applied as follows.

$$\mathbf{L}_{W_{c_i}} = \dot{\mathbf{H}}_{W_i, W_{c_i}} \quad (3.127)$$

The VSCMG motor torque is the $\hat{\mathbf{g}}_{g_i}$ component of the right-hand side of Eq. (3.126). This is found in a frame independent format as

$$u_{s_i} = \hat{\mathbf{g}}_{s_i}^T \mathbf{L}_{W_i} = \hat{\mathbf{g}}_{s_i}^T (\dot{\mathbf{H}}_{W_i, W_{c_i}} + \mathbf{r}_{W_{c_i}/W_i} \times m_{W_i} \ddot{\mathbf{r}}_{W_{c_i}/N}) \quad (3.128)$$

The inertial derivatives of the wheel and gimbal angular momentum about their respective centers of mass were found in the previous section and are reprinted here for the reader's convenience.

$$\dot{\mathbf{H}}_{W_i, W_{c_i}} = [I_{W_i, W_{c_i}}] (\dot{\boldsymbol{\omega}} + \ddot{\gamma}_i \hat{\mathbf{g}}_{g_i} + \dot{\Omega}_i \hat{\mathbf{g}}_{s_i} + \Omega_i \dot{\gamma}_i \hat{\mathbf{g}}_{t_i}) + [I_{W_i, W_{c_i}}]' \boldsymbol{\omega}_{W_i/N} + [\tilde{\boldsymbol{\omega}}] [I_{W_i, W_{c_i}}] \boldsymbol{\omega}_{W_i/N} \quad (3.129)$$

Define

$$\ddot{\mathbf{r}}_{W_{c_i}/N} = \mathbf{r}_{W_{c_i}/B}'' + [\tilde{\mathbf{r}}_{W_{c_i}/B}]^T \dot{\boldsymbol{\omega}} + 2[\tilde{\mathbf{r}}'_{W_{c_i}/B}]^T \boldsymbol{\omega} + [\tilde{\boldsymbol{\omega}}][\tilde{\boldsymbol{\omega}}] \mathbf{r}_{W_{c_i}/B} + \ddot{\mathbf{r}}_{B/N} \quad (3.130)$$

The second body frame derivative of $\mathbf{r}_{W_{c_i}/B}$ was defined in Eq. (3.17) and is reprinted here for the reader's convenience.

$$\mathbf{r}_{W_{c_i}/B}'' = (2d_i \dot{\gamma}_i \Omega_i s\theta_i - d_i \ddot{\gamma}_i c\theta_i - \ell_i \dot{\gamma}_i^2) \hat{\mathbf{g}}_{s_i} + (\ell_i \ddot{\gamma}_i - d_i \dot{\gamma}_i^2 c\theta_i) \hat{\mathbf{g}}_{t_i} - d_i \Omega_i^2 \hat{\mathbf{w}}_{2_i} + d_i \dot{\Omega}_i \hat{\mathbf{w}}_{3_i}$$

Substituting into Eq. (3.128) gives the wheel torque equation.

$$\begin{aligned}
& \left[m_{W_i} d_i \hat{\boldsymbol{w}}_{3_i}^T \right] \ddot{\boldsymbol{r}}_{B/N} + \left[\hat{\boldsymbol{g}}_{s_i}^T [I_{W_i, W_{c_i}}] + m_{W_i} d_i \hat{\boldsymbol{g}}_{s_i}^T [\tilde{\boldsymbol{w}}_{2_i}] [\tilde{\boldsymbol{r}}_{W_{c_i}/B}]^T \right] \dot{\boldsymbol{\omega}} \\
& \quad + [J_{12_i} s \theta_i + J_{13_i} c \theta_i - m_{W_i} d_i \ell_i s \theta_i] \ddot{\gamma}_i + [J_{11_i} + m_{W_i} d_i^2] \dot{\Omega}_i \\
& = -\hat{\boldsymbol{g}}_{s_i}^T \left[[I_{W_i, W_{c_i}}]' \boldsymbol{\omega}_{W_i/N} + [\tilde{\boldsymbol{\omega}}] [I_{W_i, W_{c_i}}] \boldsymbol{\omega}_{W_i/N} + m_{W_i} d_i [\tilde{\boldsymbol{w}}_{2_i}] \left[2[\tilde{\boldsymbol{r}}'_{W_{c_i}/B}]^T \boldsymbol{\omega} + [\tilde{\boldsymbol{\omega}}] [\tilde{\boldsymbol{\omega}}] \boldsymbol{r}_{W_{c_i}/B} \right] \right] \\
& \quad + (J_{13_i} s \theta_i - J_{12_i} c \theta_i) \Omega \dot{\gamma}_i - m_{W_i} d_i^2 \dot{\gamma}_i^2 c \theta_i s \theta_i + u_{s_i} \quad (3.131)
\end{aligned}$$

Removing imbalance terms gives (recall that for the simplified case $\theta_i = 0$),

$$I_{W_{s_i}} (\hat{\boldsymbol{g}}_{s_i}^T \dot{\boldsymbol{\omega}} + \dot{\Omega}_i) = -I_{W_{s_i}} \omega_t \dot{\gamma}_i + u_{s_i} \quad (3.132)$$

Chapter 4

Imbalance Parameter Adaptation

4.1 Simplified Imbalance Model

The well-used method to specify reaction wheel imbalance is to lump sources of imbalance into scalar parameters. The simplified reaction wheel imbalance model directly utilizes such specifications to model jitter as an external torque.[17, 8] Static imbalance, U_s , typically given in units of g-cm, specifies the proportionality of the square of wheel speed to the magnitude of disturbance force caused by an offset in center of mass from the geometric center of the reaction wheel. That is,

$$\mathbf{F}_{s_i} = U_{s_i} \Omega_i^2 \hat{\mathbf{u}}_i \quad (4.1)$$

where $\hat{\mathbf{u}}_i$ is an arbitrary unit vector normal to the wheel spin axis and \mathbf{F}_{s_i} is the resulting force on the spacecraft. If the reaction wheel is not coincident with the spacecraft center of mass, torque on the spacecraft resulting from the static imbalance force is given by the simplified model as

$$\mathbf{L}_{s_i} = \mathbf{r}_{W_i/B} \times \mathbf{F}_{s_i} = U_{s_i} \Omega_i^2 [\tilde{\mathbf{r}}_{W_i/B}] \hat{\mathbf{u}}_i \quad (4.2)$$

Note that the simplified model uses the approximation $\mathbf{r}_{W_{c_i}/B} \approx \mathbf{r}_{W_i/B}$ since d_i is usually very small and $\mathbf{r}_{W_i/B} \neq \mathbf{0}$.

Dynamic imbalance U_d , typically given in units g-cm², specifies the proportionality of the square of wheel speed to the magnitude of disturbance torque caused by off diagonal terms in the reaction wheel inertia tensor. That is,

$$\mathbf{L}_{d_i} = U_{d_i} \Omega_i^2 \hat{\mathbf{v}}_i \quad (4.3)$$

where $\hat{\mathbf{v}}_i$ is an arbitrary unit vector normal to the wheel spin axis and \mathbf{L}_{d_i} is the resulting torque on the spacecraft. Note that $\hat{\mathbf{u}}_i$ and $\hat{\mathbf{v}}_i$ are only required to be normal to their corresponding spin axis. This is because the lumped parameters U_{s_i} and U_{d_i} do not contain any information on orientation/location of mass imbalances about $\hat{\mathbf{g}}_{s_i}$. Additionally, the initial value of the wheel angle parameter is arbitrarily chosen, which further emphasizes the arbitrariness of the vectors $\hat{\mathbf{u}}_i$ and $\hat{\mathbf{v}}_i$ since they relate to the body frame through wheel angle θ_i .

4.2 Imbalance Parameter Adaptation

To relate the simplified model to the fully-coupled model developed within this paper, Eq. (2.39) is analyzed to identify terms that directly contribute to torque on the spacecraft. Noticing the presence of wheel speed squared and the cross product of wheel location in the term

$$m_{\text{rw}_i} d_i \Omega_i^2 [\tilde{\mathbf{r}}_{W_{c_i}/B}] \hat{\mathbf{w}}_{2_i}$$

it is equated to the simplified static imbalance model to yield

$$U_{s_i} \Omega_i^2 [\tilde{\mathbf{r}}_{W/B_i}] \hat{\mathbf{u}}_i = m_{\text{rw}_i} d_i \Omega_i^2 [\tilde{\mathbf{r}}_{W_{c_i}/B}] \hat{\mathbf{w}}_{2_i} \quad (4.4)$$

Rearranging this equation for U_{s_i} and making the approximation $\mathbf{r}_{W_{c_i}/B} \approx \mathbf{r}_{W_i/B}$ yields an expression for d_i

$$d_i = \frac{U_{s_i}}{m_{\text{rw}_i}} \quad (4.5)$$

For the dynamic imbalance, the presence of wheel speed multiplied by $[I_{\text{rw}_i, W_{c_i}}]'$ term results in an inertia value times the wheel speed squared

$$[I_{\text{rw}_i, W_{c_i}}]' \Omega_i \hat{\mathbf{g}}_{s_i}$$

Equating this term to the simplified dynamic imbalance model yields

$$U_{d_i} \Omega_i^2 \hat{\mathbf{v}}_i = [I_{\text{rw}_i, W_{c_i}}]' \Omega_i \hat{\mathbf{g}}_{s_i} = \Omega_i^2 \begin{bmatrix} 0 \\ -J_{13} \\ J_{12} \end{bmatrix} \quad (4.6)$$

Rearranging this equation for U_{d_i} yields Eq. (4.7) and agrees with the relationship found in Reference [8].

$$U_{d_i} = \sqrt{J_{13_i}^2 + J_{12_i}^2} \quad (4.7)$$

Thus, the fully-coupled model is under-constrained with respect to the implementation of the simplified model, and some combination of J_{12} and J_{13} must be selected for each wheel such that Eq. (4.7) is satisfied. Since the unit vector \hat{v}_i is arbitrary (as well as \hat{w}_{2_i} and \hat{w}_{3_i} due to the arbitrariness of initial wheel angle), the following definitions are chosen

$$J_{13_i} = U_{d_i} \quad (4.8a)$$

$$J_{12_i} = 0 \quad (4.8b)$$

To complete the discussion of characterizing RW imbalance from manufactures' specifications, the full inertia matrix needs to be defined. The balanced reaction wheel inertia tensor is

$$[I_{rw_i, W_{c_i}}] = \mathcal{P}_i \begin{bmatrix} J_{s_i} & 0 & 0 \\ 0 & J_{t_i} & 0 \\ 0 & 0 & J_{t_i} \end{bmatrix} \quad (4.9)$$

where \mathcal{P}_i is the principal axes frame of the RW. J_{s_i} and J_{t_i} are the spin axis inertia and transverse axis inertia of the RW, respectively. For there to only be J_{13_i} terms present in the \mathcal{W}_i representation of the RW's inertia tensor, the rotation matrix between \mathcal{W}_i and \mathcal{P}_i , labeled as $[\mathcal{W}_i \mathcal{P}_i]$ must be a single axis rotation about the \hat{w}_{2_i} axis:

$$[\mathcal{W}_i \mathcal{P}_i] = \begin{bmatrix} \cos(\beta_i) & 0 & -\sin(\beta_i) \\ 0 & 1 & 0 \\ \sin(\beta_i) & 0 & \cos(\beta_i) \end{bmatrix} \quad (4.10)$$

where β_i is the angle of rotation. Transforming $[I_{rw_i, W_{c_i}}]$ from the \mathcal{P}_i frame to the \mathcal{W}_i frame using Eq. (4.10) and using small angle approximations yields

$$[I_{rw_i, W_{c_i}}] = \mathcal{W}_i \begin{bmatrix} J_{s_i} & 0 & (J_{s_i} - J_{t_i})\beta_i \\ 0 & J_{t_i} & 0 \\ (J_{s_i} - J_{t_i})\beta_i & 0 & J_{t_i} \end{bmatrix} \quad (4.11)$$

However, from Eq. (4.8a), $[I_{rw_i/W_{c_i}}]$ can be written in the following form

$$[I_{rw_i/W_{c_i}}] = \omega_i \begin{bmatrix} J_{s_i} & 0 & U_{d_i} \\ 0 & J_{t_i} & 0 \\ U_{d_i} & 0 & J_{t_i} \end{bmatrix} \quad (4.12)$$

This gives the following relationship between the rotation angle, β_i , and U_{d_i}

$$\beta_i = \frac{U_{d_i}}{J_{s_i} - J_{t_i}} \quad (4.13)$$

This concludes the necessary steps to relate manufactures' specifications of RW imbalances to parameters needed for the fully-coupled jitter model. In addition, the simplified description of $[I_{rw_i/W_{c_i}}]$ seen in Eq. (4.12) simplifies the EOMs developed in the previous sections due to $J_{12_i} = J_{13_i} = 0$. In addition, Eq. (4.5), (4.8a) and (4.12) allow a direct comparison of the results of the simplified model to the fully-coupled model which is discussed in the following section.

Chapter 5

Software Implementation

This chapter describes general methodology of implementing dynamical equations of motion into a software simulation, as well as methods of validation. Section 5.1 describes the back-substitution method used to solve the coupled equations of motion of an balanced or imbalanced RW or VSCMG in a computationally, software friendly way. Section 5.2 describes the energy and angular momentum equations used to validate the fully-coupled EOMs.

5.1 Back-Substitution Method

In Chapter 2, the derivations of the translational, rotational, and motor torque equations of an imbalanced reaction wheel resulted in $N + 6$ coupled equations. Likewise, Chapter 3 derived the translational, rotational, gimbal torque, and wheel torque equations for an imbalanced variable-speed control moment gyroscope, and resulted in $2N + 6$ coupled equations - two for each VSCMG, three relating to angular acceleration, and three relating to linear acceleration. The most straightforward method of solving these coupled equations is to use the system mass matrix method. However, this method of solving the EOMs involves taking the inverse of $2N + 6$ by $2N + 6$ matrix, which can be computationally expensive when implementing the model in a software simulation. A more computationally attractive method is to use back-substitution. Although more intricate than the system mass matrix method, back-substitution can significantly reduce computation time when solving the equations of motion. Back-substitution involves substituting the equations of motion into each other so that the number of second order states in the translational and rotational EOMs

is reduced, and may be solved by taking two the inverse of two 3×3 matrices. After this, the other second order states may be solved for trivially.

The goal of back-substitution is to manipulate the rotational and translational equations of motion to conform to the following form,

$$\begin{bmatrix} [A] & [B] \\ [C] & [D] \end{bmatrix} \begin{bmatrix} \ddot{\mathbf{r}}_{B/N} \\ \dot{\boldsymbol{\omega}}_{B/N} \end{bmatrix} = \begin{bmatrix} \mathbf{v}_{\text{trans}} \\ \mathbf{v}_{\text{rot}} \end{bmatrix} \quad (5.1)$$

where $[A]$, $[B]$, $[C]$, and $[D]$ are 3×3 matrices representing $\ddot{\mathbf{r}}_{B/N}$ and $\dot{\boldsymbol{\omega}}_{B/N}$ coefficients within the translational and rotational EOMs. $\mathbf{v}_{\text{trans}}$ is a 3×1 vector that represents the right-hand side (RHS) of the translational EOM, and \mathbf{v}_{rot} is a 3×1 vector that represents the RHS of the rotational EOM. The matrices $[A]$, $[B]$, $[C]$, $[D]$ and vectors $\mathbf{v}_{\text{trans}}$, \mathbf{v}_{rot} are broken down as follows.

$$[A] = [A_{\text{hub}}] + [A_{\text{contr}}] \quad (5.2)$$

$$[B] = [B_{\text{hub}}] + [B_{\text{contr}}] \quad (5.3)$$

$$[C] = [C_{\text{hub}}] + [C_{\text{contr}}] \quad (5.4)$$

$$[D] = [D_{\text{hub}}] + [D_{\text{contr}}] \quad (5.5)$$

$$\mathbf{v}_{\text{trans}} = \mathbf{v}_{\text{trans, hub}} + \mathbf{v}_{\text{trans, contr}} \quad (5.6)$$

$$\mathbf{v}_{\text{rot}} = \mathbf{v}_{\text{rot, hub}} + \mathbf{v}_{\text{rot, contr}} \quad (5.7)$$

where $[A_{\text{hub}}]$ represents the contribution to $[A]$ from the spacecraft hub and $[A_{\text{contr}}]$ represents the contribution to $[A]$ from the effectors (i.e. RWs or VSCMGs), etc. $[A_{\text{hub}}]$ etc are the same regardless of the type of effector used, and are provided in the equation below.

$$[A_{\text{hub}}] = m_{\text{sc}}[I_{3 \times 3}] \quad (5.8)$$

$$[B_{\text{hub}}] = -m_{\text{sc}}[\tilde{\mathbf{c}}] \quad (5.9)$$

$$[C_{\text{hub}}] = m_{\text{sc}}[\tilde{\mathbf{c}}] \quad (5.10)$$

$$[D_{\text{hub}}] = [I_{\text{sc}, B}] \quad (5.11)$$

$$\mathbf{v}_{\text{trans, hub}} = \mathbf{F} - 2m_{\text{sc}}[\tilde{\boldsymbol{\omega}}]\mathbf{c}' - m_{\text{sc}}[\tilde{\boldsymbol{\omega}}]^2\mathbf{c} \quad (5.12)$$

$$\mathbf{v}_{\text{rot, hub}} = \mathbf{L}_B - [I_{\text{sc}, B}]'\boldsymbol{\omega} - [\tilde{\boldsymbol{\omega}}][I_{\text{sc}, B}]\boldsymbol{\omega} \quad (5.13)$$

The contribution matrices $[A_{\text{contr}}]$ etc are specific to the type of effector and will be solved for in the following section for a imbalanced VSCMG and in Appendix B for a balanced VSCMG, balanced RW, and imbalanced RW.

Using these vectors and matrices, $\dot{\boldsymbol{\omega}}_{B/N}$ maybe be solved for using the following equation.

$$\dot{\boldsymbol{\omega}}_{B/N} = \left([D] - [C][A]^{-1}[B] \right)^{-1} (\mathbf{v}_{\text{rot}} - [C][A]^{-1}\mathbf{v}_{\text{trans}}) \quad (5.14)$$

Likewise, $\ddot{\mathbf{r}}_{B/N}$ may be obtained by,

$$\ddot{\mathbf{r}}_{B/N} = [A]^{-1}(\mathbf{v}_{\text{trans}} - [B]\dot{\boldsymbol{\omega}}_{B/N}) \quad (5.15)$$

Now that $\ddot{\mathbf{r}}_{B/N}$ and $\dot{\boldsymbol{\omega}}_{B/N}$ are known, the other second order states may be solved for.

The following section shows the derivation of the back-substitution contribution matrices of an imbalanced VSCMG.

5.1.1 Equations of Motion

The EOMs representing a spacecraft with N imbalanced VSCMGs were derived in Chapter 3 and are repeated here for the reader's convenience. The first step is to rewrite the translational equation of motion in a convenient form. The original equation is,

$$\begin{aligned} \ddot{\mathbf{r}}_{B/N} - [\tilde{\mathbf{c}}]\dot{\boldsymbol{\omega}} + \frac{1}{m_{\text{sc}}} \sum_{i=1}^N \left[m_{G_i} [\tilde{\mathbf{g}}_{g_i}] \mathbf{r}_{G_{c_i}/G_i} - m_{W_i} d_i c \theta_i \hat{\mathbf{g}}_{s_i} + m_{W_i} \ell_i \hat{\mathbf{g}}_{t_i} \right] \ddot{\gamma}_i + \frac{1}{m_{\text{sc}}} \sum_{i=1}^N \left[m_{W_i} d_i \hat{\boldsymbol{\omega}}_{3_i} \right] \dot{\Omega}_i \\ = \ddot{\mathbf{r}}_{C/N} - 2[\tilde{\boldsymbol{\omega}}]\mathbf{c}' - [\tilde{\boldsymbol{\omega}}][\tilde{\boldsymbol{\omega}}]\mathbf{c} - \frac{1}{m_{\text{sc}}} \sum_{i=1}^N \left[m_{G_i} \dot{\gamma}_i [\tilde{\mathbf{g}}_{g_i}] \mathbf{r}'_{G_{c_i}/B} \right. \\ \left. + m_{W_i} \left[(2d_i \dot{\gamma}_i \Omega_i s \theta_i - \ell_i \dot{\gamma}_i^2) \hat{\mathbf{g}}_{s_i} - d_i \dot{\gamma}_i^2 c \theta_i \hat{\mathbf{g}}_{t_i} - d_i \Omega_i^2 \hat{\boldsymbol{\omega}}_{2_i} \right] \right] \end{aligned}$$

This equation may be abbreviated as,

$$\ddot{\mathbf{r}}_{B/N} - [\tilde{\mathbf{c}}]\dot{\boldsymbol{\omega}} + \frac{1}{m_{\text{sc}}} \sum_{i=1}^N \mathbf{u}_{r_i} \ddot{\gamma}_i + \frac{1}{m_{\text{sc}}} \sum_{i=1}^N \mathbf{v}_{r_i} \dot{\Omega}_i = \ddot{\mathbf{r}}_{C/N} - 2[\tilde{\boldsymbol{\omega}}]\mathbf{c}' - [\tilde{\boldsymbol{\omega}}]^2 \mathbf{c} - \frac{1}{m_{\text{sc}}} \sum_{i=1}^N \mathbf{k}_{r_i} \quad (5.16)$$

where,

$$\mathbf{u}_{r_i} = m_{G_i} [\tilde{\mathbf{g}}_{g_i}] \mathbf{r}_{G_{c_i}/G_i} - m_{W_i} d_i c \theta_i \hat{\mathbf{g}}_{s_i} + m_{W_i} \ell_i \hat{\mathbf{g}}_{t_i} \quad (5.17)$$

$$\mathbf{v}_{r_i} = m_{W_i} d_i \hat{\boldsymbol{\omega}}_{3_i} \quad (5.18)$$

$$\mathbf{k}_{r_i} = m_{G_i} \dot{\gamma}_i [\tilde{\mathbf{g}}_{g_i}] \mathbf{r}'_{G_{c_i}/B} + m_{W_i} [(2d_i \dot{\gamma}_i \Omega_i s \theta_i - \ell_i \dot{\gamma}_i^2) \hat{\mathbf{g}}_{s_i} - d_i \dot{\gamma}_i^2 c \theta_i \hat{\mathbf{g}}_{t_i} - d_i \Omega_i^2 \hat{\boldsymbol{\omega}}_{2_i}] \quad (5.19)$$

The next step is to rewrite the rotational equation of motion in a convenient form. The original equation is,

$$\begin{aligned} & m_{sc} [\tilde{\mathbf{c}}] \ddot{\mathbf{r}}_{B/N} + [I_{sc,B}] \dot{\boldsymbol{\omega}} + \sum_{i=1}^N \left[[I_{G_i, G_{c_i}}] \hat{\mathbf{g}}_{g_i} + m_{G_i} [\tilde{\mathbf{r}}_{G_{c_i}/B}] [\tilde{\mathbf{g}}_{g_i}] \mathbf{r}_{G_{c_i}/G_i} + [I_{W_i, W_{c_i}}] \hat{\mathbf{g}}_{g_i} \right. \\ & \left. + m_{W_i} [\tilde{\mathbf{r}}_{W_{c_i}/B}] (\ell_i \hat{\mathbf{g}}_{t_i} - d_i c \theta_i \hat{\mathbf{g}}_{s_i}) \right] \ddot{\gamma}_i + \sum_{i=1}^N \left[[I_{W_i, W_{c_i}}] \hat{\mathbf{g}}_{s_i} + m_{W_i} d_i [\tilde{\mathbf{r}}_{W_{c_i}/B}] \hat{\boldsymbol{\omega}}_{3_i} \right] \dot{\Omega}_i \\ & = \mathbf{L}_B - [I_{sc,B}]' \boldsymbol{\omega} - [\tilde{\boldsymbol{\omega}}] [I_{sc,B}] \boldsymbol{\omega} - \sum_{i=1}^N \left[[I_{G_i, G_{c_i}}]' \dot{\gamma}_i \hat{\mathbf{g}}_{g_i} + [\tilde{\boldsymbol{\omega}}] [I_{G_i, G_{c_i}}] \dot{\gamma}_i \hat{\mathbf{g}}_{g_i} + m_{G_i} [\tilde{\boldsymbol{\omega}}] [\tilde{\mathbf{r}}_{G_{c_i}/B}] \mathbf{r}'_{G_{c_i}/B} \right. \\ & \left. + m_{G_i} \dot{\gamma}_i [\tilde{\mathbf{r}}_{G_{c_i}/B}] [\tilde{\mathbf{g}}_{g_i}] \mathbf{r}'_{G_{c_i}/G_i} + [I_{W_i, W_{c_i}}] \Omega \dot{\gamma} \hat{\mathbf{g}}_{t_i} + [I_{W_i, W_{c_i}}]' \boldsymbol{\omega}_{W_i/B} + [\tilde{\boldsymbol{\omega}}] [I_{W_i, W_{c_i}}] \boldsymbol{\omega}_{W_i/B} \right. \\ & \left. + m_{W_i} [\tilde{\boldsymbol{\omega}}] [\tilde{\mathbf{r}}_{W_{c_i}/B}] \mathbf{r}'_{W_{c_i}/B} + m_{W_i} [\tilde{\mathbf{r}}_{W_{c_i}/B}] [(2d_i \dot{\gamma}_i \Omega_i s \theta_i - \ell_i \dot{\gamma}_i^2) \hat{\mathbf{g}}_{s_i} - d_i \dot{\gamma}_i^2 c \theta_i \hat{\mathbf{g}}_{t_i} - d_i \Omega_i^2 \hat{\boldsymbol{\omega}}_{2_i}] \right] \end{aligned}$$

This equation may be abbreviated as,

$$\begin{aligned} & m_{sc} [\tilde{\mathbf{c}}] \ddot{\mathbf{r}}_{B/N} + [I_{sc,B}] \dot{\boldsymbol{\omega}} + \sum_{i=1}^N \mathbf{u}_{\omega_i} \ddot{\gamma}_i + \sum_{i=1}^N \mathbf{v}_{\omega_i} \dot{\Omega}_i \\ & = \mathbf{L}_B - [I_{sc,B}]' \boldsymbol{\omega} - [\tilde{\boldsymbol{\omega}}] [I_{sc,B}] \boldsymbol{\omega} - \sum_{i=1}^N \mathbf{k}_{\omega_i} \end{aligned} \quad (5.20)$$

where,

$$\mathbf{u}_{\omega_i} = [I_{G_i, G_{c_i}}] \hat{\mathbf{g}}_{g_i} + m_{G_i} [\tilde{\mathbf{r}}_{G_{c_i}/B}] [\tilde{\mathbf{g}}_{g_i}] \mathbf{r}_{G_{c_i}/G_i} + [I_{W_i, W_{c_i}}] \hat{\mathbf{g}}_{g_i} + m_{W_i} [\tilde{\mathbf{r}}_{W_{c_i}/B}] (\ell_i \hat{\mathbf{g}}_{t_i} - d_i c \theta_i \hat{\mathbf{g}}_{s_i}) \quad (5.21)$$

$$\mathbf{v}_{\omega_i} = [I_{W_i, W_{c_i}}] \hat{\mathbf{g}}_{s_i} + m_{W_i} d_i [\tilde{\mathbf{r}}_{W_{c_i}/B}] \hat{\boldsymbol{\omega}}_{3_i} \quad (5.22)$$

$$\begin{aligned} \mathbf{k}_{\omega_i} &= [I_{G_i, G_{c_i}}]' \dot{\gamma}_i \hat{\mathbf{g}}_{g_i} + [\tilde{\boldsymbol{\omega}}] [I_{G_i, G_{c_i}}] \dot{\gamma}_i \hat{\mathbf{g}}_{g_i} + m_{G_i} [\tilde{\boldsymbol{\omega}}] [\tilde{\mathbf{r}}_{G_{c_i}/B}] \mathbf{r}'_{G_{c_i}/B} + m_{G_i} \dot{\gamma}_i [\tilde{\mathbf{r}}_{G_{c_i}/B}] [\tilde{\mathbf{g}}_{g_i}] \mathbf{r}'_{G_{c_i}/G_i} \\ & \left. + [I_{W_i, W_{c_i}}] \Omega \dot{\gamma} \hat{\mathbf{g}}_{t_i} + [I_{W_i, W_{c_i}}]' \boldsymbol{\omega}_{W_i/B} + [\tilde{\boldsymbol{\omega}}] [I_{W_i, W_{c_i}}] \boldsymbol{\omega}_{W_i/B} + m_{W_i} [\tilde{\boldsymbol{\omega}}] [\tilde{\mathbf{r}}_{W_{c_i}/B}] \mathbf{r}'_{W_{c_i}/B} \right. \\ & \left. + m_{W_i} [\tilde{\mathbf{r}}_{W_{c_i}/B}] [(2d_i \dot{\gamma}_i \Omega_i s \theta_i - \ell_i \dot{\gamma}_i^2) \hat{\mathbf{g}}_{s_i} - d_i \dot{\gamma}_i^2 c \theta_i \hat{\mathbf{g}}_{t_i} - d_i \Omega_i^2 \hat{\boldsymbol{\omega}}_{2_i}] \right] \end{aligned} \quad (5.23)$$

The gimbal torque equation is,

$$\begin{aligned}
& \hat{\mathbf{g}}_{g_i}^T \left[m_{V_i} [\tilde{\mathbf{r}}_{V_{c_i}/G_i}] \right] \ddot{\mathbf{r}}_{B/N} + \hat{\mathbf{g}}_{g_i}^T \left[[I_{V_i, V_{c_i}}] + m_{V_i} [\tilde{\mathbf{r}}_{V_{c_i}/G_i}] [\tilde{\mathbf{r}}_{V_{c_i}/B}]^T \right] \dot{\boldsymbol{\omega}} + \hat{\mathbf{g}}_{g_i}^T \left[[I_{G_i, G_{c_i}}] \hat{\mathbf{g}}_{g_i} \right. \\
& \left. + [I_{W_i, W_{c_i}}] \hat{\mathbf{g}}_{g_i} + [P_i] (\ell_i \hat{\mathbf{g}}_{t_i} - d_i c \theta_i \hat{\mathbf{g}}_{s_i}) + [Q_i] [\tilde{\mathbf{g}}_{g_i}] \mathbf{r}_{G_{c_i}/G_i} \right] \ddot{\gamma}_i + \hat{\mathbf{g}}_{g_i}^T \left[[I_{W_i, W_{c_i}}] \hat{\mathbf{g}}_{s_i} + [P_i] d_i \hat{\boldsymbol{\omega}}_{3_i} \right] \dot{\Omega}_i \\
& = -\hat{\mathbf{g}}_{g_i}^T \left[\dot{\gamma}_i [Q_i] [\tilde{\mathbf{g}}_{g_i}] \mathbf{r}'_{G_{c_i}/G_i} + [P_i] \left[(2d_i \dot{\gamma}_i \Omega_i s \theta_i - \ell_i \dot{\gamma}_i^2) \hat{\mathbf{g}}_{s_i} - d_i \dot{\gamma}_i^2 c \theta_i \hat{\mathbf{g}}_{t_i} - d_i \Omega_i^2 \hat{\boldsymbol{\omega}}_{2_i} \right] \right. \\
& \quad \left. + [I_{G_i, G_{c_i}}]' \boldsymbol{\omega}_{G_i/N} + [\tilde{\boldsymbol{\omega}}] [I_{G_i, G_{c_i}}] \boldsymbol{\omega}_{G_i/N} + [I_{W_i, W_{c_i}}] \Omega \dot{\gamma} \hat{\mathbf{g}}_{t_i} + [I_{W_i, W_{c_i}}]' \boldsymbol{\omega}_{W_i/N} \right. \\
& \quad \left. + [\tilde{\boldsymbol{\omega}}] [I_{W_i, W_{c_i}}] \boldsymbol{\omega}_{W_i/N} + m_{G_i} [\tilde{\mathbf{r}}_{G_{c_i}/V_{c_i}}] (2[\tilde{\boldsymbol{\omega}}] \mathbf{r}'_{G_{c_i}/V_{c_i}} + [\tilde{\boldsymbol{\omega}}]^2 \mathbf{r}_{G_{c_i}/V_{c_i}}) \right. \\
& \quad \left. + m_{W_i} [\tilde{\mathbf{r}}_{W_{c_i}/V_{c_i}}] (2[\tilde{\boldsymbol{\omega}}] \mathbf{r}'_{W_{c_i}/V_{c_i}} + [\tilde{\boldsymbol{\omega}}]^2 \mathbf{r}_{W_{c_i}/V_{c_i}}) + m_{V_i} [\tilde{\mathbf{r}}_{V_{c_i}/G_i}] (2[\tilde{\boldsymbol{\omega}}] \mathbf{r}'_{V_{c_i}/B} + [\tilde{\boldsymbol{\omega}}]^2 \mathbf{r}_{V_{c_i}/B}) \right] + u_{g_i}
\end{aligned} \tag{5.24}$$

where,

$$[I_{V_i, V_{c_i}}] = [I_{G_i, V_{c_i}}] + [I_{W_i, V_{c_i}}] \tag{5.25}$$

$$[I_{G_i, V_{c_i}}] = [I_{G_i, G_{c_i}}] + m_{G_i} [\tilde{\mathbf{r}}_{G_{c_i}/V_{c_i}}] [\tilde{\mathbf{r}}_{G_{c_i}/V_{c_i}}]^T \tag{5.26}$$

$$[I_{W_i, V_{c_i}}] = [I_{W_i, W_{c_i}}] + m_{W_i} [\tilde{\mathbf{r}}_{W_{c_i}/V_{c_i}}] [\tilde{\mathbf{r}}_{W_{c_i}/V_{c_i}}]^T \tag{5.27}$$

$$[P_i] = m_{W_i} \rho_{G_i} [\tilde{\mathbf{r}}_{W_{c_i}/V_{c_i}}] - m_{G_i} \rho_{W_i} [\tilde{\mathbf{r}}_{G_{c_i}/V_{c_i}}] + m_{W_i} [\tilde{\mathbf{r}}_{V_{c_i}/G_i}] \tag{5.28}$$

$$[Q_i] = m_{G_i} \rho_{W_i} [\tilde{\mathbf{r}}_{G_{c_i}/V_{c_i}}] - m_{W_i} \rho_{G_i} [\tilde{\mathbf{r}}_{W_{c_i}/V_{c_i}}] + m_{G_i} [\tilde{\mathbf{r}}_{V_{c_i}/G_i}] \tag{5.29}$$

$$[\tilde{\boldsymbol{\omega}}]^2 = [\tilde{\boldsymbol{\omega}}] [\tilde{\boldsymbol{\omega}}] \tag{5.30}$$

The wheel torque equation is,

$$\begin{aligned}
& [m_{W_i} d_i \hat{\boldsymbol{\omega}}_{3_i}^T] \ddot{\mathbf{r}}_{B/N} + [\hat{\mathbf{g}}_{s_i}^T [I_{W_i, W_{c_i}}] + m_{W_i} d_i \hat{\mathbf{g}}_{s_i}^T [\tilde{\boldsymbol{\omega}}_{2_i}] [\tilde{\mathbf{r}}_{W_{c_i}/B}]^T] \dot{\boldsymbol{\omega}} \\
& \quad + [J_{12_i} s \theta_i + J_{13_i} c \theta_i - m_{W_i} d_i \ell_i s \theta_i] \ddot{\gamma}_i + [J_{11_i} + m_{W_i} d_i^2] \dot{\Omega}_i \\
& = -\hat{\mathbf{g}}_{s_i}^T \left[[I_{W_i, W_{c_i}}]' \boldsymbol{\omega}_{W_i/N} + [\tilde{\boldsymbol{\omega}}] [I_{W_i, W_{c_i}}] \boldsymbol{\omega}_{W_i/N} + m_{W_i} d_i [\tilde{\boldsymbol{\omega}}_{2_i}] \left[2[\tilde{\mathbf{r}}'_{W_{c_i}/B}]^T \boldsymbol{\omega} + [\tilde{\boldsymbol{\omega}}] [\tilde{\boldsymbol{\omega}}] \mathbf{r}_{W_{c_i}/B} \right] \right] \\
& \quad + (J_{13_i} s \theta_i - J_{12_i} c \theta_i) \Omega \dot{\gamma} - m_{W_i} d_i^2 \dot{\gamma}_i^2 c \theta_i s \theta_i + u_{s_i} \tag{5.31}
\end{aligned}$$

5.1.2 Derivation of Back-Substitution

Solve the gimbal torque equation for $\ddot{\gamma}_i$ in terms of $\ddot{\mathbf{r}}_{B/N}$ and $\dot{\boldsymbol{\omega}}_{B/N}$ and $\dot{\Omega}_i$

$$\ddot{\gamma}_i = \mathbf{a}_{\gamma_i}^T \ddot{\mathbf{r}}_{B/N} + \mathbf{b}_{\gamma_i}^T \dot{\boldsymbol{\omega}} + c_{\gamma_i} \dot{\Omega}_i + d_{\gamma_i} \quad (5.32)$$

where,

$$\mathbf{a}_{\gamma_i} = e_{\gamma_i}^{-1} m_{V_i} [\tilde{\mathbf{r}}_{V_{c_i}/G_i}] \hat{\mathbf{g}}_{\mathbf{g}_i} \quad (5.33)$$

$$\mathbf{b}_{\gamma_i} = -e_{\gamma_i}^{-1} \left([I_{V_i, V_{c_i}}]^T \hat{\mathbf{g}}_{\mathbf{g}_i} - m_{V_i} [\tilde{\mathbf{r}}_{V_{c_i}/B}] [\tilde{\mathbf{r}}_{V_{c_i}/G_i}] \hat{\mathbf{g}}_{\mathbf{g}_i} \right) \quad (5.34)$$

$$c_{\gamma_i} = -e_{\gamma_i}^{-1} \left(\hat{\mathbf{g}}_{\mathbf{g}_i}^T [I_{W_i, W_{c_i}}] \hat{\mathbf{g}}_{\mathbf{s}_i} + d_i \hat{\mathbf{g}}_{\mathbf{g}_i}^T [P_i] \hat{\boldsymbol{\omega}}_{3_i} \right) \quad (5.35)$$

$$\begin{aligned} d_{\gamma_i} = & -e_{\gamma_i}^{-1} \hat{\mathbf{g}}_{\mathbf{g}_i}^T \left[\dot{\gamma}_i [Q_i] [\tilde{\mathbf{g}}_{\mathbf{g}_i}] \mathbf{r}'_{G_{c_i}/G_i} + [P_i] \left[(2d_i \dot{\gamma}_i \Omega_i s\theta_i - \ell_i \dot{\gamma}_i^2) \hat{\mathbf{g}}_{\mathbf{s}_i} - d_i \dot{\gamma}_i^2 c\theta_i \hat{\mathbf{g}}_{\mathbf{t}_i} - d_i \Omega_i^2 \hat{\boldsymbol{\omega}}_{2_i} \right] \right. \\ & + [I_{G_i, G_{c_i}}]' \boldsymbol{\omega}_{G_i/N} + [\tilde{\boldsymbol{\omega}}] [I_{G_i, G_{c_i}}] \boldsymbol{\omega}_{G_i/N} + [I_{W_i, W_{c_i}}] \Omega \dot{\gamma} \hat{\mathbf{g}}_{\mathbf{t}_i} + [I_{W_i, W_{c_i}}]' \boldsymbol{\omega}_{W_i/N} + [\tilde{\boldsymbol{\omega}}] [I_{W_i, W_{c_i}}] \boldsymbol{\omega}_{W_i/N} \\ & + m_{G_i} [\tilde{\mathbf{r}}_{G_{c_i}/V_{c_i}}] (2[\tilde{\boldsymbol{\omega}}] \mathbf{r}'_{G_{c_i}/V_{c_i}} + [\tilde{\boldsymbol{\omega}}]^2 \mathbf{r}_{G_{c_i}/V_{c_i}}) + m_{W_i} [\tilde{\mathbf{r}}_{W_{c_i}/V_{c_i}}] (2[\tilde{\boldsymbol{\omega}}] \mathbf{r}'_{W_{c_i}/V_{c_i}} + [\tilde{\boldsymbol{\omega}}]^2 \mathbf{r}_{W_{c_i}/V_{c_i}}) \\ & \left. + m_{V_i} [\tilde{\mathbf{r}}_{V_{c_i}/G_i}] (2[\tilde{\boldsymbol{\omega}}] \mathbf{r}'_{V_{c_i}/B} + [\tilde{\boldsymbol{\omega}}]^2 \mathbf{r}_{V_{c_i}/B}) \right] + e_{\gamma_i}^{-1} u_{\mathbf{g}_i} \quad (5.36) \end{aligned}$$

$$e_{\gamma_i} = \hat{\mathbf{g}}_{\mathbf{g}_i}^T \left[[I_{G_i, G_{c_i}}] \hat{\mathbf{g}}_{\mathbf{g}_i} + [I_{W_i, W_{c_i}}] \hat{\mathbf{g}}_{\mathbf{g}_i} + [P_i] (\ell_i \hat{\mathbf{g}}_{\mathbf{t}_i} - d_i c\theta_i \hat{\mathbf{g}}_{\mathbf{s}_i}) + [Q_i] [\tilde{\mathbf{g}}_{\mathbf{g}_i}] \mathbf{r}_{G_{c_i}/G_i} \right] \quad (5.37)$$

Solve the wheel torque equation for $\dot{\Omega}_i$ in terms of $\ddot{\mathbf{r}}_{B/N}$ and $\dot{\boldsymbol{\omega}}_{B/N}$ and $\ddot{\gamma}_i$

$$\dot{\Omega}_i = \mathbf{a}_{\Omega_i}^T \ddot{\mathbf{r}}_{B/N} + \mathbf{b}_{\Omega_i}^T \dot{\boldsymbol{\omega}}_{B/N} + c_{\Omega_i} \ddot{\gamma}_i + d_{\Omega_i} \quad (5.38)$$

where

$$\mathbf{a}_{\Omega_i} = -e_{\Omega_i}^{-1} m_{W_i} d_i \hat{\boldsymbol{\omega}}_{3_i} \quad (5.39)$$

$$\mathbf{b}_{\Omega_i} = -e_{\Omega_i}^{-1} \left([I_{W_i, W_{c_i}}]^T \hat{\mathbf{g}}_{\mathbf{s}_i} - m_{W_i} d_i [\tilde{\mathbf{r}}_{W_{c_i}/B}] [\tilde{\boldsymbol{\omega}}_{2_i}] \hat{\mathbf{g}}_{\mathbf{s}_i} \right) \quad (5.40)$$

$$c_{\Omega_i} = -e_{\Omega_i}^{-1} (J_{12_i} s\theta_i + J_{13_i} c\theta_i - m_{W_i} d_i \ell_i s\theta_i) \quad (5.41)$$

$$\begin{aligned} d_{\Omega_i} = & -e_{\Omega_i}^{-1} \left[\hat{\mathbf{g}}_{\mathbf{s}_i}^T [I_{W_i, W_{c_i}}]' \boldsymbol{\omega}_{W_i/N} + \hat{\mathbf{g}}_{\mathbf{s}_i}^T [\tilde{\boldsymbol{\omega}}] [I_{W_i, W_{c_i}}] \boldsymbol{\omega}_{W_i/N} + m_{W_i} d_i \hat{\mathbf{g}}_{\mathbf{s}_i}^T [\tilde{\boldsymbol{\omega}}_{2_i}] \left[2[\tilde{\mathbf{r}}'_{W_{c_i}/B}]^T \boldsymbol{\omega} \right. \right. \\ & \left. \left. + [\tilde{\boldsymbol{\omega}}] [\tilde{\boldsymbol{\omega}}] \mathbf{r}_{W_{c_i}/B} \right] + (J_{13_i} s\theta_i - J_{12_i} c\theta_i) \Omega \dot{\gamma} - m_{W_i} d_i^2 \dot{\gamma}_i^2 c\theta_i s\theta_i + u_{\mathbf{s}_i} \right] \quad (5.42) \end{aligned}$$

$$e_{\Omega_i} = J_{11_i} + m_{W_i} d_i^2 \quad (5.43)$$

Substitute Eq. (5.32) into Eq. (5.38).

$$\begin{aligned}
\dot{\Omega}_i &= \mathbf{a}_{\Omega_i}^T \ddot{\mathbf{r}}_{B/N} + \mathbf{b}_{\Omega_i}^T \dot{\boldsymbol{\omega}}_{B/N} + c_{\Omega_i} \left[\mathbf{a}_{\gamma_i}^T \ddot{\mathbf{r}}_{B/N} + \mathbf{b}_{\gamma_i}^T \dot{\boldsymbol{\omega}} + c_{\gamma_i} \dot{\Omega}_i + d_{\gamma_i} \right] + d_{\Omega_i} \\
&= \frac{\mathbf{a}_{\Omega_i}^T + c_{\Omega_i} \mathbf{a}_{\gamma_i}^T}{1 - c_{\Omega_i} c_{\gamma_i}} \ddot{\mathbf{r}}_{B/N} + \frac{\mathbf{b}_{\Omega_i}^T + c_{\Omega_i} \mathbf{b}_{\gamma_i}^T}{1 - c_{\Omega_i} c_{\gamma_i}} \dot{\boldsymbol{\omega}} + \frac{d_{\Omega_i} + c_{\Omega_i} d_{\gamma_i}}{1 - c_{\Omega_i} c_{\gamma_i}} \\
&= \mathbf{p}_i^T \ddot{\mathbf{r}}_{B/N} + \mathbf{q}_i^T \dot{\boldsymbol{\omega}} + s_i
\end{aligned} \tag{5.44}$$

where,

$$\mathbf{p}_i = \frac{\mathbf{a}_{\Omega_i} + c_{\Omega_i} \mathbf{a}_{\gamma_i}}{1 - c_{\Omega_i} c_{\gamma_i}} \tag{5.45}$$

$$\mathbf{q}_i = \frac{\mathbf{b}_{\Omega_i} + c_{\Omega_i} \mathbf{b}_{\gamma_i}}{1 - c_{\Omega_i} c_{\gamma_i}} \tag{5.46}$$

$$s_i = \frac{d_{\Omega_i} + c_{\Omega_i} d_{\gamma_i}}{1 - c_{\Omega_i} c_{\gamma_i}} \tag{5.47}$$

Substitute Eq. (5.32) into the translational equation of motion Eq. (5.16).

$$\begin{aligned}
\ddot{\mathbf{r}}_{B/N} - [\tilde{\mathbf{c}}] \dot{\boldsymbol{\omega}} + \frac{1}{m_{sc}} \sum_{i=1}^N \mathbf{u}_{r_i} \left[\mathbf{a}_{\gamma_i}^T \ddot{\mathbf{r}}_{B/N} + \mathbf{b}_{\gamma_i}^T \dot{\boldsymbol{\omega}} + c_{\gamma_i} \dot{\Omega}_i + d_{\gamma_i} \right] + \frac{1}{m_{sc}} \sum_{i=1}^N \mathbf{v}_{r_i} \dot{\Omega}_i \\
= \ddot{\mathbf{r}}_{C/N} - 2[\tilde{\boldsymbol{\omega}}] \mathbf{c}' - [\tilde{\boldsymbol{\omega}}]^2 \mathbf{c} - \frac{1}{m_{sc}} \sum_{i=1}^N \mathbf{k}_{r_i}
\end{aligned} \tag{5.48}$$

Group like terms.

$$\begin{aligned}
\left[I_{3 \times 3} + \frac{1}{m_{sc}} \sum_{i=1}^N \mathbf{u}_{r_i} \mathbf{a}_{\gamma_i}^T \right] \ddot{\mathbf{r}}_{B/N} + \left[-[\tilde{\mathbf{c}}] + \frac{1}{m_{sc}} \sum_{i=1}^N \mathbf{u}_{r_i} \mathbf{b}_{\gamma_i}^T \right] \dot{\boldsymbol{\omega}} + \frac{1}{m_{sc}} \sum_{i=1}^N \left[\mathbf{v}_{r_i} + \mathbf{u}_{r_i} c_{\gamma_i} \right] \dot{\Omega}_i \\
= \ddot{\mathbf{r}}_{C/N} - 2[\tilde{\boldsymbol{\omega}}] \mathbf{c}' - [\tilde{\boldsymbol{\omega}}]^2 \mathbf{c} - \frac{1}{m_{sc}} \sum_{i=1}^N \left(\mathbf{k}_{r_i} + \mathbf{u}_{r_i} d_{\gamma_i} \right)
\end{aligned} \tag{5.49}$$

Substitute Eq. (5.44) into Eq. (5.49) and group like terms. Also multiply each side of the equation by m_{sc} .

$$\begin{aligned}
\left[m_{sc} I_{3 \times 3} + \sum_{i=1}^N \left(\mathbf{u}_{r_i} \mathbf{a}_{\gamma_i}^T + \frac{(\mathbf{v}_{r_i} + \mathbf{u}_{r_i} c_{\gamma_i})(\mathbf{a}_{\Omega_i}^T + c_{\Omega_i} \mathbf{a}_{\gamma_i}^T)}{1 - c_{\Omega_i} c_{\gamma_i}} \right) \right] \ddot{\mathbf{r}}_{B/N} \\
+ \left[-m_{sc} [\tilde{\mathbf{c}}] + \sum_{i=1}^N \left(\mathbf{u}_{r_i} \mathbf{b}_{\gamma_i}^T + \frac{(\mathbf{v}_{r_i} + \mathbf{u}_{r_i} c_{\gamma_i})(\mathbf{b}_{\Omega_i}^T + c_{\Omega_i} \mathbf{b}_{\gamma_i}^T)}{1 - c_{\Omega_i} c_{\gamma_i}} \right) \right] \dot{\boldsymbol{\omega}} \\
= \mathbf{F} - 2m_{sc} [\tilde{\boldsymbol{\omega}}] \mathbf{c}' - m_{sc} [\tilde{\boldsymbol{\omega}}]^2 \mathbf{c} - \sum_{i=1}^N \left(\mathbf{k}_{r_i} + \mathbf{u}_{r_i} d_{\gamma_i} + \frac{(\mathbf{v}_{r_i} + \mathbf{u}_{r_i} c_{\gamma_i})(c_{\Omega_i} d_{\gamma_i} + d_{\Omega_i})}{1 - c_{\Omega_i} c_{\gamma_i}} \right)
\end{aligned} \tag{5.50}$$

At this point, we're done with translation. Repeat these steps for rotation. Substitute Eq. (5.32) into the rotational equation of motion Eq. (5.20) and group like terms.

$$\begin{aligned} & \left[m_{sc}[\tilde{\mathbf{c}}] + \sum_{i=1}^N \mathbf{u}_{\omega_i} \mathbf{a}_{\gamma_i}^T \right] \ddot{\mathbf{r}}_{B/N} + \left[[I_{sc,B}] + \sum_{i=1}^N \mathbf{u}_{\omega_i} \mathbf{b}_{\gamma_i}^T \right] \dot{\boldsymbol{\omega}} + \sum_{i=1}^N (\mathbf{v}_{\omega_i} + \mathbf{u}_{\omega_i} c_{\gamma_i}) \dot{\Omega}_i \\ & = \mathbf{L}_B - [I_{sc,B}]' \boldsymbol{\omega} - [\tilde{\boldsymbol{\omega}}][I_{sc,B}] \boldsymbol{\omega} - \frac{1}{m_{sc}} \sum_{i=1}^N (\mathbf{k}_{\omega_i} + \mathbf{u}_{\omega_i} d_{\gamma_i}) \end{aligned} \quad (5.51)$$

Substitute Eq. (5.44) into Eq. (5.51) and group like terms.

$$\begin{aligned} & \left[m_{sc}[\tilde{\mathbf{c}}] + \sum_{i=1}^N \left(\mathbf{u}_{\omega_i} \mathbf{a}_{\gamma_i}^T + \frac{(\mathbf{v}_{\omega_i} + \mathbf{u}_{\omega_i} c_{\gamma_i})(\mathbf{a}_{\Omega_i}^T + c_{\Omega_i} \mathbf{a}_{\gamma_i}^T)}{1 - c_{\Omega_i} c_{\gamma_i}} \right) \right] \ddot{\mathbf{r}}_{B/N} \\ & + \left[[I_{sc,B}] + \sum_{i=1}^N \left(\mathbf{u}_{\omega_i} \mathbf{b}_{\gamma_i}^T + \frac{(\mathbf{v}_{\omega_i} + \mathbf{u}_{\omega_i} c_{\gamma_i})(\mathbf{b}_{\Omega_i}^T + c_{\Omega_i} \mathbf{b}_{\gamma_i}^T)}{1 - c_{\Omega_i} c_{\gamma_i}} \right) \right] \dot{\boldsymbol{\omega}} \\ & = \mathbf{L}_B - [I_{sc,B}]' \boldsymbol{\omega} - [\tilde{\boldsymbol{\omega}}][I_{sc,B}] \boldsymbol{\omega} - \sum_{i=1}^N \left(\mathbf{k}_{\omega_i} + \mathbf{u}_{\omega_i} d_{\gamma_i} + \frac{(\mathbf{v}_{\omega_i} + \mathbf{u}_{\omega_i} c_{\gamma_i})(c_{\Omega_i} d_{\gamma_i} + d_{\Omega_i})}{1 - c_{\Omega_i} c_{\gamma_i}} \right) \end{aligned} \quad (5.52)$$

5.1.3 Back-Substitution Contribution Matrices

The contributions are,

$$[A_{\text{contr}}] = \sum_{i=1}^N \left[\mathbf{u}_{r_i} \mathbf{a}_{\gamma_i}^T + (\mathbf{v}_{r_i} + \mathbf{u}_{r_i} c_{\gamma_i}) \mathbf{p}_i^T \right] \quad (5.53)$$

$$[B_{\text{contr}}] = \sum_{i=1}^N \left[\mathbf{u}_{r_i} \mathbf{b}_{\gamma_i}^T + (\mathbf{v}_{r_i} + \mathbf{u}_{r_i} c_{\gamma_i}) \mathbf{q}_i^T \right] \quad (5.54)$$

$$[C_{\text{contr}}] = \sum_{i=1}^N \left[\mathbf{u}_{\omega_i} \mathbf{a}_{\gamma_i}^T + (\mathbf{v}_{\omega_i} + \mathbf{u}_{\omega_i} c_{\gamma_i}) \mathbf{p}_i^T \right] \quad (5.55)$$

$$[D_{\text{contr}}] = \sum_{i=1}^N \left[\mathbf{u}_{\omega_i} \mathbf{b}_{\gamma_i}^T + (\mathbf{v}_{\omega_i} + \mathbf{u}_{\omega_i} c_{\gamma_i}) \mathbf{q}_i^T \right] \quad (5.56)$$

$$\mathbf{v}_{\text{trans,contr}} = - \sum_{i=1}^N \left[\mathbf{k}_{r_i} + \mathbf{u}_{r_i} d_{\gamma_i} + (\mathbf{v}_{r_i} + \mathbf{u}_{r_i} c_{\gamma_i}) \mathbf{s}_i \right] \quad (5.57)$$

$$\mathbf{v}_{\text{rot,contr}} = - \sum_{i=1}^N \left[\mathbf{k}_{\omega_i} + \mathbf{u}_{\omega_i} d_{\gamma_i} + (\mathbf{v}_{\omega_i} + \mathbf{u}_{\omega_i} c_{\gamma_i}) \mathbf{s}_i \right] \quad (5.58)$$

This concludes the derivation of the back-substitution of imbalanced VSCMGs. Appendix B provides the back-substitution contribution matrices for balanced VSCMGs, balanced RWs, and imbalanced RWs.

5.2 Energy and Angular Momentum Validation Method

A key benefit of using fully-coupled formulations of imbalanced RWs and VSCMGs is to leverage angular momentum and energy validation tools. These tools are essential when simulating combined complex models such as flexible dynamics, fuel slosh, etc, and simply as a tool to validate the spacecraft dynamics in general. When implementing angular momentum and energy checks in a computer simulation, it is often that the integration timestep must be significantly reduced in order to propagate the spacecraft and effector states precisely enough so that the energy and angular momentum are seen as conserved. The following sections describe the equations used to valid the formulations derived within this thesis.

5.2.1 Angular Momentum

The angular momentum vector of the spacecraft + VSCMG system taken about point N is defined as

$$\mathbf{H}_{sc,N} = \mathbf{H}_{B,N} + \mathbf{H}_{W,N} + \mathbf{H}_{G,N} \quad (5.59)$$

where,

$$\mathbf{H}_{B,N} = [I_{B,B_c}] \boldsymbol{\omega} + m_B \mathbf{r}_{B_c/N} \times \dot{\mathbf{r}}_{B_c/N} \quad (5.60)$$

$$\mathbf{H}_{W,N} = [I_{W,W_c}] \boldsymbol{\omega}_{W/N} + m_W \mathbf{r}_{W_c/N} \times \dot{\mathbf{r}}_{W_c/N} \quad (5.61)$$

$$\mathbf{H}_{G,N} = [I_{G,G_c}] \boldsymbol{\omega}_{G/N} + m_G \mathbf{r}_{G_c/N} \times \dot{\mathbf{r}}_{G_c/N} \quad (5.62)$$

where the inertial derivatives $\dot{\mathbf{r}}_{B_c/N}$ etc were defined in section 3.2.2. If no external torques act on the spacecraft, then

$$\Delta \left| {}^{\mathcal{N}} \mathbf{H}_{sc,N} \right| = 0$$

that is, the change of the norm of the spacecraft angular momentum vector taken about point N and represented in the \mathcal{N} frame should be 0. This is conservation of angular momentum.

5.2.2 Energy

The total mechanical energy of the spacecraft + VSCMG system is given by

$$T_{sc} = T_B + T_G + T_W \quad (5.63)$$

where,

$$T_B = T_{B,trans} + T_{B,rot} = \frac{1}{2}m_B\dot{\mathbf{r}}_{B_c/N}^T\dot{\mathbf{r}}_{B_c/N} + \frac{1}{2}\boldsymbol{\omega}^T[I_{B,B_c}]\boldsymbol{\omega} \quad (5.64)$$

$$T_G = T_{G,trans} + T_{G,rot} = \frac{1}{2}m_G\dot{\mathbf{r}}_{G_c/N}^T\dot{\mathbf{r}}_{G_c/N} + \frac{1}{2}\boldsymbol{\omega}_{\mathcal{G}/\mathcal{N}}^T[I_{G,G_c}]\boldsymbol{\omega}_{\mathcal{G}/\mathcal{N}} \quad (5.65)$$

$$T_W = T_{W,trans} + T_{W,rot} = \frac{1}{2}m_W\dot{\mathbf{r}}_{W_c/N}^T\dot{\mathbf{r}}_{W_c/N} + \frac{1}{2}\boldsymbol{\omega}_{\mathcal{W}/\mathcal{N}}^T[I_{W,W_c}]\boldsymbol{\omega}_{\mathcal{W}/\mathcal{N}} \quad (5.66)$$

Note that each contribution to T_{sc} is the sum of the translational energy of the system about point N and the rotational energy of the system with respect to the inertial frame \mathcal{N} . If no internal or external torques are present, then

$$\Delta T_{sc} = 0$$

This is conservation of energy. Alternatively, the orbital kinetic energy of the spacecraft center of mass could be summed with the total rotational and deformational kinetic energy *about* the spacecraft center of mass to arrive at the same equation.¹

5.2.3 Energy Rate

When internal or external forces or torques are applied system energy is no longer conserved and may not be directly used as a validation tool. However, the time rate of change of energy may still be analyzed and used for validation. This is given by,

$$\dot{T}_{sc} = \dot{\mathbf{r}}_{B/N}^T \mathbf{F} + \boldsymbol{\omega}_{B/\mathcal{N}}^T \mathbf{L}_B + \sum_{i=1}^N \dot{\gamma}_i u_{g_i} + \sum_{i=1}^N \Omega_i u_{s_i} \quad (5.67)$$

If there are no unaccounted internal or external forces or torques on the system, the equation above should be numerically equivalent to the time derivative of energy as computed in Eq. (5.63).

$$\dot{T}_{sc} = \frac{d}{dt} T_{sc} \quad (5.68)$$

¹ Basilisk Technical Memorandum: FORMULATION OF THE ENERGY AND MOMENTUM OF THE SPACECRAFT, Cody Allard, 2016

In a computer simulation, the time derivative of \dot{T}_{sc} may be computed numerically and compared to the theoretical energy rate given by Eq. (5.67) to validate the dynamics. This form of dynamics validation is particularly useful in the situation where the spacecraft attitude is being controlled closed-loop by means of torquing the VSCMGs.

Chapter 6

Numerical Simulation Results

6.1 Spacecraft with N Imbalanced Reaction Wheels

Numeric simulations are provided to demonstrate the fully-coupled imbalanced reaction wheel model. Angular momentum is calculated to confirm that when no external disturbances are present angular momentum is conserved, and system energy is calculated to show that when no external disturbances or reaction wheel motor torques are present, energy is conserved. The fully-coupled model is directly compared to the simplified model using the formulation developed in Section 4.2. Simulation parameters used are given in Table 6.1.

The first simulation that is included simulates three RWs. The purpose of this simulation is to show the effect of RW jitter on a spacecraft that is initially inertially fixed, and therefore the only perturbations to the spacecraft will be due to the RW jitter. Accordingly, the spacecraft has no external forces present and has zero initial velocity and zero initial angular velocity. The spacecraft's attitude is parameterized in terms of Modified Rodriguez Parameters (MRPs). The RWs are initially spinning with specified values seen in Table 6.1. Also, to give further confirmation in the model, the motor torque in each RW has a nonzero time history and can be seen in Figure 6.3(b). Note that the wheel orientation matrix $[G_s]$ (which is useful for many controls applications [24]) is formulated such that each column contains the spin axis unit vector for the i th wheel, $\hat{\mathbf{g}}_{s_i}$, and has dimension $3 \times N$.

$$[G_s] = \begin{bmatrix} \hat{\mathbf{g}}_{s_1} & \cdots & \hat{\mathbf{g}}_{s_N} \end{bmatrix} \quad (6.1)$$

Figures 6.1-6.4 show simulation results for the fully-coupled and simplified RW imbalance

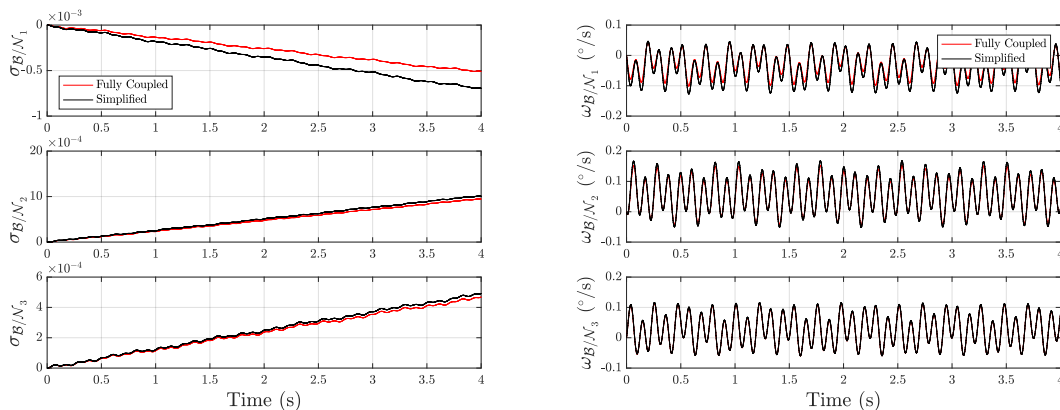
Table 6.1: : Simulation parameters for the fully-coupled model. Note that wheel parameters apply to all wheels unless otherwise specified.

Parameter	Notation	Value	Units
Number of reaction wheels	N	3	-
Total spacecraft mass	m_{sc}	662	kg
Hub mass	m_{hub}	644	kg
Wheel mass	m_{rw}	6	kg
Hub inertia tensor about hub CoM	$[I_{hub,B_c}]$	${}^B \begin{bmatrix} 550 & 0.1045 & -0.0840 \\ 0.1045 & 650 & 0.0001 \\ -0.0840 & 0.0001 & 650 \end{bmatrix}$	kg·m ²
Hub CoM. location wrt B	$\mathbf{r}_{B_c/B}$	${}^B [1 \ -2 \ 10]^T$	cm
Wheel orientation matrix	$[G_s]$	${}^B \begin{bmatrix} 0.7887 & -0.2113 & -0.5774 \\ -0.2113 & 0.7887 & -0.5774 \\ 0.5774 & 0.5774 & 0.5774 \end{bmatrix}$	-
Wheel static imbalance	U_s	1920	g·cm
Wheel static imbalance	U_d	1540	g·cm ²
Wheel CoM offset (derived from U_s)	d	3.2	mm
Wheel inertia tensor about wheel CoM (derived from U_d)	$[I_{rw,W_c}]$	${}^W \begin{bmatrix} 0.0796 & 0 & 2.0E-4 \\ 0 & 0.0430 & 0 \\ 2.0E-4 & 0 & 0.0430 \end{bmatrix}$	kg·m ²
Wheel 1 location vector	$\mathbf{r}_{W_1/B}$	${}^B [0.6309 \ -0.1691 \ 0.4619]^T$	
Wheel 2 location vector	$\mathbf{r}_{W_2/B}$	${}^B [-0.1691 \ 0.6309 \ 0.4619]^T$	
Wheel 3 location vector	$\mathbf{r}_{W_3/B}$	${}^B [-0.4619 \ -0.4619 \ 0.4619]^T$	m
Initial position	$\mathbf{r}_{B/N}$	${}^N [0 \ 0 \ 0]^T$	m
Initial velocity	$\mathbf{v}_{B/N}$	${}^N [0 \ 0 \ 0]^T$	m/s
Initial attitude MRP	$\boldsymbol{\sigma}_{B/N}$	$[0 \ 0 \ 0]^T$	-
Initial angular velocity	$\boldsymbol{\omega}_{B/N}$	${}^B [0 \ 0 \ 0]^T$	deg/s
Initial wheel speeds	Ω	-558, -73, 242	RPM
Initial wheel angles	θ	43, 179, 346	deg
Commanded wheel torques	u_s	10, -25, 17.5	mN·m

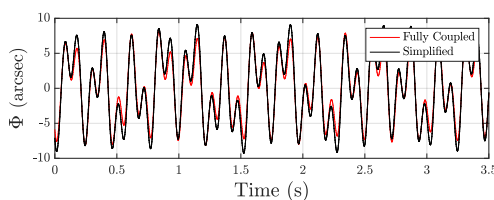
model with $N = 3$ wheels. In Figure 6.1, the attitude of the spacecraft is shown to be drifting due to the imbalance in the RWs. The impact of jitter is visible in the spacecraft's body rates. Note that the simplified model compares well with the higher-fidelity angular velocity values, but the attitude does slowly drift from the fully-coupled model. For simulations that last longer than a few seconds this could cause significant error. Figure 6.1(c) shows the principal angle with the drift subtracted out, so that only the jitter is visible. This shows that the RW jitter results in a perturbation amplitude of around 8 arcseconds. These parameters are important to consider when performing analysis of spacecraft pointing stability.

The translational position and velocity are shown in Figs. 6.2(a) and 6.2(b), respectively. These plots demonstrate that there is a non-zero effect due to RW jitter on the position and velocity of the spacecraft. The position and velocity comparison of the fully-coupled and simplified model show that the simplified model is not able to track either position or angular velocity well for the given set of initial conditions. The wheel rates seen in Figure 6.3(a) agree with the time history of the motor torque seen in Figure 6.3(b). The fact that the wheel speed data for the fully-coupled model and simplified model agree as shown in Figure 6.3(a) demonstrates that the variation in wheel speed is primarily due to the coupling between the hub's angular velocity and wheel speed.

Figure 6.4 shows the change in energy and momentum plotted versus time for the fully-coupled and simplified models. Energy is plotted for a 3.5 second duration because the motor torque is zero during this time and the change in energy should be zero. However, Figure 6.4(a) shows that using the simplified model causes energy to fluctuate whereas the fully-coupled model only includes integration error. Angular momentum, by definition, should be conserved for a closed system under the influence of internal torques, and is thus plotted for the entire duration of the simulation in Figure 6.4(b). It can be seen that the simplified model violates conservation of angular momentum and the fully-coupled model only exhibits integration error. For numerical simulations of a spacecraft, angular momentum and energy conservation is an important check to validate EOMs. For long simulation times the error in the simplified model will grow. This need for validation checks and error propagations are important characteristics to consider between both



(a) Attitude MRP of the spacecraft for the fully- (b) Body rates of the spacecraft for the fully-coupled and simplified models with $N = 3$



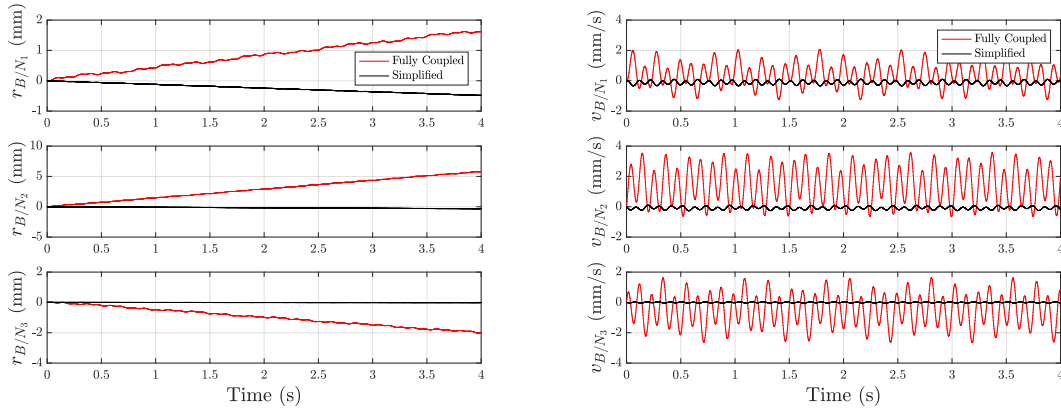
(c) Principal angle jitter for the fully-coupled and simplified models with $N = 3$

Figure 6.1: Attitude, principle angle, and body rates of spacecraft

models. A second simulation is included in the following section to directly compare results of the two models using a fixed-axis scenario.

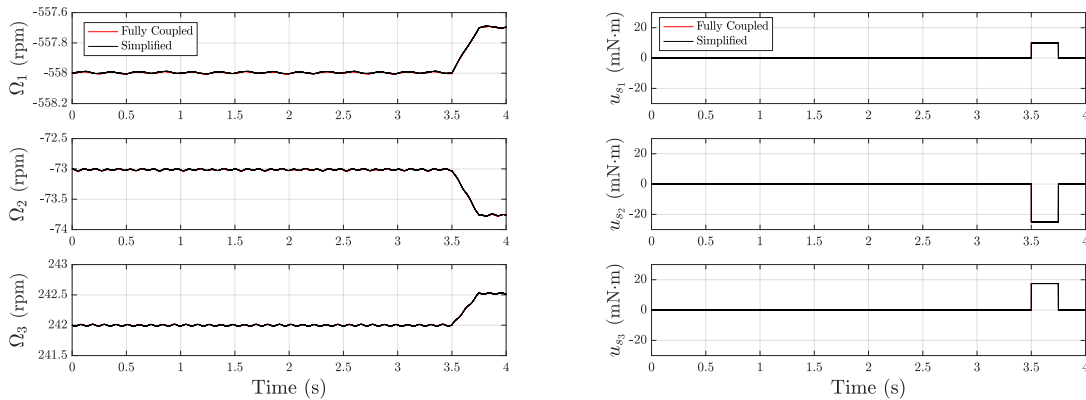
6.2 Reaction Wheel Jitter Comparison Using a Fixed-Axis Rotation Scenario

The fully-coupled model is directly compared to the simplified model using a fixed-axis scenario in order to focus on the comparison of jitter. These simulations involve similar initial conditions as seen in Table 6.1, except only one RW is included for simplicity. Figure 6.5(a) shows principal angle jitter of the spacecraft (drift subtracted out) for each model. This result gives confidence that the imbalance parameter adaptation method developed in section 4 is accurate for converting manufacturers' specifications on RW imbalances to the parameters needed for the fully-coupled simulation. However, this also shows that there is a noticeable difference between the two simulations which is a result of the fully-coupled simulation modeling the RW jitter as in



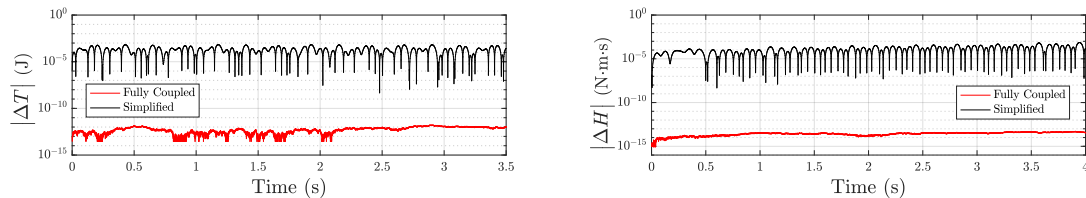
(a) Inertial position of the spacecraft for the fully-coupled and simplified models with $N = 3$ (b) Inertial velocity of the spacecraft for the fully-coupled and simplified models with $N = 3$

Figure 6.2: Position and velocity of the spacecraft



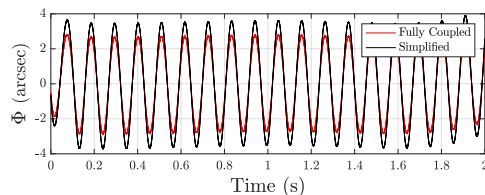
(a) Wheel speeds for the fully-coupled and simplified models with $N = 3$ (b) Open-loop wheel motor torques for the fully-coupled and simplified models with $N = 3$

Figure 6.3: Wheel angle, wheel speed, and motor torque of RWs

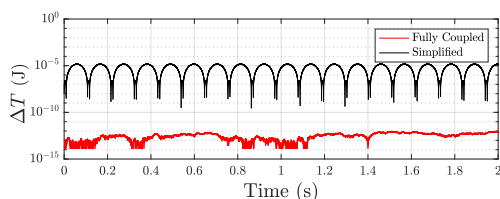


(a) System energy Δ for the fully-coupled and simplified models with $N = 3$ (b) System angular momentum Δ for the fully-coupled and simplified models with $N = 3$

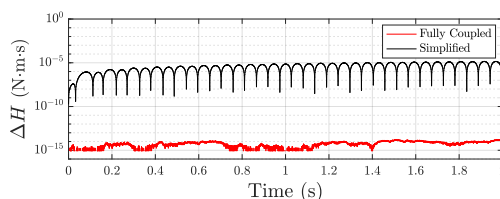
Figure 6.4: Change in energy and momentum of the spacecraft



(a) Comparison of principal angle jitter results for the fully-coupled and simplified models with $N = 1$



(b) Comparison of energy results for the fully-coupled and simplified models with $N = 1$



(c) Comparison of momentum results for the fully-coupled and simplified models with $N = 1$

Figure 6.5: Comparison of results for the fully-coupled and simplified models with $N = 1$

internal rather than an external force and torque on the spacecraft. Figures 6.5(b) and 6.5(c) show the energy and momentum, respectively, for each model for the one wheel simulation. This data further demonstrates that the simplified model is not appropriate where energy and momentum tools are needed for validation purposes.

6.3 Spacecraft with N Imbalanced VSCMGs

Numeric simulations are provided to demonstrate the fully-coupled imbalanced VSCMG model. Angular momentum is calculated to confirm that when no external disturbances are present angular momentum is conserved. System energy is calculated to show that when no external disturbances or internal torques are present, energy is conserved. The system energy rate of the fully-coupled and simplified models are compared to the theoretical value as defined in section 5.2. In all plots, the fully-coupled model is directly compared to the simplified model using the formulation developed in Section 4.2. Simulation parameters used are given in Table 6.2. The scenario used to demonstrate the fully-coupled imbalanced VSCMG EOMs involves a rigid spacecraft hub and $N = 4$ VSCMGs. Figures 6.6-6.12 show the results of the simulation.

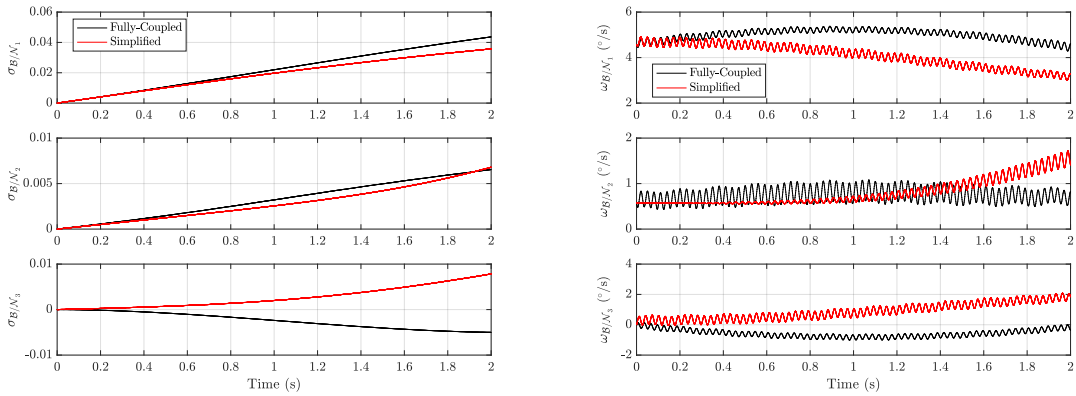
Table 6.2: : Simulation parameters for the fully-coupled model. Note that wheel parameters apply to all wheels unless otherwise specified.

Parameter	Notation	Value	Units
Number of VSCMGs	N	4	-
Total spacecraft mass	m_{sc}	862	kg
Hub mass	m_B	750	kg
Wheel mass	m_W	4	kg
Gimbal mass	m_G	24	kg
Hub inertia tensor about hub CoM	$[I_{hub, B_c}]$	${}^B \begin{bmatrix} 900 & 4.15 & 2.93 \\ 4.15 & 800 & 2.75 \\ 2.93 & 2.75 & 600 \end{bmatrix}$	$\text{kg}\cdot\text{m}^2$
Hub CoM location wrt B	$\mathbf{r}_{B_c/B}$	${}^B \begin{bmatrix} -0.02 & 0.01 & 10 \end{bmatrix}^T$	cm
Wheel static imbalance	U_s	32	$\text{g}\cdot\text{cm}$
Wheel dynamic imbalance	U_d	15.4	$\text{g}\cdot\text{m}^2$
Wheel CoM offset (derived from U_s)	d	8.0	mm
Wheel inertia tensor about wheel CoM (derived from U_d)	$[I_{W, W_c}]$	${}^W \begin{bmatrix} 0.2 & 0 & 1.54\text{E}-2 \\ 0 & 0.1 & 0 \\ 1.54\text{E}-2 & 0 & 0.1 \end{bmatrix}$	$\text{kg}\cdot\text{m}^2$
Gimbal inertia tensor about gimbal CoM (derived from U_d)	$[I_{G, G_c}]$	${}^W \begin{bmatrix} 9 & 0.81 & 0.24 \\ 0.81 & 11 & 0.93 \\ 0.24 & 0.93 & 5 \end{bmatrix}$	$\text{kg}\cdot\text{m}^2$
VSCMG 1 location vector	$\mathbf{r}_{G_1/B}$	${}^B \begin{bmatrix} -30 & 0 & 0 \end{bmatrix}^T$	cm
VSCMG 2 location vector	$\mathbf{r}_{G_2/B}$	${}^B \begin{bmatrix} 30 & 0 & 0 \end{bmatrix}^T$	cm
VSCMG 3 location vector	$\mathbf{r}_{G_3/B}$	${}^B \begin{bmatrix} 0 & -30 & 0 \end{bmatrix}^T$	cm
VSCMG 4 location vector	$\mathbf{r}_{G_4/B}$	${}^B \begin{bmatrix} 0 & 30 & 0 \end{bmatrix}^T$	cm
Initial position	$\mathbf{r}_{B/N}$	${}^N \begin{bmatrix} 0 & 0 & 0 \end{bmatrix}^T$	m
Initial velocity	$\mathbf{v}_{B/N}$	${}^N \begin{bmatrix} 0 & 0 & 0 \end{bmatrix}^T$	m/s
Initial attitude MRP	$\boldsymbol{\sigma}_{B/N}$	$\begin{bmatrix} 0 & 0 & 0 \end{bmatrix}^T$	-
Initial angular velocity	$\boldsymbol{\omega}_{B/N}$	${}^B \begin{bmatrix} 4.58 & 0.57 & 0 \end{bmatrix}^T$	deg/s
Initial wheel speeds	Ω	2000, 350, -11, 2	RPM
Initial wheel angles	θ	0, 0, 0, 0	deg
Initial gimbal speeds	$\dot{\gamma}$	-1.72, 0.63, 0, 0	deg/s
Initial gimbal angles	γ	0, 0, 0, 0	deg
Commanded wheel torques	u_s	0, 250, -250, 0	mN·m
Commanded gimbal torques	u_g	100, -100, 0, 0	mN·m

Figure 6.6 shows the attitude and body rates of the spacecraft for the duration of the simulation. In Figure 6.6(a), the spacecraft attitude computed using the simplified model is shown to rapidly drift from that of the fully-coupled model. The third MRP component in particular drifts in the opposite direction. This information is reflected in the spacecraft body rates as shown in Figure 6.6(b). The body rates as computed by the simplified model drift rapidly from those using the fully-coupled model, although the higher frequency variations are similar in amplitude. It is evident from this data that the body rates and attitude MRP of the spacecraft would likely be wildly different between the simplified and fully-coupled models if the simulation were propagated for longer than $t = 2$ seconds. Figure 6.7 shows the principle angle of the spacecraft with respect to inertial. Figure 6.7(a) shows the raw principle angle computed from the attitude MRP in Figure 6.6(a) and reflects much of the same information. After 2 second, the two models show principle angles that are different by several degrees. Figure 6.7(b) shows the higher frequency modes of the principle angle by subtracting out a polynomial fit of the data shown in Figure 6.7(a) to act as a high-pass filter of sorts.

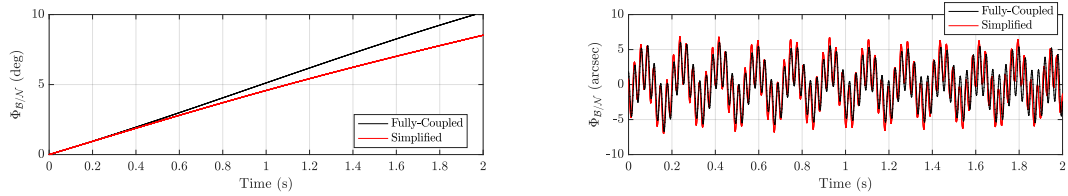
Figure 6.8 shows the translational position and velocity. These plots demonstrate that there is a non-zero effect due to VSCMG jitter on the position and velocity of the spacecraft. The position and velocity comparison of the fully-coupled and simplified model show that the simplified model is not able to track either position or angular velocity well for the given set of initial conditions. In Figure 6.8(b), it is evident that the simplified model has wildly underestimated the magnitude of the imbalance vibration effect on spacecraft velocity.

Figure 6.9 shows the VSCMG gimbal rate and wheel speeds. Again, it is evident that the simplified model has underestimated the effect of the vibration on each of the rates. The gimbal rate of VSCMG 1 in particular, shown in Figure 6.9(a), varies greatly between the two models. The fully-coupled model has a high frequency chatter with an amplitude of approximately 75 deg/s, whereas the simplified model shows no visible signs of chatter and slowly drifts in the same overall trend as the fully-coupled model. The wheel speed for gimbal 1, however, does not appear to closely match the same trend between the fully-coupled and simplified models. VSCMG 2 shows similar



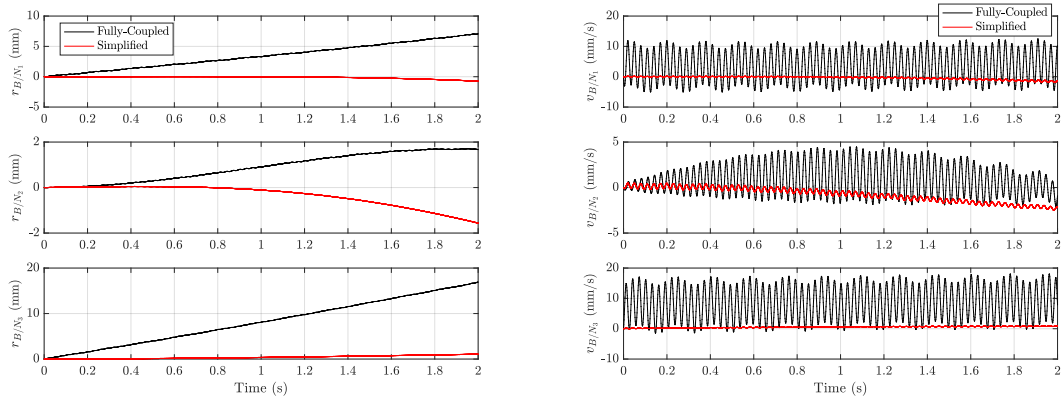
(a) Attitude MRP of the spacecraft for the fully-coupled and simplified models with $N = 4$ (b) Body rates of the spacecraft for the fully-coupled and simplified models with $N = 4$

Figure 6.6: Attitude and body rates of the spacecraft



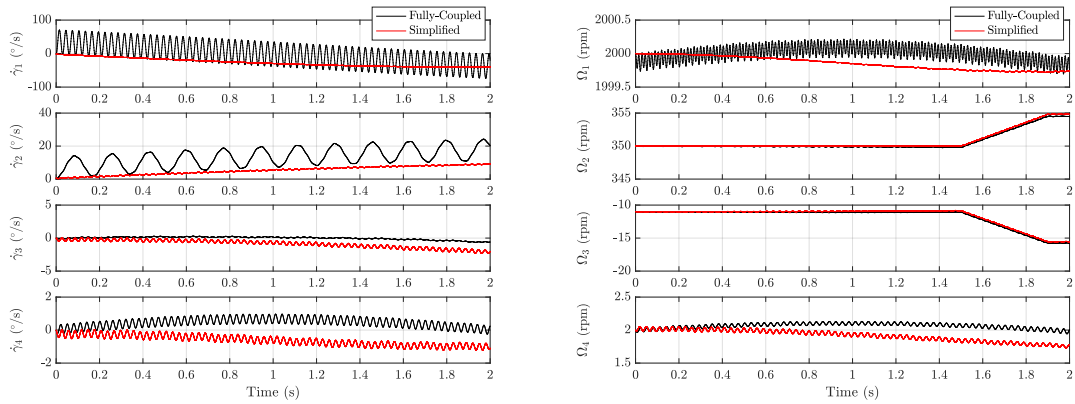
(a) Principal angle for the fully-coupled and simplified models with $N = 4$ (b) Principal angle jitter for the fully-coupled and simplified models with $N = 4$

Figure 6.7: Principle angle and jitter of the spacecraft



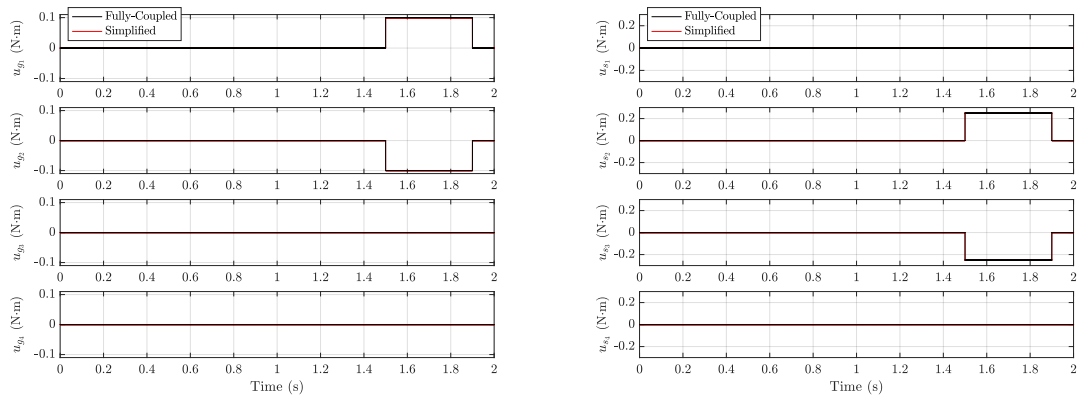
(a) Inertial position of the spacecraft for the fully-coupled and simplified models with $N = 4$ (b) Inertial velocity of the spacecraft for the fully-coupled and simplified models with $N = 4$

Figure 6.8: Position and velocity of the spacecraft



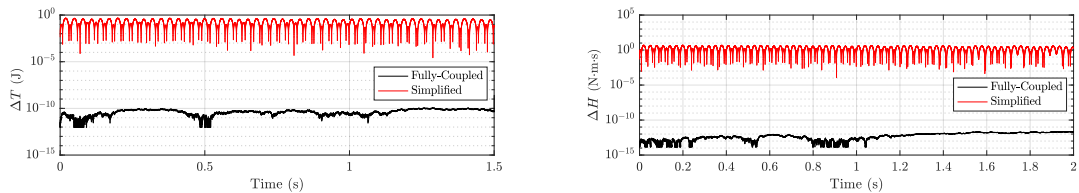
(a) Wheel speeds for the fully-coupled and simplified models with $N = 4$ (b) Open-loop wheel motor torques for the fully-coupled and simplified models with $N = 4$

Figure 6.9: Wheel speed and gimbal rate of the VSCMGs



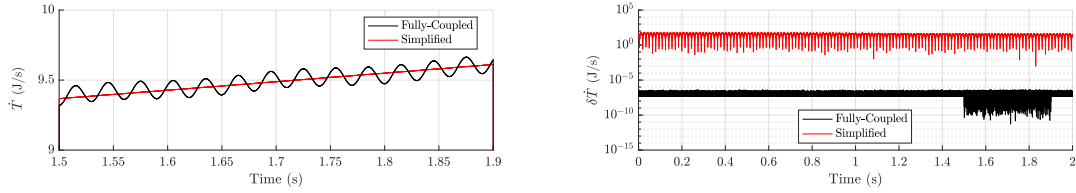
(a) Open-loop gimbal torques for the fully-coupled and simplified models with $N = 4$ (b) Open-loop wheel torques for the fully-coupled and simplified models with $N = 4$

Figure 6.10: Wheel torque and gimbal torque of the VSCMGs



(a) System energy Δ for the fully-coupled and simplified models with $N = 4$ (b) System angular momentum Δ for the fully-coupled and simplified models with $N = 4$

Figure 6.11: Change in energy and angular momentum of the system



(a) System energy rate for the fully-coupled and simplified models with $N = 4$ (b) System energy rate error for the fully-coupled and simplified models with $N = 4$

Figure 6.12: Energy rate and energy rate error of the system

information regarding gimbal rate. The wheel speeds and gimbal rates agree with the time history of the applied wheel and gimbal torques as shown in Figures 6.10(b) and 6.10(a), respectively. The effect of the wheel torque is evident from looking at the wheel rates. The effect of the gimbal torque on the gimbal rates is not evident to the eye since the gimbal has a significantly larger moment of inertia.

Figure 6.11 shows the change in energy and angular momentum of the system for the fully-coupled and simplified models. Energy is plotted for a 1.5 second period since the wheel and gimbal torques are zero during this time and energy should be conserved. However, Figure 6.11(a) shows that using the simplified model causes energy to fluctuate whereas the fully-coupled model only includes integration error. Angular momentum, by definition, should be conserved for a closed system under the influence of internal torques, and is thus plotted for the entire duration of the simulation in Figure 6.11(b). It can be seen that the simplified model violates conservation of angular momentum and the fully-coupled model only exhibits integration error. For numerical simulations of a spacecraft, angular momentum and energy conservation is an important check to validate EOMs. For long simulation times the error in the simplified model will grow. This need for validation checks and error propagations are important characteristics to consider between both models.

Figure 6.12 shows the energy rate of and the energy rate error of the system for the fully-coupled and simplified models. Figure 6.12(a) shows the energy rate during the time period that the VSCMG has nonzero wheel and gimbal torques (from $t = 1.5$ s to $t = 1.9$ s), thus highlighting

the difference between the fully-coupled and simplified models. The fully-coupled model has clearly visible fluctuation whereas the simplified model does not. Figure 6.12(b) shows the absolute error between the theoretical energy rate based on the internal torques and the numerically calculated energy rate based on numerically differentiating the energy T_{sc} , as described in section 5.2.3. It is clear that the simplified model violates the theoretical energy rate, whereas the fully-coupled model has little error. Due to numerically differentiating the system energy T_{sc} , the comparison does show a larger error than in Figures 6.11(a)-6.11(b): approximately 10^{-7} compared to 10^{-12} .

Chapter 7

Conclusions

Most previous work related to modeling jitter due to momentum exchange device (MED) imbalances models the effect as an external force and torque on the spacecraft. In reality, this effect is an internal force and torque on the spacecraft and thus requires a different formulation. The work presented in this thesis develops the general fully-coupled model of reaction wheel (RW) and variable-speed control moment gyroscope (VSCMG) imbalances. The fully-coupled model allows for momentum and energy validation to be implemented in a simulation. Additionally, a discussion is included that aids in converting manufacturers' specifications of RW imbalances to the parameters needed for the fully-coupled simulation.

Simulation results are provided to demonstrate the fully-coupled model compared to the simplified model for RWs and VSCMGs. Energy is shown to be conserved when the motor torques are zero, and momentum is conserved throughout the length of the simulations. Energy rate is shown to closely match the theoretical energy rate for the imbalanced VSCMG model. This provides validation of the fully-coupled models and highlights drawbacks to the simplified model, which violates conservation of momentum and energy. A comparison between the fully-coupled model and the simplified model shows that the imbalance parameter adaptation is adequate because the fully-coupled and simplified models give similar high-level results, for a fixed-axis scenario. However, because the simplified model is not valid in terms of conservation of energy and conservation of angular momentum it is undesirable when including additional complex dynamical models such as flexible dynamics or fuel slosh and causes error propagation to be a concern for lengthy simulation

times.

The research presented within this thesis validated the EOMs and software implementation using with energy and angular momentum results from two completely independent software suites. Additionally, the states versus time were validated between the two simulations. This level of validation shows that the EOMs and software implementation method are correct beyond doubt.

Implementations of the fully-coupled RW and VSCMG models derived within this thesis will be released open-source in 2017 as part of the Basilisk astrodynamics software.¹

¹ <http://hanspeterschaub.info/bskMain.html>

Bibliography

- [1] J. Wertz and W. Larson. Space Mission Analysis and Design. 3rd edition, 1999.
- [2] A. Vanderburg and J. Johnson. A Technique for Extracting Highly Precise Photometry for the Two-Wheeled Kepler Mission. Publications of the Astronomical Society of the Pacific, 126(944):948, 2014.
- [3] H. Schaub and J. Junkins. Singularity Avoidance Using Null Motion and Variable-speed Control Moment Gyros. Journal of Guidance, Control, and Dynamics, 23(1):11–16, 2000.
- [4] T. Sasaki, J. Alcorn, H. Schaub, and T. Shimomura. Convex Optimization for Power Tracking of Double-Gimbal Variable-Speed Control Moment Gyros. AIAA Journal of Spacecraft and Rockets, 2017.
- [5] J. Chabot and H. Schaub. Spherical Magnetic Dipole Actuator for Spacecraft Attitude Control. Journal of Guidance, Control, and Dynamics, pages 911–915, 2016.
- [6] J. Alcorn. The Contributions of Walter Haussermann to Rocket Development. International Astronautical Congress, Oct. 3–7 2011.
- [7] M. Sidi. Spacecraft Dynamics and Control: A Practical Engineering Approach. Cambridge Aerospace Series. Cambridge University Press, 1997.
- [8] F. Markley and J. Crassidis. Fundamentals of Spacecraft Attitude Determination and Control, volume 33. Springer, 2014.
- [9] L. Dewell, N. Pedreiro, C. Blaurock, K. Liu, J. Alexander, and M. Levine. Precision Telescope Pointing and Spacecraft Vibration Isolation for the Terrestrial Planet Finder Coronagraph. SPIE Space Telescope Optomechanics and Dynamics, 2005.
- [10] M. Rizzo, S. Rinehart, J. Alcorn, D. Fixsen, A. Gore, A. Rau, S. Weinreich, A. Cotto, et al. Building an Interferometer at the Edge of Space: Pointing and Phase Control System for BETTII. SPIE Space Telescopes and Instrumentation, 2014.
- [11] D. Cheon, D. Choi, E. Jang, and H. Oh. Disturbance Reduction on the Small Satellite Actuator. In International Conference on Instrumentation Control and Automation (ICA), pages 31–34. IEEE, 2011.
- [12] D. Kamesh, R. Pandiyan, and A. Ghosal. Passive Vibration Isolation of Reaction Wheel Disturbances Using a Low Frequency Flexible Space Platform. Journal of Sound and Vibration, 331(6):1310–1330, 2012.

- [13] J. Park, A. Palazzolo, and R. Beach. MIMO Active Vibration Control of Magnetically Suspended Flywheels for Satellite IPAC Service. Journal of Dynamic Systems, Measurement, and Control, 130(4):041005, 2008.
- [14] J. Park and A. Palazzolo. Magnetically Suspended VSCMGs For Simultaneous Attitude Control And Power Transfer IPAC Service. Journal of Dynamic Systems, Measurement, and Control, 132(5):051001, 2010.
- [15] R. Masterson and D. Miller. Development of Empirical and Analytical Reaction Wheel Disturbance Models. AIAA Structures, Structural Dynamics, and Materials, 1999.
- [16] R. Masterson, D. Miller, and R. Grogan. Development and Validation of Reaction Wheel Disturbance Models: Empirical Model. Academic Press Journal of Sound and Vibration, 2002.
- [17] L. Liu. Jitter and Basic Requirements of the Reaction Wheel Assembly In the Attitude Control System. Massachusetts Institute of Technology.
- [18] H. Gutierrez. Performance Assessment and Enhancement of Precision Controlled Structures During Conceptual Design. PhD thesis, Massachusetts Institute of Technology, 1999.
- [19] D. Li, X. Chen, and B. Wu. Analysis of Reaction-Wheels Imbalance Torque Effects On Satellite Attitude Control System. In Control and Decision Conference (CCDC), 2016 Chinese, pages 3722–3725. IEEE, 2016.
- [20] K. Liu, P. Maghami, and C. Blaurock. Reaction Wheel Disturbance Modeling, Jitter Analysis, and Validation Tests for Solar Dynamics Observatory. 2008.
- [21] S. Miller, P. Kirchman, and J. Sudey. Reaction Wheel Operational Impacts On the GOES-N Jitter Environment. In AIAA Guidance, Navigation and Control Conference and Exhibit, pages 2007–6736, 2007.
- [22] D. Kim. Micro-vibration Model and Parameter Estimation Method of a Reaction Wheel Assembly. Journal of Sound and Vibration, 333(18):4214–4231, 2014.
- [23] Y. Zhang and J. Zhang. Disturbance Characteristics Analysis of CMG Due to Imbalances and Installation Errors. IEEE Transactions on Aerospace and Electronic Systems, 50(2):1017–1026, 2014.
- [24] H. Schaub and J. Junkins. Analytical Mechanics of Space Systems. AIAA Education Series, Reston, VA, 3rd edition, 2014.
- [25] C. Allard, H. Schaub, and S. Piggott. General Hinged Solar Panel Dynamics Approximating First-Order Spacecraft Flexing. In AAS Guidance and Control Conference, Breckenridge, CO, Feb. 5–10 2016. Paper No. AAS-16-156.
- [26] C. Allard, M. Diaz-Ramos, and H. Schaub. Spacecraft Dynamics Integrating Hinged Solar Panels and Lumped-mass Fuel Slosh Model. In AIAA/AAS Astrodynamics Specialist Conference, Long Beach, CA, Sept. 12–15 2016.
- [27] J. Alcorn, C. Allard, and H. Schaub. Fully-Coupled Dynamical Jitter Modeling of a Rigid Spacecraft With Imbalanced Reaction Wheels. In AIAA SPACE 2016, Long Beach, CA, Sep. 13–16 2016. Paper No. 2490836.

- [28] M. Margenet, H. Schaub, and S. Piggott. Modular attitude guidance development using the basilisk software framework. In AIAA SPACE 2016, Long Beach, CA, Sep. 13–16 2016. Paper No. 2490836.
- [29] C. Allard, M. Diaz Ramos, and H. Schaub. Spacecraft dynamics integrating hinged solar panels and lumped-mass fuel slosh model. In AIAA SPACE 2016, Long Beach, CA, Sep. 13–16 2016. Paper No. 2490836.
- [30] C. Allard, H. Schaub, and S. Piggott. General hinged solar panel dynamics approximating first-order spacecraft flexing. In AAS Guidance and Control Conference, Breckenridge, CO, Feb. 5–10 2016. Paper No. AAS-16-156.
- [31] S. Piggott, J. Alcorn, M. Margenet, P. Kenneally, and H. Schaub. Flight Software Development Through Python. 2016 Workshop on Spacecraft Flight Software, Dec. 13-15 2016.
- [32] J. Alcorn. Simulating Attitude Actuation Options Using the Basilisk Astrodynamics Software Architecture. International Astronautical Congress, Sep. 26–30 2016.
- [33] H. Schaub and V. J. Lappas. Redundant Reaction Wheel Torque Distribution Yielding Instantaneous l_2 Power-optimal Attitude Control. AIAA Journal of Guidance, Control, and Dynamics, 32(4):1269–1276, July–Aug. 2009.
- [34] R. Blenden and H. Schaub. Regenerative Power-optimal Reaction Wheel Attitude Control. AIAA Journal of Guidance, Control, and Dynamics, 35(4):1208–1217, July–Aug. 2012.
- [35] J. Alcorn, H. Schaub, and S. Piggott. Attitude Control Performance Analysis Using Discretized Thruster With Residual Tracking. In AAS Guidance and Control Conference, Breckenridge, CO, Feb. 5–10 2016. Paper No. AAS-16-038.

Appendix A

Basilisk Software Architecture

A.1 Basilisk Overview

The Basilisk astrodynamics software is being developed by the University of Colorado Boulder's Autonomous Vehicle Systems (AVS) Laboratory and the Laboratory for Atmospheric and Space Physics (LASP). Basilisk provides deterministic, integrated faster than realtime simulation while at the same time providing HWIL simulation capabilities using a modular and fast C/C++ architecture.[32] This source code is then wrapped in Python allowing the convenience of a fully scriptable Python user interface. The modular architecture and fully-coupled dynamical representation allows for complex actuators to be simulated without sacrificing accuracy. Basilisk has been used internally by the University of Colorado/LASP for simulation of flexible dynamics [30], fuel slosh[29], reaction wheel jitter[27], thrust pulsing algorithm evaluation[35], guidance algorithm development[28], and for analysis and support of ADCS sub-system developments. Basilisk offers many of the same core benefits as Commercial-off-the-Shelf (COTS)/Government-off-the-Shelf (GOTS) softwares and is open-source, cross-platform, and has a fully-scriptable user interface using the common programming language Python.

The Basilisk framework has been designed from inception to support several different (often competing) requirements.

- **Speed:** Even though the system is operated through a Python interface, the underlying simulation executes entirely in C/C++ which allows for maximum execution speed. The



Figure A.1: The Basilisk logo.

requirement for the Mars mission are sufficiently accurate vehicle simulation with at least a 365x realtime speeds (“*a year in a day*”).

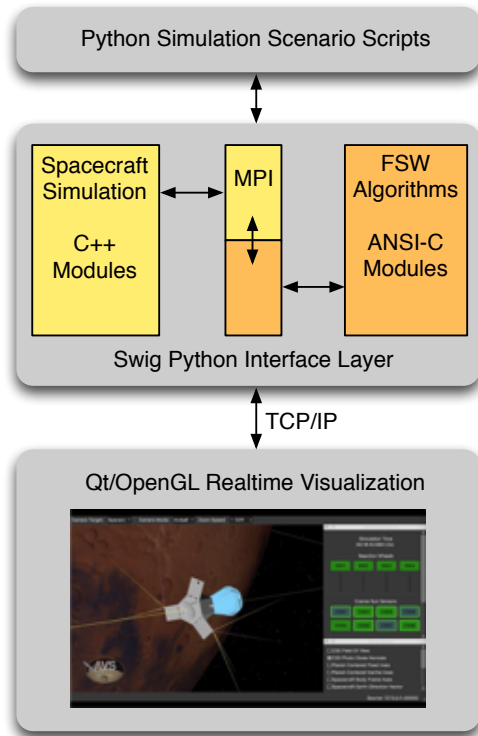
- **Reconfiguration:** The user interface executes natively in Python which allows the user to change task-rates, model/algorithm parameters, and output options dynamically on the fly.
- **Analysis:** Python-standard analysis products like `numpy`¹ and `matplotlib`² are actively used to facilitate rapid and complex analysis of data obtained in a simulation run without having to stop and export to an external tool. This capability also applies to the Monte-Carlo engine available natively in the Basilisk framework.
- **HWIL:** Basilisk provides synchronization to realtime via clock tracking modules. This allows the package to synchronize itself to one or more timing frames in order to provide deterministic behavior in a realtime environment. External communication is handled via the Boost library³ with ethernet currently available and serial planned in the near future.

Figure A.1 shows the Basilisk logo. The name Basilisk was chosen to reflect both the reptilian (Python) nature of the product-design as well as a nod to the speed requirements as the South American common basilisk runs so fast that it can even run across water.

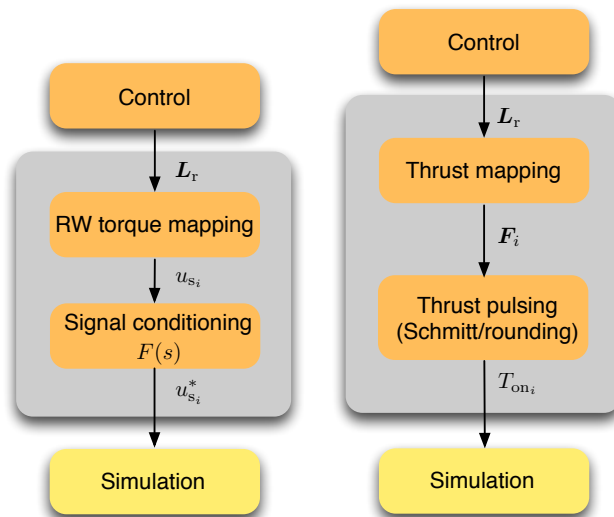
¹ <http://www.numpy.org/>

² <http://matplotlib.org/>

³ <http://www.boost.org>



(a) Basilisk architecture diagram.



(b) Example of thruster FSW algorithm (c) Example of RW FSW algorithm

Figure A.2: Basilisk simulation and FSW architecture

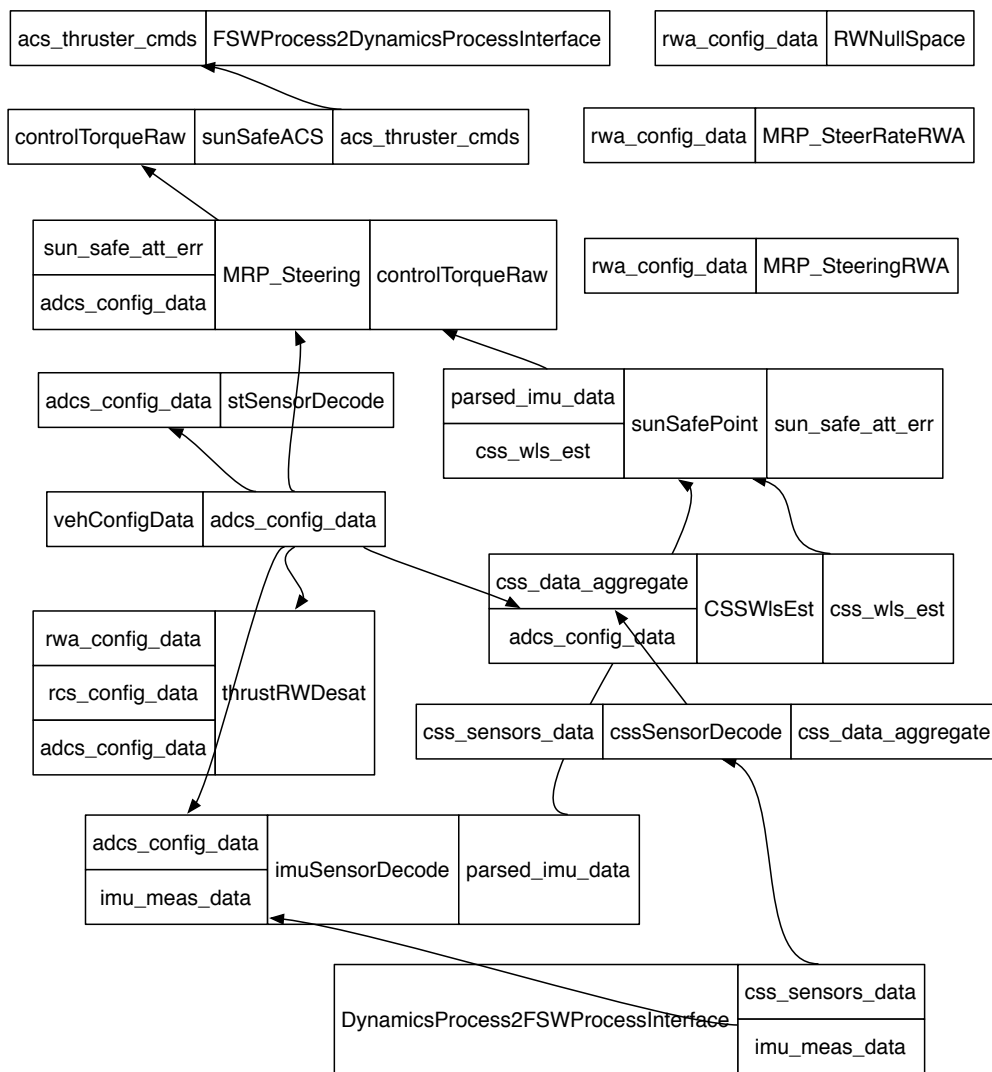


Figure A.3: Basilisk message passing interface

Figure A.2(a) shows a diagram of the Basilisk software architecture. The Python user interface layer allows the simulation to be easily reconfigured which allows the user complete freedom in creating their own simulation modules and FSW modules. Scenario scripts utilizing the user-defined simulation can be used to configure spacecraft properties, initial conditions, events, and various simulation parameters such as timing. The Python user interface layer abstracts logging/analysis which allows a single compilation of the source code to support completely different simulations. Most simulation modules are written in C++ to allow for object-oriented development while the FSW modules are written in C to allow for easy portability to flight targets. Simulation modules and FSW modules communicate through the message passing interface (MPI), which is a singleton pattern. Figure A.3 shows an auto-generated visualization of the Basilisk message passing interface. The MPI allows data traceability and ease of test. The MPI is capable of visual data mapping, which allows the user to visualize data flow between modules. Modules are limited in their ability to subscribe to messages and write messages, thus setting limitations on the flow of information and the power of modules to control data generation.[32] The messaging system is also instrumented to track data exchange, allowing the user to visualize exactly what data movement occurred in a given simulation run. The Python interface to the C/C++ layer relies on the Simplified Wrapper and Interface Generator (SWIG) software⁴, a cross-platform, open-source software tasked solely with interfacing C/C++ with scripting languages. Basilisk is inherently cross-platform in nature, currently used on Mac, Windows, and Linux systems.

A.2 Basilisk Dynamics Architecture

The Basilisk dynamics engine heavily leverages the back-substitution method as described in section 5.1. The equations of motion of the spacecraft hub are contained entirely within $[A_{\text{hub}}]$, $[B_{\text{hub}}]$, $[C_{\text{hub}}]$, $[D_{\text{hub}}]$ matrices and $\mathbf{v}_{\text{trans,hub}}$, $\mathbf{v}_{\text{rot,hub}}$ vectors. Each attachment to the spacecraft, whether it be reaction wheel, VSCMG, solar panel, fuel tank, etc, is considered either a dynamic effector or a state effector and has its own contribution matrices and vectors. The dynamics

⁴ <http://swig.org/>

manager class aggregates all contributions and solves the aggregate system EOMs. States belonging to the effectors such as $\dot{\Omega}_i$ or $\ddot{\gamma}_i$ are solved for within the corresponding effector class. Additionally, each effector is responsible for registering its own states with the dynamics manager, and computing its energy, momentum, and mass contributions at each timestep.

The Basilisk dynamics engine relies heavily on Eigen C++ libraries⁵ in order to perform the massive amount of matrix algebra required to solve the spacecraft system of equations.

A.3 Visualization

Basilisk has an accompanying visualization that allows the user to observe the simulated spacecraft's operations realtime. The visualization uses Qt⁶ /OpenGL⁷ to visualize the spacecraft, planets, and various qualitative data and indicators for sensors and actuators. Simulation events and device faults may be triggered directly from the visualization. Figure A.4 shows an example of the visualization with a spacecraft in Mars orbit. The control panel on the right hand side allows the user to view sensor and actuator data and trigger events. Reference frame axes may be enabled/disabled from the control panel. The visualization also demonstrates thruster plumes and the field of view of sensors such as star trackers and course sun sensors.

⁵ <https://eigen.tuxfamily.org/>

⁶ <https://www.qt.io/>

⁷ <https://www.opengl.org/>

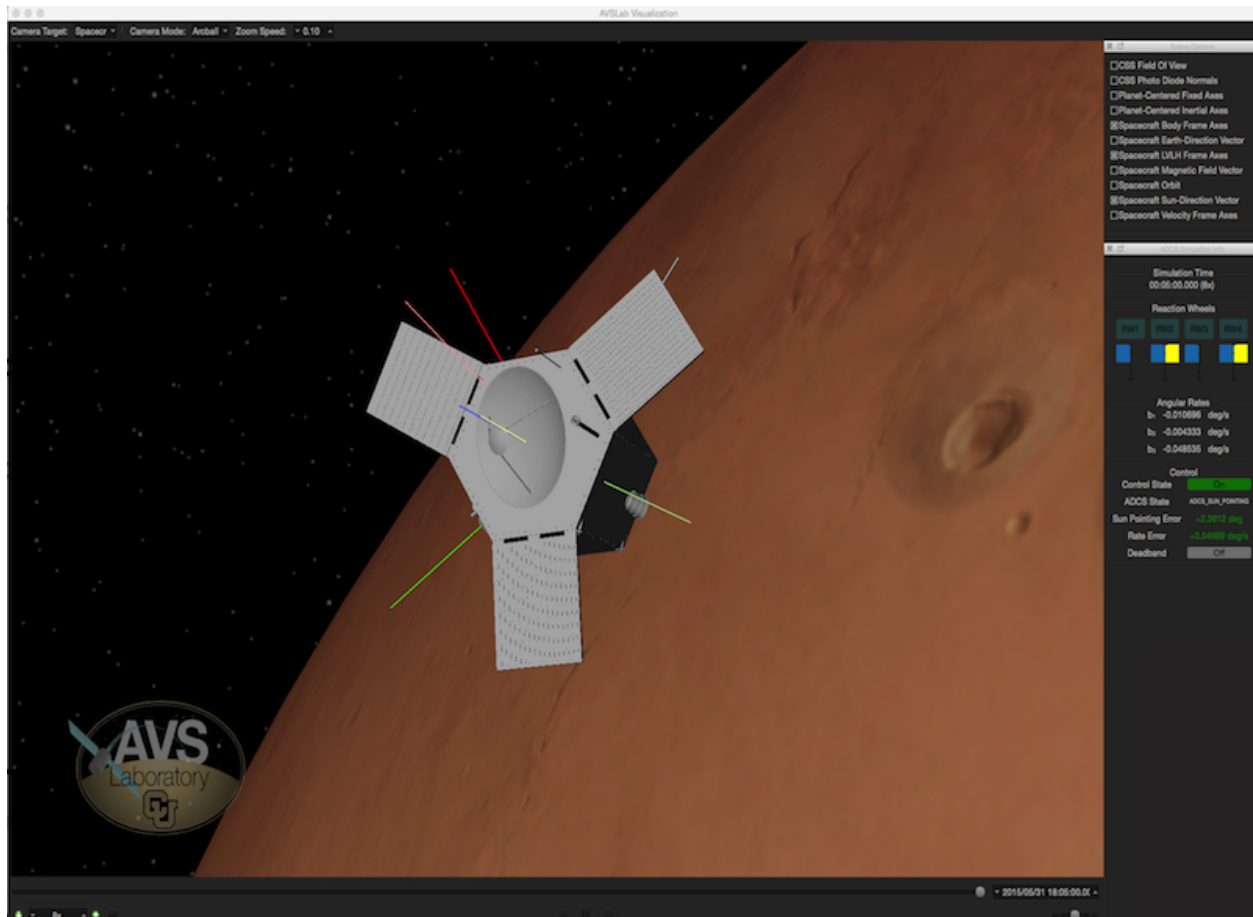


Figure A.4: Basilisk visualization example of a Mars orbiting spacecraft.

Appendix B

Additional Back-Substitution Derivations

B.1 Back-Substitution Derivations

Chapter 5 provided the derivation of the back-substitution contribution matrices for an imbalanced VSCMG as an example. This section provides the derivation of the back-substitution contribution matrices of a balanced RW, imbalanced RW, and balanced VSCMG for reference, and builds upon the the material presented in Chapter 5. Consideration should be given to implementing these equations in software separately from imbalanced VSCMG equations, since it is more computationally efficient to have a separate set of equations to solve rather than zero out imbalance terms or gimbal states.

B.1.1 Balanced Reaction Wheel Back-Substitution

B.1.1.1 Equations of Motion

The equations of motion of a balanced reaction wheel were provided in Chapter 2, and are repeated here for the reader's convenience. The translational equation of motion is not coupled with $\dot{\Omega}$ as show below.

$$m_{sc}[I_{3 \times 3}]\ddot{\mathbf{r}}_{B/N} - m_{sc}[\tilde{\mathbf{c}}]\dot{\boldsymbol{\omega}}_{B/N} = \mathbf{F}_{ext} - 2m_{sc}[\tilde{\boldsymbol{\omega}}_{B/N}]\mathbf{c}' - m_{sc}[\tilde{\boldsymbol{\omega}}_{B/N}][\tilde{\boldsymbol{\omega}}_{B/N}]\mathbf{c} \quad (\text{B.1})$$

The rotational equation of motion includes $\dot{\Omega}$ terms, and is thus coupled with the wheel motion as seen below.

$$m_{sc}[\tilde{\mathbf{c}}]\ddot{\mathbf{r}}_{B/N} + [I_{sc,B}]\dot{\boldsymbol{\omega}}_{B/N} + \sum_{i=1}^N J_{s_i} \hat{\mathbf{g}}_{s_i} \dot{\Omega}_i = -[\tilde{\boldsymbol{\omega}}_{B/N}][I_{sc,B}]\boldsymbol{\omega}_{B/N} - \sum_{i=1}^N (\boldsymbol{\omega}_{B/N} \times J_{s_i} \Omega_i \hat{\mathbf{g}}_{s_i}) + \mathbf{L}_B \quad (\text{B.2})$$

The motor torque equation is coupled with $\dot{\boldsymbol{\omega}}_{B/N}$ as shown below.

$$\dot{\Omega}_i = \frac{u_{s_i}}{J_{s_i}} - \hat{\mathbf{g}}_{s_i}^T \dot{\boldsymbol{\omega}}_{B/N} \quad (\text{B.3})$$

B.1.1.2 Back-Substitution Derivation

Since translation is not coupled with wheel speed, the back-substitution equation may be obtained by simply plugging Eq. (B.3) into Eq. (B.2)

$$m_{sc}[\tilde{\mathbf{c}}]\ddot{\mathbf{r}}_{B/N} + ([I_{sc,B}] - \sum_{i=1}^N J_{s_i} \hat{\mathbf{g}}_{s_i} \hat{\mathbf{g}}_{s_i}^T) \dot{\boldsymbol{\omega}}_{B/N} = -[\tilde{\boldsymbol{\omega}}_{B/N}][I_{sc,B}]\boldsymbol{\omega}_{B/N} - \sum_{i=1}^N (\hat{\mathbf{g}}_{s_i} u_{s_i} + \boldsymbol{\omega}_{B/N} \times J_{s_i} \Omega_i \hat{\mathbf{g}}_{s_i}) - [I'_{sc,B}]\boldsymbol{\omega}_{B/N} + \mathbf{L}_B \quad (\text{B.4})$$

The contribution matrices using for solving the coupled EOMs may now be defined.

B.1.1.3 Back-Substitution Contribution Matrices

The back-substitution contribution matrices provide the dynamical contribution of the RWs to the general form given by Eq. (5.1). Thus, any terms that do not contain RW terms are known

and are the same for any type of device. The following are defined from the coefficients of Eq. (B.4)

$$[A_{\text{contr}}] = [0_{3 \times 3}] \quad (\text{B.5})$$

$$[B_{\text{contr}}] = [0_{3 \times 3}] \quad (\text{B.6})$$

$$[C_{\text{contr}}] = [0_{3 \times 3}] \quad (\text{B.7})$$

$$[D_{\text{contr}}] = - \sum_{i=1}^N J_{s_i} \hat{\mathbf{g}}_{s_i} \hat{\mathbf{g}}_{s_i}^T \quad (\text{B.8})$$

$$\mathbf{v}_{\text{trans,contr}} = \mathbf{0} \quad (\text{B.9})$$

$$\mathbf{v}_{\text{rot,contr}} = - \sum_{i=1}^N (\hat{\mathbf{g}}_{s_i} u_{s_i} + \boldsymbol{\omega}_{\mathcal{B}/\mathcal{N}} \times J_{s_i} \Omega_i \hat{\mathbf{g}}_{s_i}) \quad (\text{B.10})$$

B.1.2 Imbalanced Reaction Wheel Back-Substitution

B.1.2.1 Equations of Motion

The equations of motion of an imbalanced reaction wheel were provided in Chapter 2, and are repeated here for the reader's convenience. The translational equation of motion is

$$\ddot{\mathbf{r}}_{\mathcal{B}/\mathcal{N}} - [\tilde{\mathbf{c}}] \dot{\boldsymbol{\omega}}_{\mathcal{B}/\mathcal{N}} + \frac{1}{m_{\text{sc}}} \sum_{i=1}^N m_{\text{rw}_i} d_i \hat{\boldsymbol{\omega}}_{3_i} \dot{\Omega}_i = \ddot{\mathbf{r}}_{\mathcal{C}/\mathcal{N}} - 2[\tilde{\boldsymbol{\omega}}_{\mathcal{B}/\mathcal{N}}] \mathbf{c}' - [\tilde{\boldsymbol{\omega}}_{\mathcal{B}/\mathcal{N}}][\tilde{\boldsymbol{\omega}}_{\mathcal{B}/\mathcal{N}}] \mathbf{c} + \frac{1}{m_{\text{sc}}} \sum_{i=1}^N m_{\text{rw}_i} d_i \Omega_i^2 \hat{\boldsymbol{\omega}}_{2_i} \quad (\text{B.11})$$

The rotational equation of motion is

$$\begin{aligned} & m_{\text{sc}} [\tilde{\mathbf{c}}] \ddot{\mathbf{r}}_{\mathcal{B}/\mathcal{N}} + [I_{\text{sc},\mathcal{B}}] \dot{\boldsymbol{\omega}}_{\mathcal{B}/\mathcal{N}} + \sum_{i=1}^N \left([I_{\text{rw}_i, W_{c_i}}] \hat{\mathbf{g}}_{s_i} + m_{\text{rw}_i} d_i [\tilde{\mathbf{r}}_{W_{c_i}/\mathcal{B}}] \hat{\boldsymbol{\omega}}_{3_i} \right) \dot{\Omega}_i \\ &= \sum_{i=1}^N \left[m_{\text{rw}_i} [\tilde{\mathbf{r}}_{W_{c_i}/\mathcal{B}}] d_i \Omega_i^2 \hat{\boldsymbol{\omega}}_{2_i} - [I_{\text{rw}_i, W_{c_i}}]' \Omega_i \hat{\mathbf{g}}_{s_i} - [\tilde{\boldsymbol{\omega}}_{\mathcal{B}/\mathcal{N}}] \left([I_{\text{rw}_i, W_{c_i}}] \Omega_i \hat{\mathbf{g}}_{s_i} + m_{\text{rw}_i} [\tilde{\mathbf{r}}_{W_{c_i}/\mathcal{B}}] \mathbf{r}'_{W_{c_i}/\mathcal{B}} \right) \right] \\ & \quad - [\tilde{\boldsymbol{\omega}}_{\mathcal{B}/\mathcal{N}}] [I_{\text{sc},\mathcal{B}}] \boldsymbol{\omega}_{\mathcal{B}/\mathcal{N}} - [I_{\text{sc},\mathcal{B}}]' \boldsymbol{\omega}_{\mathcal{B}/\mathcal{N}} + \mathbf{L}_B \quad (\text{B.12}) \end{aligned}$$

The motor torque equation is

$$\begin{aligned} & [m_{\text{rw}_i} d_i \hat{\boldsymbol{\omega}}_{3_i}^T] \ddot{\mathbf{r}}_{\mathcal{B}/\mathcal{N}} + [(J_{11_i} + m_{\text{rw}_i} d_i^2) \hat{\mathbf{g}}_{s_i}^T + J_{13_i} \hat{\boldsymbol{\omega}}_{3_i}^T - m_{\text{rw}_i} d_i \hat{\boldsymbol{\omega}}_{3_i}^T [\tilde{\mathbf{r}}_{W_i/\mathcal{B}}]] \dot{\boldsymbol{\omega}}_{\mathcal{B}/\mathcal{N}} + [J_{11_i} + m_{\text{rw}_i} d_i^2] \dot{\Omega}_i \\ &= -J_{13_i} \omega_{w_{2_i}} \omega_{s_i} + \omega_{w_{2_i}} \omega_{w_{3_i}} (J_{22_i} - J_{33_i} - m_{\text{rw}_i} d_i^2) - m_{\text{rw}_i} d_i \hat{\boldsymbol{\omega}}_{3_i}^T [\tilde{\boldsymbol{\omega}}_{\mathcal{B}/\mathcal{N}}] [\tilde{\boldsymbol{\omega}}_{\mathcal{B}/\mathcal{N}}] \mathbf{r}_{W_i/\mathcal{B}} + u_{s_i} + \hat{\mathbf{g}}_{s_i}^T \boldsymbol{\tau}_{\text{ext},i} \quad (\text{B.13}) \end{aligned}$$

B.1.2.2 Derivation of Back-Substitution

First, we solve the motor torque equation for $\dot{\Omega}_i$.

$$\begin{aligned} \dot{\Omega}_i = & - \left(\frac{m_{rw_i} d_i \hat{\mathbf{w}}_{3_i}^T}{J_{11_i} + m_{rw_i} d_i^2} \right) \ddot{\mathbf{r}}_{B/N} - \frac{1}{J_{11_i} + m_{rw_i} d_i^2} [(J_{11_i} + m_{rw_i} d_i^2) \hat{\mathbf{g}}_{s_i}^T \\ & + J_{13_i} \hat{\mathbf{w}}_{3_i}^T - m_{rw_i} d_i \hat{\mathbf{w}}_{3_i}^T [\tilde{\mathbf{r}}_{W_i/B}]] \dot{\boldsymbol{\omega}}_{B/N} + \frac{1}{J_{11_i} + m_{rw_i} d_i^2} \left(\omega_{w_{2_i}} \omega_{w_{3_i}} (J_{22_i} \right. \\ & \left. - J_{33_i} - m_{rw_i} d_i^2) - J_{13_i} \omega_{w_{2_i}} \omega_{s_i} - m_{rw_i} d_i \hat{\mathbf{w}}_{3_i}^T [\tilde{\boldsymbol{\omega}}_{B/N}] [\tilde{\boldsymbol{\omega}}_{B/N}] \mathbf{r}_{W_i/B} + u_{s_i} \right) \end{aligned} \quad (\text{B.14})$$

The following coefficients are defined from Eq. (B.14), and are used to de-clutter the final equations.

$$\mathbf{a}_{\Omega_i} = - \frac{m_{rw_i} d_i}{J_{11_i} + m_{rw_i} d_i^2} \hat{\mathbf{w}}_{3_i} \quad (\text{B.15})$$

$$\mathbf{b}_{\Omega_i} = - \frac{1}{J_{11_i} + m_{rw_i} d_i^2} [(J_{11_i} + m_{rw_i} d_i^2) \hat{\mathbf{g}}_{s_i} + J_{13_i} \hat{\mathbf{w}}_{3_i} + m_{rw_i} d_i [\tilde{\mathbf{r}}_{W_i/B}] \hat{\mathbf{w}}_{3_i}] \quad (\text{B.16})$$

$$\begin{aligned} c_{\Omega_i} = & \frac{1}{J_{11_i} + m_{rw_i} d_i^2} \left(\omega_{w_{2_i}} \omega_{w_{3_i}} (J_{22_i} - J_{33_i} - m_{rw_i} d_i^2) - J_{13_i} \omega_{w_{2_i}} \omega_{s_i} \right. \\ & \left. - m_{rw_i} d_i \hat{\mathbf{w}}_{3_i}^T [\tilde{\boldsymbol{\omega}}_{B/N}] [\tilde{\boldsymbol{\omega}}_{B/N}] \mathbf{r}_{W_i/B} + u_{s_i} + \hat{\mathbf{g}}_{s_i}^T \boldsymbol{\tau}_{ext,i} \right) \end{aligned} \quad (\text{B.17})$$

Rewrite Eq. (B.14) in compact form.

$$\dot{\Omega}_i = \mathbf{a}_{\Omega_i}^T \ddot{\mathbf{r}}_{B/N} + \mathbf{b}_{\Omega_i}^T \dot{\boldsymbol{\omega}}_{B/N} + c_{\Omega_i} \quad (\text{B.18})$$

Plugging the equation above into Eq. (B.11) and multiplying both sides by m_{sc} , we arrive at,

$$\begin{aligned} & \left[m_{sc} [I_{3 \times 3}] + \sum_{i=1}^N m_{rw_i} d_i \hat{\mathbf{w}}_{3_i} \mathbf{a}_{\Omega_i}^T \right] \ddot{\mathbf{r}}_{B/N} + \left[-m_{sc} [\tilde{\mathbf{c}}] + \sum_{i=1}^N m_{rw_i} d_i \hat{\mathbf{w}}_{3_i} \mathbf{b}_{\Omega_i}^T \right] \dot{\boldsymbol{\omega}}_{B/N} \\ & = \mathbf{F} - 2m_{sc} [\tilde{\boldsymbol{\omega}}_{B/N}] \mathbf{c}' - m_{sc} [\tilde{\boldsymbol{\omega}}_{B/N}] [\tilde{\boldsymbol{\omega}}_{B/N}] \mathbf{c} + \sum_{i=1}^N \left[m_{rw_i} d_i \Omega_i^2 \hat{\mathbf{w}}_{2_i} - m_{rw_i} d_i c_{\Omega_i} \hat{\mathbf{w}}_{3_i} \right] \end{aligned} \quad (\text{B.19})$$

So the same step for the rotational EOM.

$$\begin{aligned}
& \left[m_{sc}[\tilde{\mathbf{c}}] + \sum_{i=1}^N \left([I_{rw_i, W_{c_i}}] \hat{\mathbf{g}}_{s_i} + m_{rw_i} d_i [\tilde{\mathbf{r}}_{W_{c_i}/B}] \hat{\mathbf{w}}_{3_i} \right) \mathbf{a}_{\Omega_i}^T \right] \ddot{\mathbf{r}}_{B/N} \\
& + \left[[I_{sc, B}] + \sum_{i=1}^N \left([I_{rw_i, W_{c_i}}] \hat{\mathbf{g}}_{s_i} + m_{rw_i} d_i [\tilde{\mathbf{r}}_{W_{c_i}/B}] \hat{\mathbf{w}}_{3_i} \right) \mathbf{b}_{\Omega_i}^T \right] \dot{\boldsymbol{\omega}}_{B/N} \\
& = -[\tilde{\boldsymbol{\omega}}_{B/N}] [I_{sc, B}] \boldsymbol{\omega}_{B/N} - [I_{sc, B}]' \boldsymbol{\omega}_{B/N} + \mathbf{L}_B \\
& + \sum_{i=1}^N \left[m_{rw_i} [\tilde{\mathbf{r}}_{W_{c_i}/B}] d_i \Omega_i^2 \hat{\mathbf{w}}_{2_i} - [I_{rw_i, W_{c_i}}]' \Omega_i \hat{\mathbf{g}}_{s_i} - [\tilde{\boldsymbol{\omega}}_{B/N}] \left([I_{rw_i, W_{c_i}}] \Omega_i \hat{\mathbf{g}}_{s_i} + m_{rw_i} [\tilde{\mathbf{r}}_{W_{c_i}/B}] \mathbf{r}'_{W_{c_i}/B} \right) \right. \\
& \quad \left. - \left([I_{rw_i, W_{c_i}}] \hat{\mathbf{g}}_{s_i} + m_{rw_i} d_i [\tilde{\mathbf{r}}_{W_{c_i}/B}] \hat{\mathbf{w}}_{3_i} \right) c_{\Omega_i} \right] \quad (\text{B.20})
\end{aligned}$$

We now have all the information needed to define the back-substitution contributions matrices for imbalanced reaction wheels.

B.1.2.3 Back-Substitution Contribution Matrices

The imbalanced reaction wheel back-substitution contribution matrices are given by,

$$[A_{\text{contr}}] = \sum_{i=1}^N m_{rw_i} d_i \hat{\mathbf{w}}_{3_i} \mathbf{a}_{\Omega_i}^T \quad (\text{B.21})$$

$$[B_{\text{contr}}] = \sum_{i=1}^N m_{rw_i} d_i \hat{\mathbf{w}}_{3_i} \mathbf{b}_{\Omega_i}^T \quad (\text{B.22})$$

$$[C_{\text{contr}}] = \sum_{i=1}^N \left([I_{rw_i, W_{c_i}}] \hat{\mathbf{g}}_{s_i} + m_{rw_i} d_i [\tilde{\mathbf{r}}_{W_{c_i}/B}] \hat{\mathbf{w}}_{3_i} \right) \mathbf{a}_{\Omega_i}^T \quad (\text{B.23})$$

$$[D_{\text{contr}}] = \sum_{i=1}^N \left([I_{rw_i, W_{c_i}}] \hat{\mathbf{g}}_{s_i} + m_{rw_i} d_i [\tilde{\mathbf{r}}_{W_{c_i}/B}] \hat{\mathbf{w}}_{3_i} \right) \mathbf{b}_{\Omega_i}^T \quad (\text{B.24})$$

$$\mathbf{v}_{\text{trans, contr}} = \sum_{i=1}^N \left[m_{rw_i} d_i \Omega_i^2 \hat{\mathbf{w}}_{2_i} - m_{rw_i} d_i c_{\Omega_i} \hat{\mathbf{w}}_{3_i} \right] \quad (\text{B.25})$$

$$\begin{aligned}
\mathbf{v}_{\text{rot, contr}} = \sum_{i=1}^N \left[m_{rw_i} [\tilde{\mathbf{r}}_{W_{c_i}/B}] d_i \Omega_i^2 \hat{\mathbf{w}}_{2_i} - [I_{rw_i, W_{c_i}}]' \Omega_i \hat{\mathbf{g}}_{s_i} - [\tilde{\boldsymbol{\omega}}_{B/N}] \left([I_{rw_i, W_{c_i}}] \Omega_i \hat{\mathbf{g}}_{s_i} \right. \right. \\
\left. \left. + m_{rw_i} [\tilde{\mathbf{r}}_{W_{c_i}/B}] \mathbf{r}'_{W_{c_i}/B} \right) - \left([I_{rw_i, W_{c_i}}] \hat{\mathbf{g}}_{s_i} + m_{rw_i} d_i [\tilde{\mathbf{r}}_{W_{c_i}/B}] \hat{\mathbf{w}}_{3_i} \right) c_{\Omega_i} \right] \quad (\text{B.26})
\end{aligned}$$

B.1.3 Balanced VSCMG Back-Substitution

B.1.3.1 Equations of Motion

The balanced VSCMG equations of motion are reproduced here for the reader's convenience. The balanced translational equation of motion as derived in Eq. (3.26) is given below. Note that translation is not coupled with $\dot{\Omega}$ or $\ddot{\gamma}_i$.

$$m_{sc}\ddot{\mathbf{r}}_{B/N} - m_{sc}[\tilde{\mathbf{c}}]\dot{\boldsymbol{\omega}} = \mathbf{F} - 2m_{sc}[\tilde{\boldsymbol{\omega}}]\mathbf{c}' - m_{sc}[\tilde{\boldsymbol{\omega}}]^2\mathbf{c}$$

The rotational equation of motion includes $\dot{\Omega}_i$ and $\ddot{\gamma}_i$ terms, and is thus coupled with VSCMG motion as seen below.

$$\begin{aligned} m_{sc}[\tilde{\mathbf{c}}]\ddot{\mathbf{r}}_{B/N} + [I_{sc,B}]\dot{\boldsymbol{\omega}} + \sum_{i=1}^N I_{V_{g_i}} \hat{\mathbf{g}}_{g_i} \ddot{\gamma}_i + \sum_{i=1}^N I_{W_{s_i}} \hat{\mathbf{g}}_{s_i} \dot{\Omega}_i \\ = \mathbf{L}_B - [I_{sc,B}]\boldsymbol{\omega} - [\tilde{\boldsymbol{\omega}}][I_{sc,B}]\boldsymbol{\omega} - \sum_{i=1}^N \left[+ I_{W_{t_i}} \Omega \dot{\gamma}_i \hat{\mathbf{g}}_{t_i} + \Omega_i \dot{\gamma}_i (I_{W_{s_i}} - I_{W_{t_i}}) \hat{\mathbf{g}}_{t_i} \right. \\ \left. + [\tilde{\boldsymbol{\omega}}][I_{G_i, G_{c_i}}] \dot{\gamma}_i \hat{\mathbf{g}}_{g_i} + [\tilde{\boldsymbol{\omega}}][I_{W_i, W_{c_i}}] \boldsymbol{\omega}_{W_i/B} \right] \end{aligned}$$

The gimbal torque equation as derived in Eq. (3.124) is given below.

$$I_{V_{g_i}} (\hat{\mathbf{g}}_{g_i}^T \dot{\boldsymbol{\omega}} + \ddot{\gamma}_i) = u_{g_i} + (I_{V_{s_i}} - I_{V_{t_i}}) \omega_s \omega_t + I_{W_{s_i}} \Omega_i \omega_t$$

The wheel torque equation as derived in Eq. (3.132) is given below.

$$I_{W_{s_i}} (\hat{\mathbf{g}}_{s_i}^T \dot{\boldsymbol{\omega}} + \dot{\Omega}_i) = -I_{W_{s_i}} \omega_t \dot{\gamma}_i + u_{s_i}$$

B.1.3.2 Back-Substitution Derivation

Solve the gimbal torque equation for $\ddot{\gamma}_i$ in terms of $\dot{\boldsymbol{\omega}}_{B/N}$.

$$\ddot{\gamma}_i = \frac{1}{I_{V_{g_i}}} \left(u_{g_i} + (I_{V_{s_i}} - I_{V_{t_i}}) \omega_s \omega_t + I_{W_{s_i}} \Omega_i \omega_t - I_{V_{g_i}} \hat{\mathbf{g}}_{g_i}^T \dot{\boldsymbol{\omega}} \right) \quad (\text{B.27})$$

Solve the wheel torque equation for $\dot{\Omega}_i$ in terms of $\dot{\boldsymbol{\omega}}_{B/N}$

$$\dot{\Omega}_i = -\omega_t \dot{\gamma}_i - \hat{\mathbf{g}}_{s_i}^T \dot{\boldsymbol{\omega}} + \frac{u_{s_i}}{I_{W_{s_i}}} \quad (\text{B.28})$$

Plug Eq. (B.27) and Eq. (B.28) into the rotational equation of motion and group like terms.

$$\begin{aligned}
m_{sc}[\tilde{\mathbf{c}}]\ddot{\mathbf{r}}_{B/N} + \left[[I_{sc,B}] - \sum_{i=1}^N (I_{V_{g_i}} \hat{\mathbf{g}}_{g_i} \hat{\mathbf{g}}_{g_i}^T + I_{W_{s_i}} \hat{\mathbf{g}}_{s_i} \hat{\mathbf{g}}_{s_i}^T) \right] \dot{\boldsymbol{\omega}} \\
= \mathbf{L}_B - [I_{sc,B}]' \boldsymbol{\omega} - [\tilde{\boldsymbol{\omega}}][I_{sc,B}] \boldsymbol{\omega} - \sum_{i=1}^N \left[(u_{s_i} - I_{W_{s_i}} \omega_t \dot{\gamma}_i) \hat{\mathbf{g}}_{s_i} + I_{W_{s_i}} \Omega \dot{\gamma}_i \hat{\mathbf{g}}_{t_i} \right. \\
\left. + (u_{g_i} + (I_{V_{s_i}} - I_{V_{t_i}}) \omega_s \omega_t + I_{W_{s_i}} \Omega_i \omega_t) \hat{\mathbf{g}}_{g_i} + [\tilde{\boldsymbol{\omega}}][I_{G_i, G_{c_i}}] \dot{\gamma}_i \hat{\mathbf{g}}_{g_i} + [\tilde{\boldsymbol{\omega}}][I_{W_i, W_{c_i}}] \boldsymbol{\omega}_{W_i/B} \right] \quad (\text{B.29})
\end{aligned}$$

We now have all the information needed to define the back-substitution contribution matrices for a balanced VSCMG.

B.1.3.3 Back-Substitution Contribution Matrices

The balanced VSCMG back-substitution contribution matrices are given by,

$$[A_{\text{contr}}] = [0_{3 \times 3}] \quad (\text{B.30})$$

$$[B_{\text{contr}}] = [0_{3 \times 3}] \quad (\text{B.31})$$

$$[C_{\text{contr}}] = [0_{3 \times 3}] \quad (\text{B.32})$$

$$[D_{\text{contr}}] = - \sum_{i=1}^N [I_{V_{g_i}} \hat{\mathbf{g}}_{g_i} \hat{\mathbf{g}}_{g_i}^T + I_{W_{s_i}} \hat{\mathbf{g}}_{s_i} \hat{\mathbf{g}}_{s_i}^T] \quad (\text{B.33})$$

$$\mathbf{v}_{\text{trans,contr}} = \mathbf{0} \quad (\text{B.34})$$

$$\begin{aligned}
\mathbf{v}_{\text{rot,contr}} = - \sum_{i=1}^N \left[(u_{s_i} - I_{W_{s_i}} \omega_t \dot{\gamma}_i) \hat{\mathbf{g}}_{s_i} + I_{W_{s_i}} \Omega \dot{\gamma}_i \hat{\mathbf{g}}_{t_i} + (u_{g_i} + (I_{V_{s_i}} - I_{V_{t_i}}) \omega_s \omega_t + I_{W_{s_i}} \Omega_i \omega_t) \hat{\mathbf{g}}_{g_i} \right. \\
\left. + [\tilde{\boldsymbol{\omega}}][I_{G_i, G_{c_i}}] \dot{\gamma}_i \hat{\mathbf{g}}_{g_i} + [\tilde{\boldsymbol{\omega}}][I_{W_i, W_{c_i}}] \boldsymbol{\omega}_{W_i/B} \right] \quad (\text{B.35})
\end{aligned}$$